DEPOSITIONAL SYSTEMS AND PERMEABILITY DISTRIBUTION OF FLUVIAL-ALLUVIAL-EOLIAN DEPOSITS OF SIERRA LADRONES FORMATION, APPLIED TO PETROLEUM MIGRATION IN THE ALBUQUERQUE BASIN NEW MEXICO

by

Adi Fernando Mulyadi

Submitted in Partial Fulfilment of the Requirements for the Master of Science in Petroleum Geology

New Mexico Institute of Mining and Technology
Department of Geoscience

Socorro, New Mexico

May, 1995

ACKNOWLEDGMENTS

I thank Dr. Dave W. Love for educating me while in the field, his guidance and technical assistance to complete this independent study. I also thank to Dr. Peter S. Mozley who inspired me with some ideas in the petroleum migration and to Dr. David B. Johnson for improving this study.

Special thanks are due other to Pertamina, the Indonesian oil goverment, which gave me opportunity to study my M.S in New Mexico Tech, LCP International Institute as an Pertamina colleague in the US, Pat, Ted, and Indonesian students in New Mexico Tech who help and contribute transportation during the field work.

For my Mom, Dad, Brothers, Sisters, and Nunung

ABSTRACT

The Upper Sierra Ladrones Formation southwest of Bosque, New Mexico is located in southern half-graben of the Albuquerque Basin. The 21- 30 meter thick deposits within my study area show fining-upward vertical sequences. The various types of lithofacies are produced by combinations of fluvial, alluvial, and eolian systems. These processes control the lateral and vertical geometry of each lithofacies. Some are more continuous than others. Vertical aggradation reflects decreasing stream power in channels, but also occurs on floodplains and in eolian settings. Some lithofacies interfinger and pinch-out. Different depositional processes may take place laterally at the same depositional level within the sequence.

Depositional systems control the permeability distribution in my study area, especially gravelly sandstones and sandstone lithofacies of channel-fill deposits. Gravelly sands have the biggest permeability value, followed by sandstone lithofacies derived from fluvial systems and finally sandy lithofacies from the eolian system. Their permeability values are reduced by increasing cementation and soil development and decreasing grain size distribution. Paleoflow in channels is determined by the sedimentary structures and is generally from a NW direction. Concretions and differential cementation are also oriented NW-SE.

Oil migration occur in layers having laterally continuous permeability distributions. The changes of permeability through time are caused by cementation. Such changes affect the direction of migration as well.

TABLE OF CONTENTS

LIST OF FIGURES

LIST OF TABLES

CHAPTER 1 INTRODUCTION

Petroleum geologists are developing alternative techniques for increasing oil production while reducing costs of production. Two alternative ideas are to explore for new oil wells or stimulate oil production from formerly non-productive zones. In order to develop or to stimulate oil production, the permeability distribution and depositional model of the prospective area should be known. Therefore, geologic units within the site, the permeability patterns within the geologic units, and lateral correlation of permeability and lithofacies distribution are required to achieve this goal.

Hydrocarbons commonly migrate both laterally and vertically in the opposite direction of water movement (Braester et al., 1991). These lateral and vertical migration pathways are governed by temperature, capillary pressure, density of oil, and water buoyancy. The flows follow simple geometric rules, and therefore can be estimated. In most cases, vertical migration controls major hydrocarbon accumulation (Pratsch, 1991).

The purpose of this study is to achieve better understanding of relationships between the depositional system and permeability distribution applied to petroleum migration. This study classifies the deposits into lithofacies. The term "lithofacies" is defined as "a body of rock with certain specified attributes that distinguish it from other rock units" (Leeder, 1982). Conybeare, (1979) implies lithofacies is "a lateral change of rock type within a time-stratigraphic unit in response to a change in depositional environment". This change may reflect a change of climatic, paleogeographic, or other aspects. Depositional systems in the study area are interpreted from the lateral and vertical distribution of lithofacies. Both lateral and vertical lithofacies distribution govern the permeability behavior and distribution of petroleum. The lithologies are not always wide-spread; they may pinch out. Allen, (1974) determined that the sedimentology in alluvial-fluvial systems is controlled by autocyclic and allocyclic responses. Autocyclic adjustments control river movement as the result of changes in energy within a sedimentary basin. Allocyclic responses , on the other hand, control the river as a result of climatic and tectonic changes. Because Allen's (1974) models for depositional shifts in river systems are good for distinguishing different kinds of depositional situations, results of this study will be compared to the models. Instead of merely describing the area with ten vertical measured sections, this study also measures the permeability value of each unconsolidated sandy lithofacies. The permeability distributions are determined by measuring the orientation of concretions.

Although previous workers in the study area utilized architectural elements for their classification, this study uses lithofacies. None-the-less direct comparisons may still be made between the present and past.

The field site chosen is approximately 1.3 km long and located southwest of Bosque, New Mexico, south of the areas studied by Davis, (1990,1993), Lohmann, (1992), and Gotkowitz (1993) (Figure 1.1). This study traces deposits of fluvial-alluvial-eolian systems continuing south of their mapped areas. This study concentrates on gravelly sands and sandstone lithofacies, because their permeability is measurable and continuous through out the mapped area. Interbedded sand-silt-clay and paleosols are not considered in as much detail in this study because they have lower permeability. This field site was chosen because of the presence of continuous sandstone and gravelly sand lithofacies that are generally bounded by clay-silt and paleosol lithofacies along the mapped area. This permeable and continuous lithofacies will represent a good example of reservoir lithofacies for estimating petroleum migration. Besides, there were several previous workers that had already done permeability measurements within Bosque site.

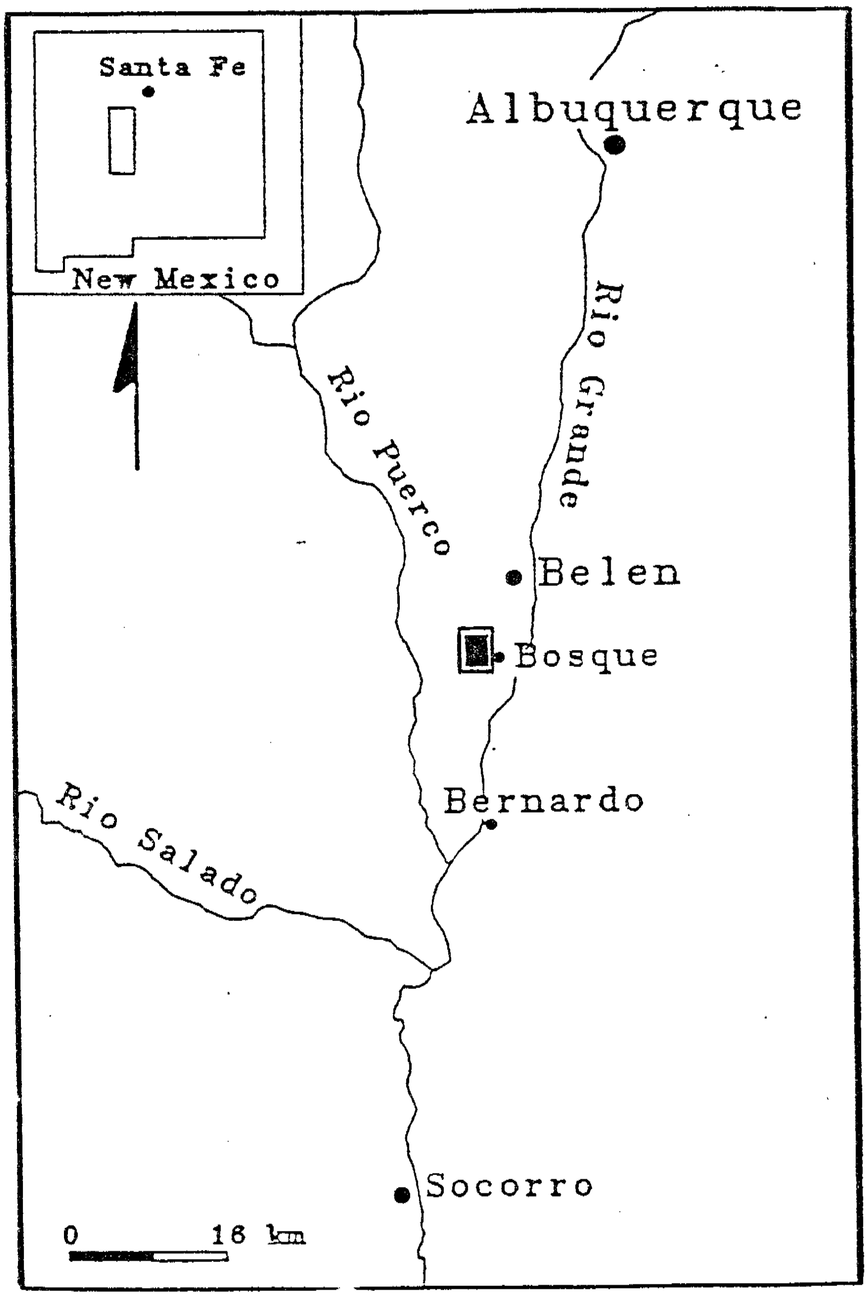

Figure 1.1. Site location of the Field area (black box)

CHAPTER 2 GEOLOGIC SITE

2.1 Site Location

The study area is located southwest of Bosque, Valencia County, central New Mexico. It is 48 - 60 km north of Socorro. The field site is in the south-central portion of Albuquerque Basin, along north-south trending eastern escarpment of the Llano de Albuquerque (Lozinsky 1988 ; figure 2.1). The site is bounded by latitudes 34^0 32" 15' - 34^0 33" 45' N and 106^0 48" 00' - 106^0 48" 30' W longitudes on the Veguita quadrangle map with scale of 1 : 24.000. The basin fill is exposed at the surface by down cutting of valleys rather than uplift of the basin center in Late Pleistocene (Lozinsky et al., 1991). The bluffs are 100 m high but I only studied the middle 30 m of exposures along 1. 3 km.

2.2 Basin-Filling History of the Albuquerque Basin

Sediments within the mapped area are composed of fluvial-alluvial-eolian deposits (Davis, 1990,1993; Lohmann, 1992), which comprise the upper part of Sierra Ladrones Formation. Fluvial deposits are distributed by three major rivers, Rio Puerco, Rio Grande and Rio San Jose. The Rio Grande is the largest perennial river to traverse the Bosque site. The ancestral Rio Grande had braided character in the Albuquerque basin (Lozinsky, 1988). Both Rio Puerco and Rio San Jose were sometimes braided rivers (Stephens et al., 1988) flowed to the east, coalesced and fed the Rio Grande.

The Sierra Ladrones and Popatosa Formations are units that filled the Albuquerque Basin and form Santa Fe Group (Table 2.1). From Late Oligocene (30 Ma) until Late Miocene (5 Ma), the Albuquerque Basin formed by rifting in two major episodes (Chapin and Seager, 1975; Seager et al., 1984). The Popatosa Formation is the first deposit that accumulates in the basin during that time. This formation was deposited in a closed basin system.

Figure 2.1 Stratigraphic relationship of Popatosa and Sierra Ladrones Formations that form the Santa Fe Group (Lozinsky, 1991). Units 1 to 3 are specific to the Gabaldon badlands.

Lithologic unit			Age
Santa Fe Group	Sierra Ladrones Formation		Pleistocene / Pliocene
Santa Fe Group	Popotosa Formation	unit 3	Miocene
Santa Fe Group	Popotosa Formation	unit 2	Miocene
Santa Fe Group	Popotosa Formation	unit 1	Miocene
unit of Isleta #2 well			Oligocene
Baca Formation			Eocene

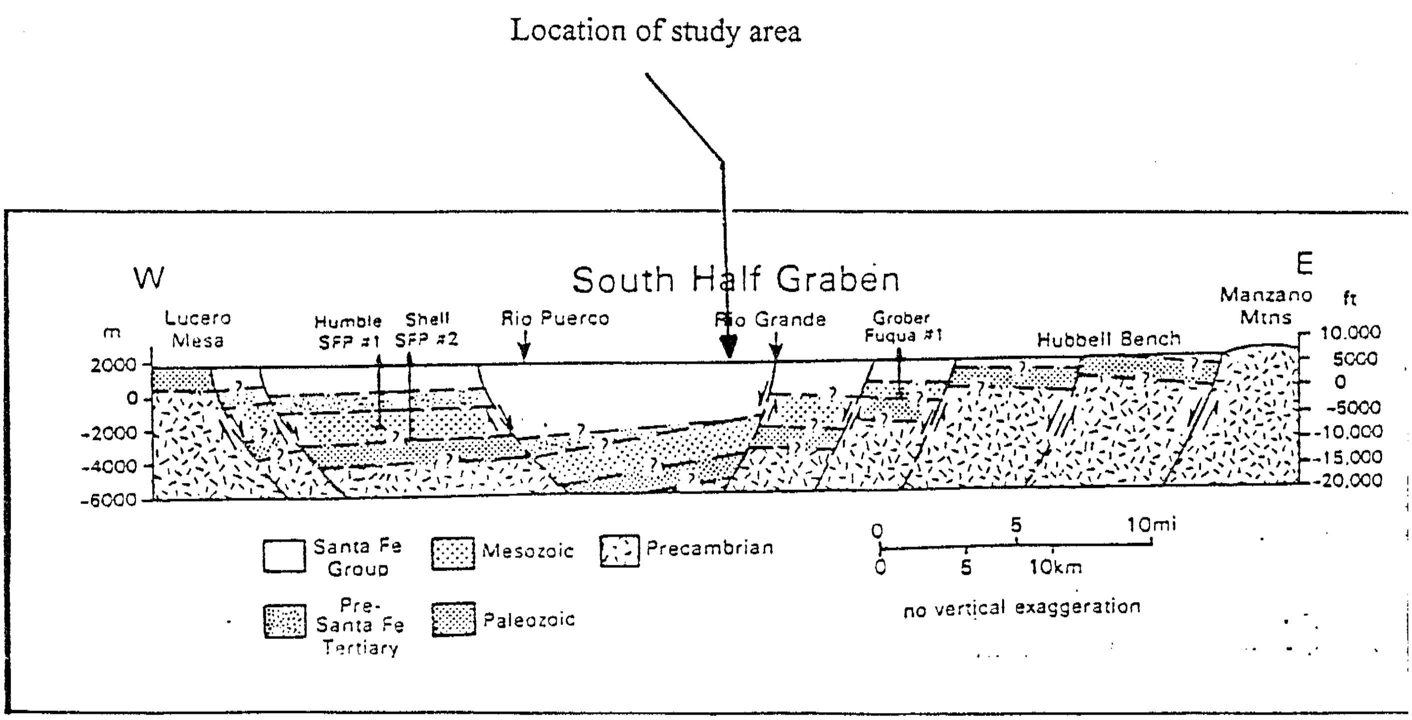

Figure 2.2. Position of field area in the South Albuquerque Basin half-graben systems (Lozinsky, 1988)

Sierra Ladrones Formation, on the other hand, began to be deposited when the Rio Grande flowed across the basin and deposited sediment on top of the basin floor facies of the Popatosa Formation (Lozinsky et al., 1991).

Based on outcrop and borehole analysis, there are three primary depositional facies which are: basin-margin alluvial fans, eolian facies, and playa facies at the center of the basin (Lozinsky, 1988). During Pliocene-Pleistocene time, alluvial - fluvial - eolian depositional facies of Sierra Ladrones Formation aggraded in the Albuquerque Basin. The Popatosa and Sierra Ladrones Formation are separated by a distinctive boundary of fluvial deposits along the axis of the basin. The sediments are now inclined about 1-2 m per 1 km southward. The aggradational system in Bosque site is dominated by several vertical sequences of fluvial-alluvial-eolian deposits and pedogenic overprints.

2.3 Previous Workers of the Upper Sierra Ladrones Formation

The Bosque site has been studied by Lohmann (1992), Gotkowitz (1993) and Davis, (1990; 1993). Their studies emphasized heterogeneity of the aquifer for hydrologic importance. Young et al. (1982) and Lozinsky et al. (1988; 1991) studied the Sierra Ladrones Formation. Although their area was not in my study area, they contributed valuable information. Young et al. (1982) determined that the pebbles along the Llano de Albuquerque escarpment were derived from three main rivers : Rio Grande, Rio Puerco, and Rio San Jose. Lozinsky et al. (1988 and 1991) described the general depositional system of the Albuquerque basin where sedimentation and rifting took place (Figure 2.2 and 2.3). Harris (1991) did point counts on coarse sand grains from three major distributary rivers, Rio Grande, Rio Puerco, and Rio San Jose as well as deposits from the Bosque site. Davis (1990,1993) separated the deposits within the Bosque site into seventeen elements. Lohmann (1992) described similar deposits by using

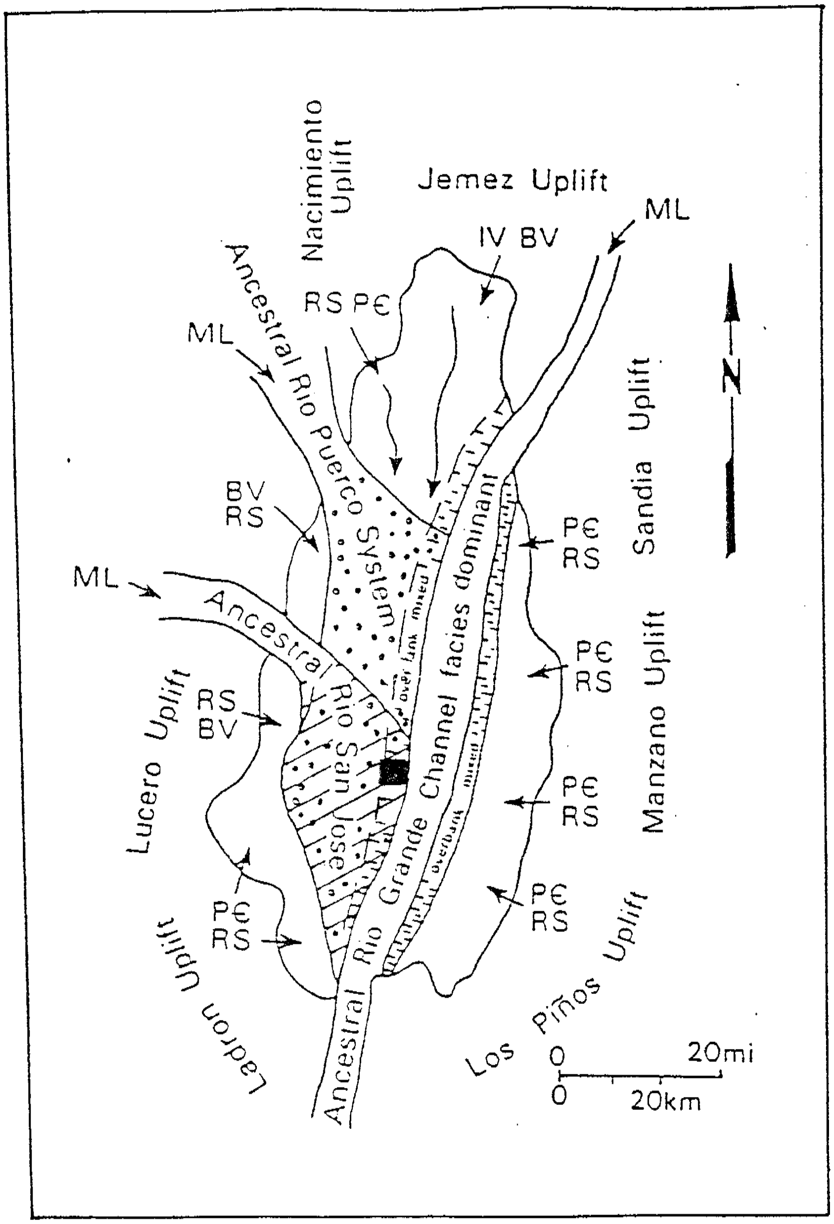

Figure 2.2 Hypothetical geometry of Albuquerque Basin during deposition of upper Sierra Ladrones Formation (Lozinsky, 1988) Arrows indicate source areas and clast types derived rom those areas. PЄ = Precambrian, RS= Reworked sedimentary rocks, IV=intermediate volcanic rocks, BV=mafic volcanic rocks, ML=mixed lithologies, Approximate location of Bosque site is shown by black circle.

Davis' classification but he grouped the seventeen facies into four groups , CH I, CH II, OF and Paleosols. Both Davis (1990, 1993 and Lohmann (1992) utilized Miall's (1985,1988) architectural element model (AEM; see Table 2.1). Facies presented in Table 2.1 basically are similar to the lithofacies in my study area, such as Gm, Gt, and Gms are the similar to Gs lithofacies in my classification; St, Sfl are similar with Ss1; Smb, Sr are similar to Ss2; Sl and Sm are similar to Ss3. Fr, Fm, Fsc are similar to paleosols lithofacies (P); Fr,Fm,Fsc and P are similar to ISS lithofacies. However, not all of the Davis' classification are found in my study area. Some of them are probably continuous or pinch-out. Therefore, I utilized different lithofacies with different symbol too

Chapin and Cather (1995) determined the boundary between Popatosa Formation and Sierra Ladrones Formation as the onset of the through flowing ancestral Rio Grande. Mozley, (1995, in revision) discusses the paleocurrents of Upper Sierra Ladrones Formation based on distribution of the concretions within the Bosque site.

Table 2.1. Comparison of facies grouping for definition of Architectural Elements at Bosque Site (Mulyadi, 1995; Lohmann, 1992; modification from Davis 1990).

Facies Present (Mulyadi, 1995)	Facies Present (Lohman, 1992)	Description / Comments
Gs, Ss1, Ss2	Gm,Gt,Sp,St,Sl,Sgm (CH-1)	Channel element consists dominantly gravelly and coarse sand facies
Ss1, Ss2	Gms,St,Sp,Sfl,Sh,Sl,Smb, Fl,Fm,Fsc (CH-2)	Sand and sand-sized clay clasts dominate with local lag gravel deposits
Ss3, Ss4 P	--- P,Sm,Fsc (P)	Eolian deposits Soil and Stacked Soils
ISS	Fr,Fm,Fsc,P (OF)	Overbank fines

CHAPTER 3 METHODOLOGY

As an extension of Lohmann's (1992), Davis' (1993) and Gotkowitz' (1993) field work, this study will also quantify the geologic features near Bosque, New Mexico, with the following methodology: i) lithofacies description and lateral mapping of geologic deposits , ii) measuring the permeability of individual coarse facies, iii) relate the observed sedimentary structures to depositional environment, iv) correlate the measured vertical sections to obtain a 2-D horizontal lithofacies distribution, and v) relate the depositional system to the permeability distribution. These last two are approached in the discussion section.

3.1 Lithofacies Description and Lateral Mapping

Consecutive vertical sections were measured and described using a jacob staff, shovel and 100 m tape. Even with ten vertical sections over 1.3 km of outcrop the depositional facies could not be correlated from section to section, therefore, horizontal tracing between the sections was done by walking to define the boundary geometry of each lithofacies.

Sections were located on a topographic base map (Veguita 7.5 minute quadrangle map). Areal photographs were also used for morphologic description and location of the outcrops. Three sections were done in 1993, and the rest finished during summer, 1994.

Based on the vertical sections, I classify the deposits into four lithofacies. Lithofacies and geometric description such as thickness, lateral distribution, and cross-sectional shapes of the deposits were determined during measuring sections. An "Apple Core" computer program was used after field data were collected for producing better plots of the vertical sections.

3.2 Permeability Measurement

A mini-airpermeameter (Davis et al., 1994) was used to obtain permeability values. This method is well-suited to obtaining in situ measurements on outcrops of dry sediment. First, I selected the permeable deposits such as sands and gravels, because the mini-airpermeameter cannot be applied to deposits of silt and clay due to their sizes. Before applying the mini-airpermeameter I cleaned a vertical surface and let the exposure dry for several days. The measurements were taken by putting the tip of the mini-air-permeameter directly to the outcrop surface. The permeameter measures the amount of time it takes to blow a volume of air into the outcrop. The value that I obtained was time (in seconds) , so to convert these values to obtain real permeability I used the formula (from Davis et al., 1994) :

$$k = \frac{2 \mu q P_1}{a\, G_o\, (b_D)\, (P_1^2 - P_o^2)}$$

Where k = permeability [m^2]; μ = viscosity of air [Pa s]; q = volumetric flow rate [m^3/s]; P1 = pressure applied tip seal / outcrop interface [Pa]; a radius of tip seal orifice [m]; Go= geometric factor [dimesionless]; b_D = dimensionless tip seal radius (b/a) [dimensionless]; b = outer radius of tip seal [m]; and a = inner radius of tip seal [m].

All values except k and q are not known but the time is known, thus, q can be calculated and k can also be ultimately known. An example of calibration is shown in appendix IV.

3.3 Relation Between Sedimentary Structures and Depositional Environment

Sedimentary structures provide information about depositional mechanisms. From the depositional mechanisms, lateral distribution, and vertical sequence we can interpret the appropriate sedimentary environment. However, some of the structures are not obvious. They might be obliterated by soil development or they might be locally absent, or they might be similar in many environments. For example, ripple stratification may form in fluvial and eolian environments. Therefore, instead of just comparing the orientation and geometry of sedimentary structures, vertical and lateral relationships are also applied to interpret an appropriate depositional environment (Table 3.1, 3.2 and 3.3)

The most common sedimentary structures in sandy gravel deposits at the Bosque site are (1) pebble imbrication, which is comprised of various orientations depending on depositional environment; (2) cross bedding, which is also has variety forms depending on depositional environment, such as: channel fill cross bedding, sand dunes cross bedding, micro delta cross bedding; (3) parallel lamination and (4) scour.

Table 3.1 Basic types of stratifications and mecanisms in eolian deposits (Hunter, 1977)

Depositional process	Character of depositional surface	Type of stratification	Dip angle	Thickness of strata Sharpness of contacts	Segregation of grain types Size grading	Packing	Form of strata
Tractional deposition	Rippled	Subcritically climbing translatent stratification	Stratification: low (typically 0°–20°, maximum ~30°) Depositional surfaces: similarly low	Thin (typically 1–10 mm, maximum ~5 cm) Sharp, erosional	Distinct Inverse	Close	Tabular, planar
		Supercritically climbing translatent stratification	Stratification: variable (0°–90°) Depositional surfaces: intermed. (10°–25°)	Intermediate (typically 5–15 mm) Gradational	Distinct Inverse except in contact zones	Close	Tabular, commonly curved
		Ripple-foreset cross-lamination	Relative to translatent stratification: intermed. (5°–20°)	Individual laminae: thin (typically 1–3 mm) Sharp or gradational, nonerosional		Close	Tabular, concave-up or sigmoidal
		Rippleform lamination	Generalized: intermed. (typically 10°–25°)		Individual laminae and sets of laminae: indistinct Normal and inverse, neither greatly predominating	Close	Very tabular, wavy
	Smooth	Plane-bed lamination	Low (typically 0°–15° max.?)	Sets of laminae: intermediate (typically 1–10 cm) Sharp or gradational, nonerosional		Close	Very tabular, planar
Largely grainfall deposition	Smooth	Grainfall lamination	Intermed. (typically 20°–30°, min. 0°, max. ~40°)			Intermediate	Very tabular, follows preexistent topography
Grainflow deposition	Marked by avalanches	Sandflow cross-stratification	High (angle of repose) (typically 28°–34°)	Thick (typically 2–5 cm) Sharp, erosional or nonerosional	Distinct to indistinct Inverse except near toe	Open	Cone-shaped, tongue-shaped, or roughly tabular

Table 3.2 Facies and charateristic structures of fluvial (Braided rivers; Mial, A. D., 1977)

	Facies identifier	Lithofacies	Sedimentary structures	Interpretation
Gravel	Gm	Gravel, massive or crudely bedded; minor sand, silt, or clay lenses	Ripple marks, cross-strata in sand units, gravel imbrication	Longitudinal bars, channel-lag deposits
	Gt	Gravel, stratified	Broad, shallow trough cross-strata, imbrication	Minor channel fills
	Gp	Gravel, stratified	Planar cross-strata	Linguoid bars or deltaic growths from older bar remnants
Sand	St	Sand, medium to very coarse; may be pebbly	Solitary or grouped cross-strata	Dunes (lower-flow regime)
	Sp	Sand, medium to very coarse; may be pebbly	Solitary or grouped planar cross-strata	Linguoid bars, sand waves (upper- and lower-flow regimes)
	Sr	Sand, very fine to coarse	Ripple marks of all types, including climbing ripples	Ripples (lower-flow regime)
	Sh	Sand, very fine to very coarse; may be pebbly	Horizontal lamination, parting or streaming lineation	Planar bed flows (lower- and upper-flow regimes)
	Ss	Sand, fine to coarse; may be pebbly	Broad, shallow scours (including cross-stratification)	Minor channels or scour hollows
	Fl	Sand (very fine), silt, mud, interbedded	Ripple marks, undulatory bedding, bioturbation, plant rootlets, caliche	Deposits of waning floods, overbank deposits
Mud	Fm	Mud, silt	Rootlets, desiccation cracks	Drape deposits formed in pools of standing water

Source: Miall, A. D., 1977, A review of the braided-river depositional environment: Earth Science Rev., v. 13, Table III, p. 20, reprinted by permission of Elsevier Science Publishers, Amsterdam.

Table 3.3 Classification of common primary sedimentary structures (Sam Boggs, JR., 1995)

MORPHOLOGICAL CLASSIFICATION \ GENETIC CLASSIFICATION	Depositional structures: Suspension-settling and current- and wave-formed structures	Depositional structures: Wind-formed structures	Depositional structures: Chemically and biochemically precipitated structures	Erosional structures: Scour marks	Erosional structures: Tool marks	Deformation structures: Slump structures	Deformation structures: Load and founder structures	Deformation structures: Injection (fluidization) structures	Deformation structures: Fluid-escape structures	Deformation structures: Desiccation structures	Deformation structures: Impact structures (rain, hail, spray)	Biogenic structures: Bioturbation structures	Biogenic structures: Biostratification structures
STRATIFICATION AND BED-FORMS													
Bedding and lamination													
Laminated bedding	X	X	X										
Graded bedding	X											X	
Massive (structureless) bedding	X											X	
Bedforms													
Ripples	X	X											
Dunes	X	X											
Antidunes	X												
Cross-lamination													
Cross-bedding	X	X											
Ripple cross-lamination	X	X											
Flaser and lenticular bedding	X												
Hummocky cross-bedding	X												
Irregular stratification													
Convolute bedding and lamination							X						
Flame structures							X						
Ball and pillow structures							X						
Synsedimentary folds and faults						X							
Dish and pillar* structures									X				
Channels				X									
Scour-and-fill structures				X									
Mottled bedding												X	
Stromatolites													X
BEDDING-PLANE MARKINGS													
Groove casts: striations: bounce, brush, prod, and roll marks					X								
Flute casts				X									
Parting lineation	X												
Load casts							X						
Tracks, trails, burrows†												X	
Mudcracks and syneresis cracks										X			
Pits and small impressions											X		
Rill and swash marks	X												
OTHER STRUCTURES													
Sedimentary sills and dikes								X					

*Not wholly stratification structures †Not wholly bedding-plane markings

Chapter 4 GEOLOGICAL RESULTS

4.1 Lithofacies Description

Sediments in my study area can be divided into four facies : gravelly sands (Gs), sands and sandstone (Ss1, Ss2, Ss3, and Ss4), interbedded sand-silt-clay (ISS), and paleosols (P). These lithofacies are distinguished from one to another by the color, texture and lateral and vertical geometry (Figure 4.1). Each lithofacies may be repeated in some sections, or may not even exist in one section. Detailed description of each vertical section is given in appendix I. Measurement of each section began in lower gravelly sands (Gs). Two datums were used to tie sections together. First, for sections 1 to 6, the datum is the basal upper gravelly sands (known as "lower Fred"). Second, for the sections 6 to 10, the datum is the base of the slabby sands, where present at the middle of the section.

4.1.1 Gravelly Sands (Gs)

The studied section is restricted by two gravelly sands that occupy the base and the top of the mapped units. Both of them are commonly well cemented by calcite. These gravelly sands are light to medium gray, poorly sorted, traceable throughout the study area from north to south, and have variable thickness across the outcrop from 0.6 to more than 2.4 m. Sedimentary structures such as imbrication, scour, cross-bedding, and irregular graded bedding are well preserved in these beds (Figure 4.2, 4.3). Mud-balls within the gravelly sands range from 2 to 50 cm in diameter . Figure 4.2 shows the lower gravelly sands containing pebbles and cobbles that fine upward. These beds are highly resistant to erosion. In some sections, the upper boundary of these gravels is irregular; and in other sections the gravels are graded. The lower boundary is commonly scoured.

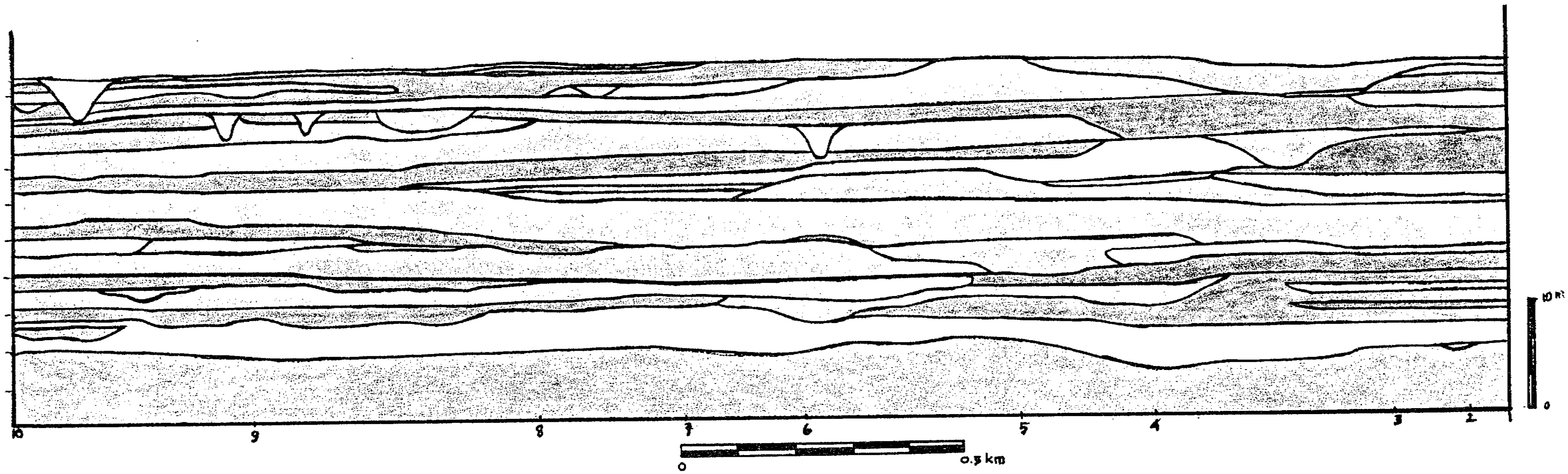

O = Gravelly sands

O = Sandstones type 1

O = Sandstones type 2

O= Sandstones type 3

O= Sandstones type 4

O= Interbedded sand-silt-clay

O= Sandy clay and clay Paleosols

Figure 4.1 General lithofacies sequences of my study area. They consist of four lithofacies that are present in my study area.

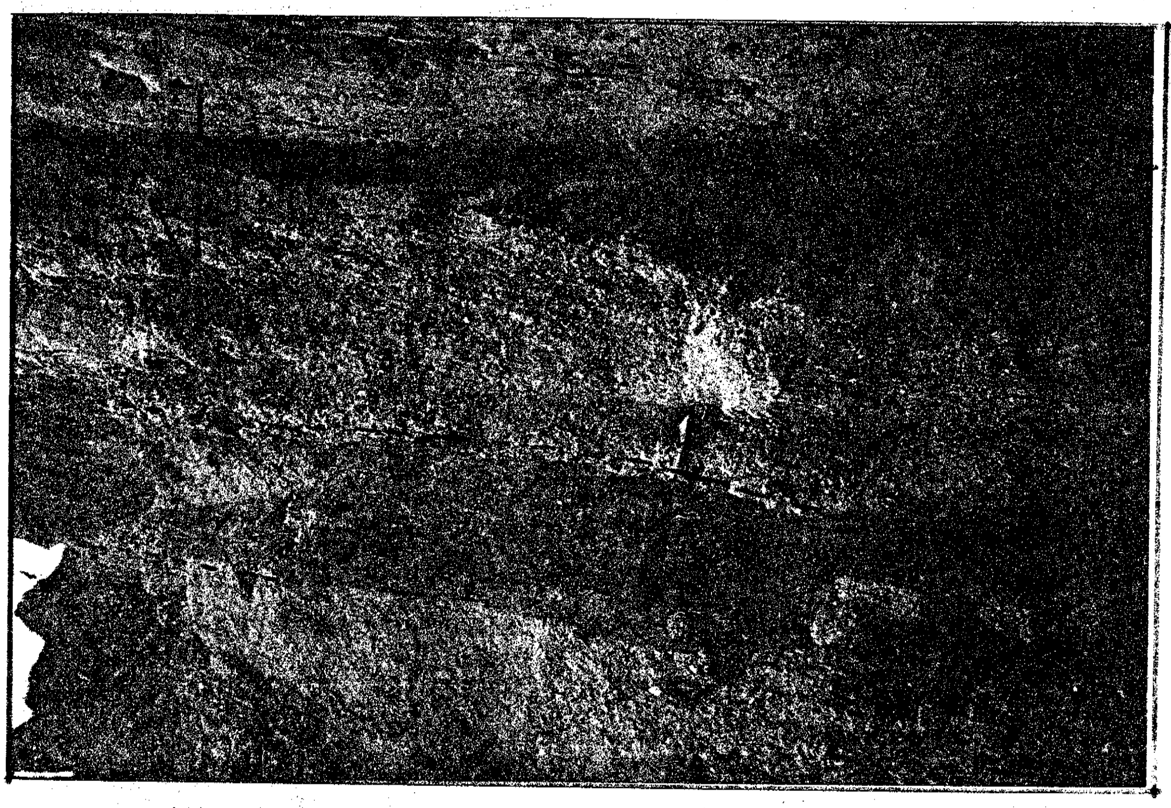

Figure 4.2. This figure shows several sets of fining upward of cemented cross bedded gravelly sands (Gs) and white calcite coatings around the grains in the lower gravelly sand . Lower boundary shows the mud balls with size range 2-10 cm. Scoured structures are obvious at the lower boundary. The upper boundary is flat and sometimes laminated. Location is between sections 3 - 4.

Figure 4.3. This figure shows two sets fining upward of lower cemented gravelly sand that consists of mud-balls and imbrication structures. A) first set, B) second set. This imbrication shows the flow direction is to S15E to S 35E. Location is between section 2 and 3.

Figure 4.3 shows well preserved mud-balls and pebble imbrication in lower gravelly sands. General paleoflow from this imbrication is S 15 E to S 35 E. These sands are 1 - 1.5 m thick. In general these beds fine upward. The bottom gravelly sands overlie cemented coarse-grained sandstone at some places. At other places, bottom gravelly sands are interbedded with light gray, coarse, medium sorted, and orange, lower medium, well sorted sands. The top gravelly sands commonly overlie interbedded sand-silt-clay units and are continuous laterally to the south.

In the middle of some local sections (sections 2, 8), similar light gray, poorly sorted gravelly sands fine upward, but are thinner (60cm-90cm), structureless, not continuous, and not well cemented. The general appearance of these units is similar to the previous gravels with an undulous lower boundary and gentle slope (Figure 4.4). These layers are considered as the same as the bottom gravelly sands, as we called "lower Fred"

Outcrop morphology of the upper and lower gravelly sands is steep to cliffy and remains largely the same laterally across the study area. In the middle of the map area the upper gravelly sands are less cemented. The local gravelly sands have a gentle slope due to non resistance to erosion.

4.1.2 Sandstones (Ss)

In my study area, there are four types of sandstones. Three of them have a light gray - tan color (10 YR 6/4). Generally, they are differentiated by texture and geometry. The fourth one is characterized by its orange-reddish color (5YR 6/6) and is described in more detail later in paleosols lithofacies. In most of the sections these types of sandstone beds are repeated, but these units are bordered by other types of sandstones, interbedded sand-silt-clay, or paleosol.

Type 1 sandstones (Ss1) are commonly continuous laterally across the outcrops and lie above gravelly sands (Gs) (Figure 4.5). Other type 1 sandstones also present as channels. Sedimentary structures in this typical lithofacies are not obvious. These beds are

Figure 4.4. This figure shows uncemented gravelly sands (Gs). This layer pinches out to the left. Morphology of this bed is flat-undulous at the base and nearly flat at the top. Location along section 2.

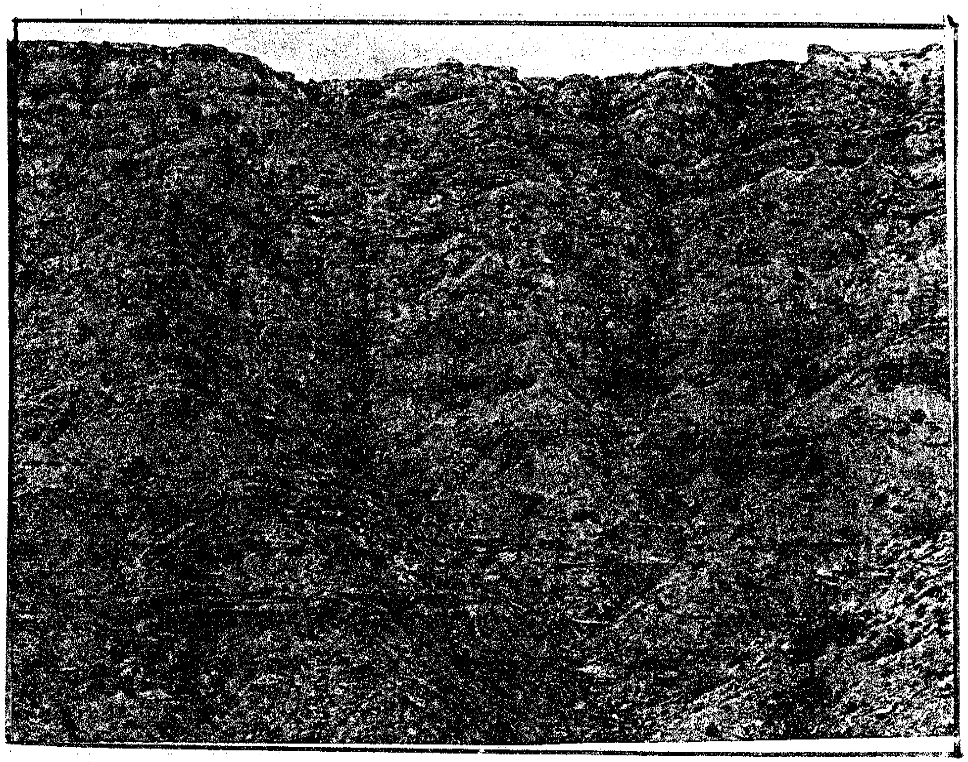

Figure 4.5 This figure shows type 1 (Ss1) of uncemented sandstone. This sandstone commonly overlies the gravelly sands with gentle slope. The same typical sandstone is repeated above this layer discontinuously. Location is in section 8.

easily distinguished by gentle slope, tan-gray color, and loose lower medium to upper coarse grained sands. Some places these beds are cemented by calcite as shown by concretions. A few pebbles commonly exist in these beds. The thickness ranges from 0.60 m to 2.25 m. The boundaries some of these beds are commonly undulous and graded at the base and irregular at the top. Some of them have scoured at the base.

Type 2 sandstones (Ss2) look similar to type 1, because they are light gray - tan. Type 2 sandstones are lighter gray color, and are thicker and finer grained (Figure 4.6). Most of the type 2 sands occupy the middle of the measured sections. These beds are not continuous laterally throughout the mapped area, but they are traceable for a few hundred m. These beds are also repeated vertically. A few thin carbonate nodules exist in some local sections of these beds. Type 2 sandstones are distinguished from type 1 by very well cemented into tabular bodies and preserve low angle trough cross-bedding, horizontal lamination, cracks, and insects holes (Figure 4.7). The upper and lower boundaries for these beds are mostly irregular. Thickness varies from 30-60 cm. The type 2 sandstones form a continuous slabby sands from section 6 to section 10 in the middle of the section. Therefore, this typical sandstone is used as a base of the datum for section 6 to 10.

Type 3 sandstones (Ss3) are orange in color (5YR 6/6). In my mapped section, there are 3 or more layers of these beds (Figure 4.9). These beds are easily distinguished by their color from a distance. Some of them are not continuous, but at least one is continuous across the mapped area. The thickness of orange sandstones that are not continuous ranges approximately from 0.3 to 2 m. Type 3 sandstones also consist of uniform grain size from upper fine to lower medium sand. Carbonate nodules is another typical secondary structures that are also common in some of the local sections of type 3 sandstones. These sandstones are partially cemented, form steep slopes and locally have poorly preserved tangential cross bedding over several meters in their lower parts. These sands will be further discussed with paleosols lithofacies.

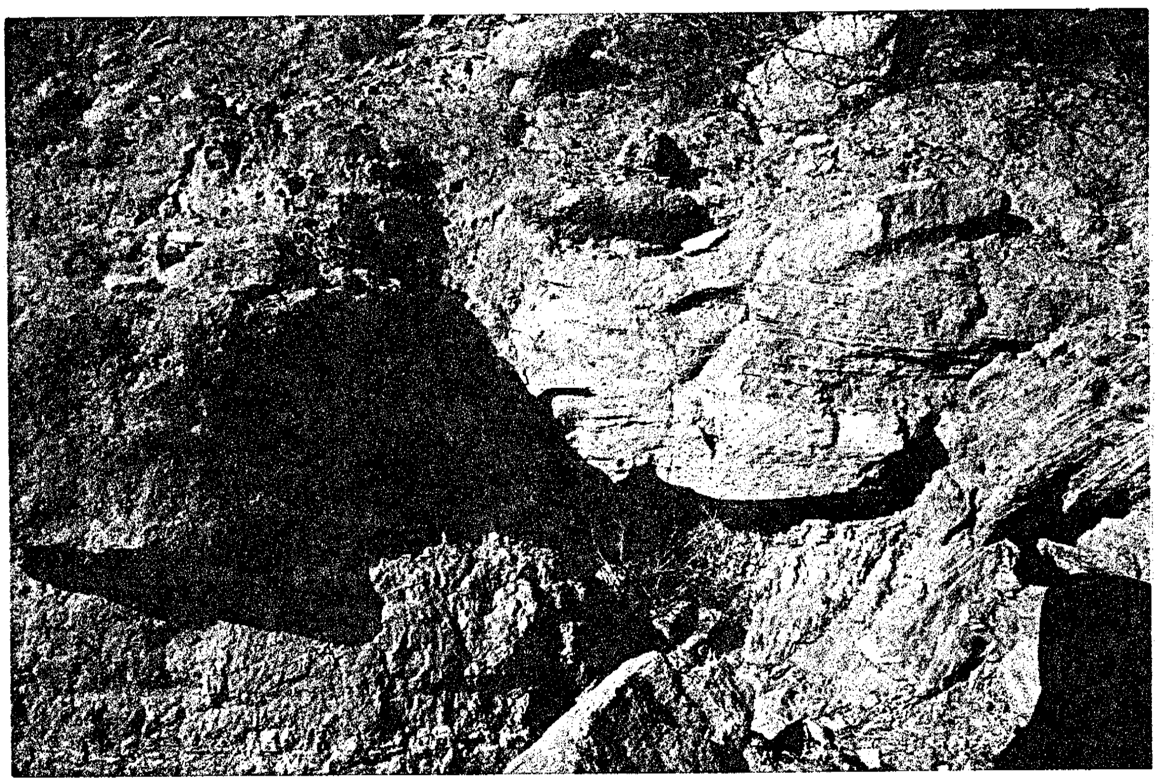

Figure 4.6. This figure shows type 2 (Ss2) of cemented sandstone lithofacies with undulous at lower boundary, low angle cross-bedding, and hammer as a scale. Location is in between sections 2 and 3

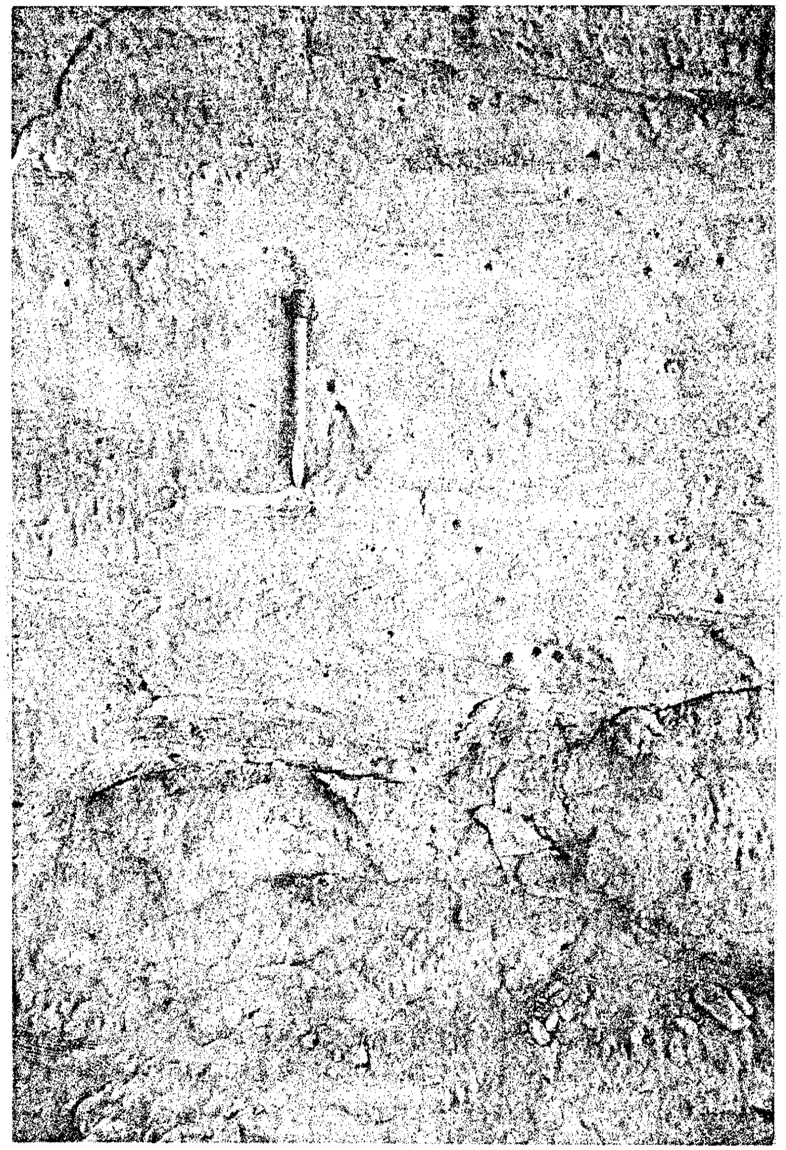

Figure 4.7. This figure shows another sandstone type 2 (Ss2) with trough and ripple cross-bedding, and modern insect holes. Carbonate nodules are scattered throughout. Location is in between section 2 and 3.

Figure 4.8. This figure shows sandstones type 2 (Ss2) with horizontal lamination, climbing ripples, and burrows. In the middle of the section is a 2-3 cm thick unit with horizontal lamination. A scoured brown clay drape overlies this bed. Location is in between section 1 and 2.

A)

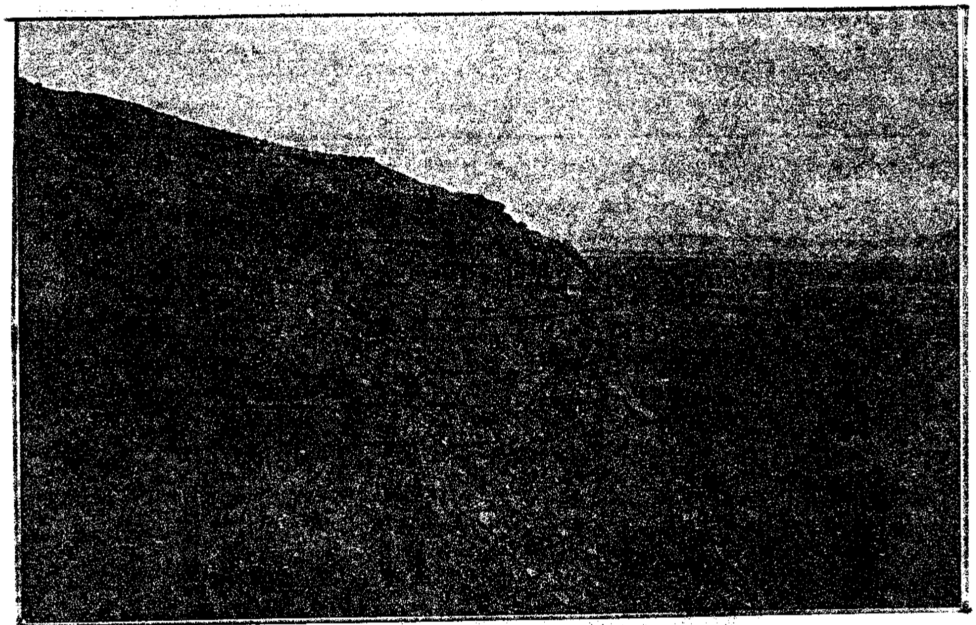

B)

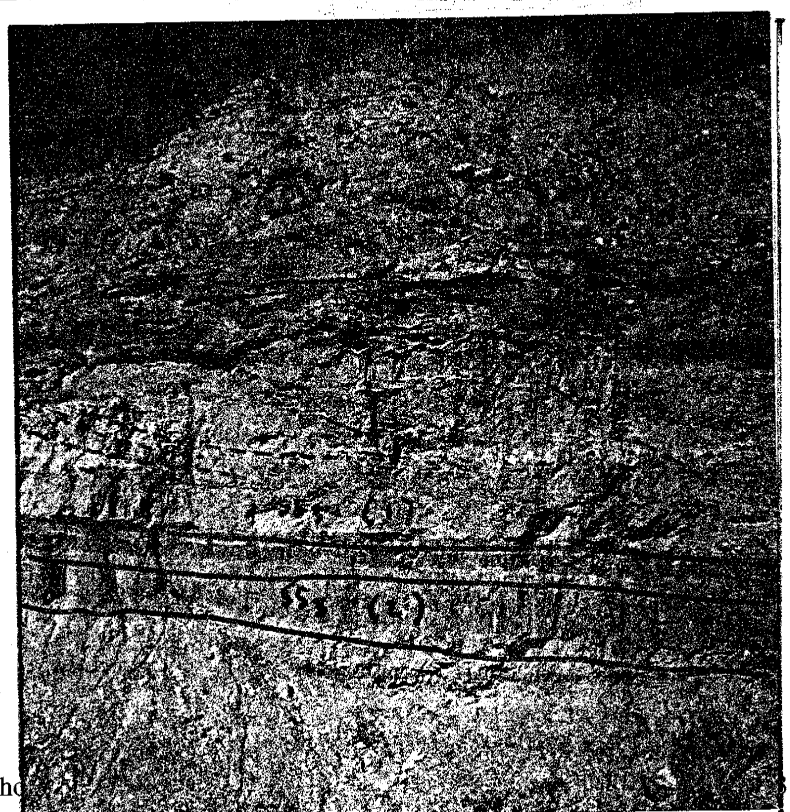

Figure 4.9. **A**. Sh (Ss3) lithofacies (Above). The intervening beds are sandy clay (Paleosols=P), interbedded sand-silt-clay (ISS) . Location is in between sections 9 and 10. **B**. Shows two beds (1 and 2) of well cemented orange sandstones (Ss3) and an intervening paleosol (P). Orange sandstone 2 has faint large dimension tangential cross-bedding that indicates eolian deposition. Location is in between sections 3 and 4.

Morphology of these units are commonly are steep to cliffy such as section 1 to 4 and section 7 to 10.

Type 4 sandstone (Ss4) is characterized by light gray to tan color and upper fine to lower medium sands. These beds are not laterally continuous; for example, the thickest part of one unit in section 3 becomes thinner toward the south and north and pinches out near section 5. Horizontal lamination is the most common sedimentary structure in these beds. Climbing-ripple and low angle trough cross bedding are present only in local sections (Figure 4.8). In some sections sedimentary structures are not obvious. The thickness ranges from 0.2 m to 1.8 m. The upper and lower boundaries of these units are also irregular. Similar beds are also repeated vertically in some local sections (e.g. Section 6).

4.1.3 Interbedded sand-silt-clay (ISS)

Interbedded sand-silt-clay units are composed of dark brown clay, light gray to tan sand and tan silt with clay. These beds have variable total thickness from 0.45 to 2.7 m, in layers generally a few cm thick. The units occupy the top of sections (underlie gravelly sands) and the lower part of the section (above the type 2 sands). The ratio of sand-silt-clay thickness is variable. Most of the sections show the ratio of sand-silt-clay ranges from 4:1:3 to 5:1:2. Sands commonly are only 30 - 80 cm thick. Carbonate nodules commonly overlie the clay layers. Reddish-dark brown clay commonly underlies the lower part of these beds. In section 2 (Appendix II), the sand units are thicker and well cemented, but clay-silt units become thinner toward section 3. Between sections 4 and 5, the clay ratio increases and clay layers become darker (Figure 4.10).

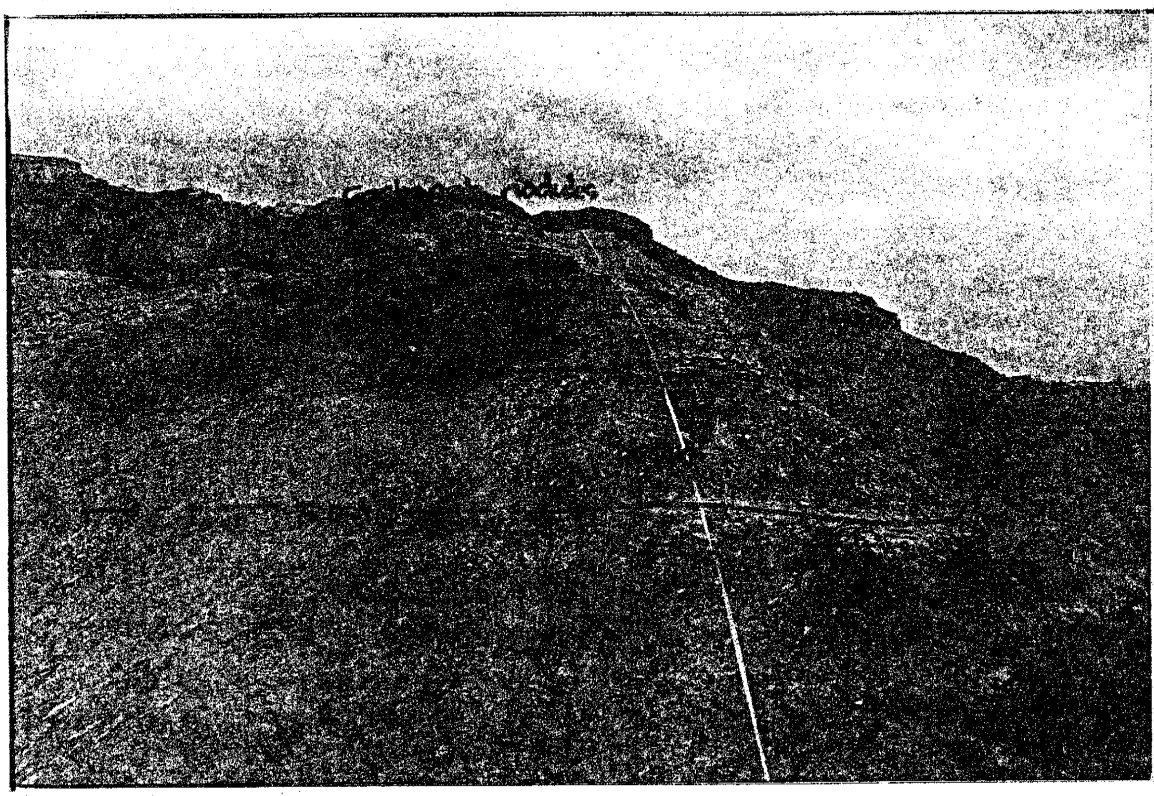

Figure 4.10 This figure shows the two sets interbedded of sand-silt-clay lithofacies (1 and 2) overlying reddish-dark brown clay soil (P). Carbonate nodules overlie these beds. Thin horizontal laminations are common in the silt, boundary clay-silt and sand-silt. Location is in section 5 .

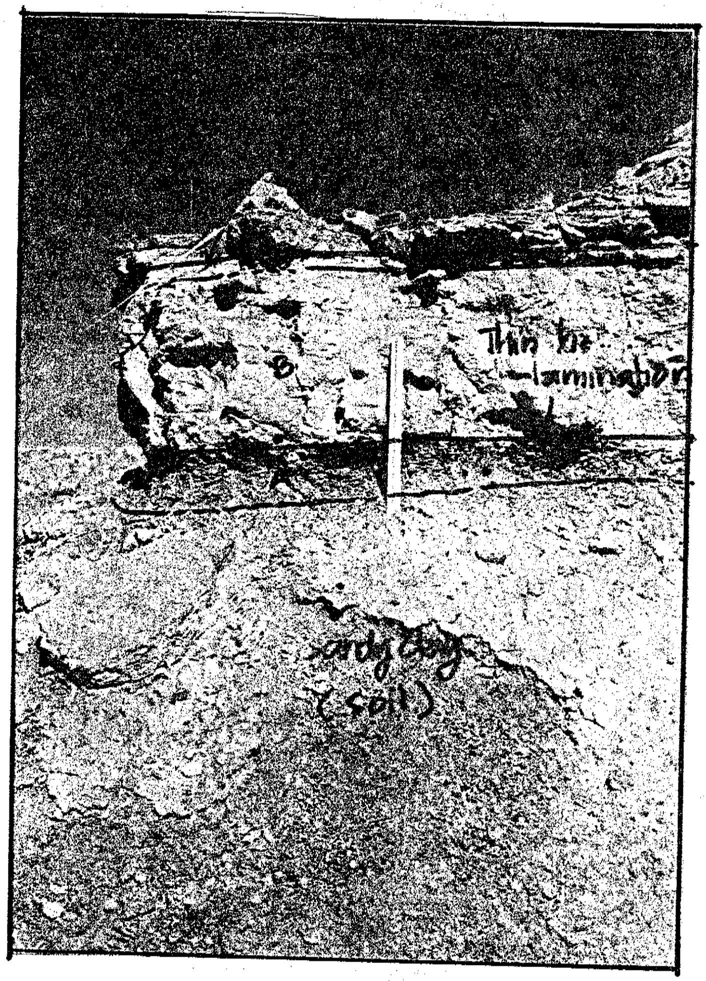

Figure 4.11. This figure shows 45 cm Interbedded sand-silt-clay lithofacies overlies the reddish-dark brown clay soil. A. A 10 cm thin horizontal lamination, B. A 32 cm laminated sand, and C. A 3 cm laminated silt.

Sedimentary structures such as thin horizontal lamination are common in between sandstone and silt, and clay and silt. Figure 4.11 shows the interbedded sand-silt-clay 45 cm thick. From the bottom, letter (A) indicates 10 cm dark brown clay with mud cracks and thin horizontal lamination. Letter (B) indicates a 30 cm tan churned sandy clay with horizontal lamination. Letter (C) is a 5 cm light tan well cemented sand-silt with thin horizontal lamination. Carbonate nodules are above the clay units.

4.1.4 Paleosols (P)

Paleosols are recognized by the absence of sedimentary structures, color, carbonate, and clay contents (Mack et al., 1993). Paleosols in the mapped area are comprised of two types: sand and clay paleosols. This section will briefly describe the soil lithofacies within the Bosque site.

Sandy paleosols appear as lower fine - upper medium sands, 0.9 - 3 meters thick, orange-red 5 YR 6/6 or 0.3-1.5 - meter thick dark brown clayey sand. Sedimentary structures are poorly preserved and/or not obvious. The geometry of these soils are tabular or lens-shaped. These soils are commonly underlain by loose gravels at the bottom and overlain by clay paleosol or by laminated sand-silt-clay.

Most of the orange sand paleosols are cemented. Carbonate nodules within these beds are not well formed and are present locally. The carbonate nodules are spherical-elongated and distributed tabular (plane-sheet shape). The length is approximately 3 to 10 cm. The diameter is approximately 1 to 5 cm.

Clay paleosols are primarily composed of light tan silt and dark brown clay (7.5 YR 3/3). These units are distinguished by carbonate nodules within the beds, and churned, darker, and structureless compared to laminated sand-silt-clay units. The carbonate nodules that commonly are present peripherally at the boundary of sandstones typical 2, 3, 4, and interbedded sand-silt-clay. In most sections, these units are recognized by their dark brown color and are continuous over hundreds of meters. In some places these beds are interbedded with silty clay, and have relict thin discontinuous horizontal lamination. These beds have gentle outcrop slope and commonly have more resistant sandstones at the bottom and the top. The thickness is variable from 0.3 - 1.6 meters. Original sedimentary structures are not obvious, and the clays have been churned (Figure 4.12).

Figure 4.12 . This figure shows churned clay with relict silty-clay horizontal lamination Elongated-spherical carbonate nodules are distributed peripherally at the boundary between sand and clay. Location : section 9.

4.1.5 Permeability Results

As previously described permeability calibration from field measurements is based on the formula given by Goggin et al., (1988; see Appendix IV herein for one example). Once variables within the formula have been established, permeability values are obtained by converting the "time" (Table 4.1) to darcies.

According to the Table 4.1, the highest permeability value is in gravely sands (Gs) with a mean permeability value of 49 darcies. The lowest permeability value from measurements is the interbedded sand-silt-clay (ISS) facies, which has mean permeability value of 17.5 darcies. However, the lowest permeability value should be paleosol lithofacies due to clay enrichment.

In permeable lithofacies, on the other hand, cementation is the main factor reducing the permeability value. The reduction is indicated by the difference permeability value at the same lithofacies. For example, the permeability values of Ss4 in section 6 ranges from 22.90-24.13 darcies, but permeability value of Ss4 in section 10 ranges from 22.69-25.75 darcies. These lithofacies in section 6 and 10 have similar characteristic but different physical condition such as consolidation.

Table 4.1 PERMEABILITY MEASUREMENT

Lithofacies (Units)	Time (Average) sec.	Grain size	Section	q 10^{-5}	v 10^{-3}	Ff	Fg	Pn	ΔP	P1	Permeability (k) [m2] 10^{-11}	[darcy]
1. Gravelly Sands (Gs)	2.88	very coarse -cob.	6	1.909	18.9	0.155	1.744	1464.8	108.447	1550.42	4.785	48.32
2. Sandstone Type (Ss2)	3.57	lower coarse-uc	6	1.541	15.25	0.1360	1.744	1514.17	77.903	1599.792	3.745	37.82
3. Sandstone Type (Ss4)	5.54	lower fine-upper med.	6	0.9928	9.828	0.1149	1.744	1581.46	32.40	1667.08	2.315	23.38
4. Sandstone Type (ISS)	7.43	lower fine-clay	6	0.7402	7.329	0.1083	1.744	1608.37	11.43	163.99	1.700	17.17
5. Sandstone Type (Ss4)	5.38	upper fine-lower med.	6	1.022	10.118	0.11586	1.744	1577.05	34.826	1662.67	2.389	24.13
6. Sandstone Type (Ss4)	5.65	upper fine-upper med.	6	0.9734	9.637	0.1143	1.744	1583.07	30.79	1668.69	2.268	22.90
7. Sandstone Type (Ss2)	3.33	lower coarse-upper coarse	6	1.651	16.35	0.1414	1.744	1500.10	87.03	1585.72	4.049	40.89
8. Gravelly sands (Gs)	2.75	very coarse-cob.	10	2	19.80	0.1607	1.744	1452.32	116	1537.94	5.058	51.08
9. Sandstone Type (Ss2)	3.65	lower coarse-upper coarse	10	1.507	14.92	0.1345	1.744	1518.98	75.081	1604.60	3.652	36.88
10. Sandstone Type (Ss4)	5.06	lower med.-upper med.	10	1.086	10.75	0.1179	1.744	1569.76	40.138	1655.82	2.550	25.75
11. Sandstone Type (Ss2)	4.07	lower coarse-upper coarse	10	1.351	13.37	0.127	1.744	1538.86	62.13	1624.60	3.2339	32.65
12. Sandstone Type (Ss4)	5.56	lower fine-lower med.	10	0.989	9.794	0.1148	1.744	1580.77	32.10	1666.39	2.308	23.31
13. Sandstone Type (Ss4)	5.70	upper fine-lower med.	10	0.965	9.55	0.1141	1.744	1583.78	30.08	1669.40	2.247	22.69
14. Sandstone Type (Ss2)	3.43	lower coarse-upper coarse	10	1.603	15.8	0.1386	1.744	1507.05	83.049	1592.67	3.914	39.53

CHAPTER 5 INTERPRETATION

5.1 Lithofacies distribution

In this chapter, lithofacies interpretation emphasizes energy of the transport and depositional media, source, and environment of deposition. Gravelly sands and sandstone lithofacies are the two main interests, because their permeability is measurable and they are the most common constituents within the study area. Sedimentary textures and structures are the best indicators of the depositional mechanisms and depositional environments (Table 5.1).

5.1.1 Gravelly sands (Gs)

Gravelly sands (Gs) that bound the bottom and the top of the section indicate the mapped area has had at least two episodes of high stream competence. Poorly sorted gravel to coarse sands and sandy matrix present in gravelly sands can be interpreted as being deposited under high flow velocity (lower flow regime) from bed load, which forms large scale cross bedding (Figure 5.1, 5.2 and 5.3).

As the stream power decreases, lower plane bed results. With decreasing stream power, only smaller grains can be transported. In this condition, ripple cross and / or planar lamination structures may be formed.

Figure 5.1 General fining upward of gravelly sands (Gs) units in my study area.

Sands
(with lamination)
Sands
(with ripples)

Gravelly sands
(with large scale cross bedding)

Table 5.1 Summary of common lithofacies at the Bosque, New Mexico.

Lithofacies	Units	Description	Sedimentary Structures	Paleocurrents
Gravelly sands (Gs)	Gravelly sands (Gs)	Light gray, very coarse sand-cobles, poorly sorted, well rounded, well cemented.	Imbrication, trough cross-bedding, hz. lamination, graded, scoured	S 15^0 E - S 35^0 E N/A
Sandstones (Ss)	Sandstone Type 1 (Ss-1)	Light gray, lower coarse-upper coarse sand with pebbles, well rounded, poorly sorted	Graded bedding	S 33^0 E - S 25^0 E
	Sandstone Type 2 (Ss-2)	Light gray-tan, upper medium-lower coarse sand, well rounded, med.sorted, cemented	Climbing ripples, low angle cross bedding, parallel lamiantion	S 29^0 E - S 25^0 E
	Sandstone Type 3 (Ss-3)	Light gray-tan, upper fine-upper medium sand, well rounded, well sorted, concretions	Sand sheet, low angle trough cross bedding, climbing riple	N/A
	Sandstone Type 4 (Ss-4)	Orange-reddish, upper fine-upper medium sand, well rounded,well sorted, med-well cemented, nodules	Relict tangential Cross-bedding	
Interbedded Sand-Silt-Clay (ISS)	Interbedded Sand-Silt-Clay (ISS)	Dark brown - tan - whitish, uper fine sand-clay, well sorted and well rounded for ss.	Thin hz. lamination	N/A
Paleosols (P)	Clayey Sands (P-1)	Brown - reddish, churned, mud balls	N/A	N/A
	Sandstone Type 4 (P2/Ss-4)	Orange-reddish, upper fine-lower medium sand,nodules	Local tangential cross-bedding	N/A
	Clay (P-3)	Light brown - dark brown, red, churned, draping, nodules	N/A	N/A

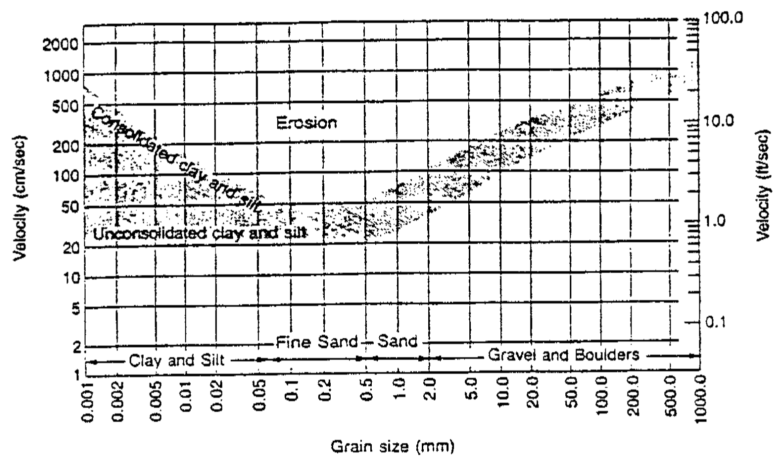

Figure 5.2. The Hjulstörm diagram, as modified by Sundborg, showing the critical current velocity required to move quartz grains on a plane bed at a water depth of 1 m. (After Sunborg, A., 1956, The River Klaräven, a study of fluvial processes: Geografiska Annaler, Ser. A, v. 38. Fig. 16, pp. 197).

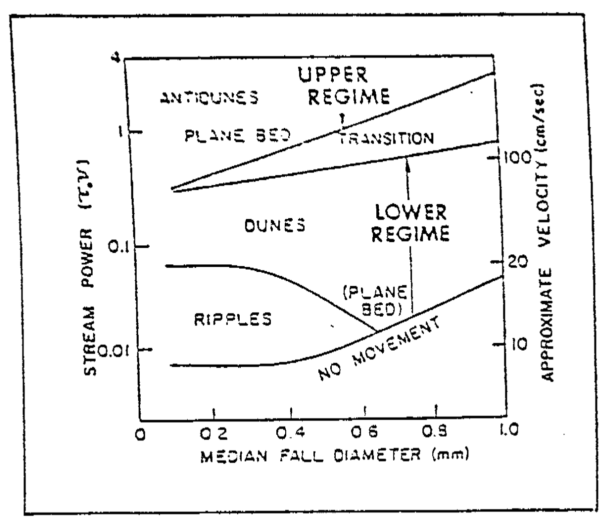

Figure 5.3. Relationship between stream power, median grain size, and bed form (From Simon, Richardson, and Nordin, 1965). Stream velocities shown at the right are approximate values for the grain size of 0.4 mm and extrapolated to 1 ft. flow depth.

The transition of gravelly sands at Bosque site to general thinning of the same gravelly sands toward the south, fining upward, plane and laminated at the upper boundary of these gravelly sands can be interpreted to show that the stream power decreases and/or decreasing the water depth toward south.

Thus, the general fining upward sequences of the gravelly sands without erosional surface between the bedforms is probably formed under waning flow in lower flow regime (Figure 5.3). The thicker gravelly sands at the center of my study area can be interpreted as local high energy flow and/or can be taken to mean flows of longer duration or short duration with high stream power condition.

Preserved imbrication and trough cross bedding in some gravelly sands shows that the paleocurrent depositing these beds trended southeast. They also indicate that these gravelly sands are derived northwest of my study area. Harris (1991, unpublished) also demonstrated that an ancestral Rio Puerco is the dominant source for the coarse Bosque sediments.

Based on the description above and geometry (in Figure 4.1), the consolidated gravelly sands are interpreted to have formed wide-spread braided channel systems. The streams moved back and forth , scoured, and reworked the previous deposits. According to the orientation of preserved imbrications, it is possible that the stream was the ancestral Rio Puerco (See Figure 2.2).

5.1.2 Sandstones (Ss)

Sandstones in the mapped area are comprised of four different kinds. Two of them are fluvial. Type 1 (Ss1) is characterized by lower fine - pebbly sands, medium sorted, rounded, with continuous and discontinuous horizontal lamination, graded bedding, and has no silt or clay. Position some of these beds above gravelly sands with graded bedding and thin horizontal laminations indicate that the energy of the stream decreased from gravelly sands to sandstones type 1. By relating vertically the graded boundary from these sandstones to the gravelly sands, it can be interpreted that the sands deposited with grade bedding within the same facies as gravelly sands in channel-fill deposits or channel-lag deposits as the discharge waned under lower-flow regime (Figure 5.3 and Table 3.2). Some Ss1 with undulous and scoured lower contact may be deposited under upper flow regime.

Sandstone type 2 (Ss2) is finer than sandstones type 1 and is characterized by light to dark gray, lower medium to upper coarse sandstone, well cemented, poor - medium sorted, with trough cross bedding, or ripple cross lamination. Some of these sandstone layers do not continue laterally, but form channels. Continuous layers commonly form tabular bodies. Based on the geometry and sedimentary structures, the type 2 sandstones can be interpreted as fluvial in origin. The type 2 sandstones formed as tabular bodies may be deposited on flood plains as crevasse splays under lower-flow regime. Sandstones type 2 with ripple cross laminations were deposited in narrow channels as a result of suspension load systems. Local sandstones type 2 that are isolated can be interpreted as arroyos because there is no fluvial systems during that time. However, they might also not as arroyos if the main fluvial systems are not located in the study area; they are still able to interpreted as crevasse splays. The source of type 2 beds is not known, because no petrology has been done, but trough cross beds suggest a northwesterly source. If the discharge decreases at the Bosque site through time, the source could be the same as that for the gravelly sands.

The other two uniform upper fine-lower medium, well sorted, light gray-tan, well rounded sands are distinguished from sandstones type 1 and 2 by , geometry, better sorting and some typical sedimentary structures. Type 3 sandstones are characterized by uniform grain size and faint large-dimension tangential cross bedding (vertically 6-8 m), which is typical of eolian deposits (Rubin and Hunter, 1984), that has been followed by carbonate cement. Sandstones type 3 (Ss3) has been altered to become soil. Soil development is characterized by orange - reddish (5 YR, 6/6) color, lack of sedimentary structures, distribution of carbonate nodules within the bed, peripheral along the boundary (Surdam et al., 1993), or along the tangential cross-bedding. This red color derived from goethite or hematite shows the products of weathering (Berner, 1971; Walker, 1971).

The type 4 sandstones (Ss4) look similar with sandstones type 3 (Ss3) in grain-size and sorting. They are distinguished by the color, in which sandstones type 3 is orange (see section between 5 and 6 in Figure 4.1), but type 4 is light gray to tan. Unlike sandstone type 3 with faint large-tangential cross bedding, sandstones type 4 have sedimentary structures such as low angle sand sheet and thin laminated structures. The lamination, climbing ripples structures can be formed either in fluvial or eolian deposits. In fluvial systems, lamination with upper fine-lower medium grain-sized may be formed under either lower or upper flow regimes (Figure 5.3). In upper flow regime, scoured lower boundaries are usually present. However, the lower contact of the type 3 and 4 sandstones are mostly flat. Therefore, these units could be fluvial lower flow regime. Climbing ripples are present in type 4 sandstones; cross bedding, on the other hand, is not present in type 4 sandstones. In eolian systems, climbing ripple structure can be formed in grainfall deposits on dunes (Fryberger et. al., 1979; Kocurek, 1981; Hunter, 1977; Rubin and Hunter, 1984; see Table 3.1). Similar well sorted beds and low angle sand sheets are interpreted to show wind velocity up to 1200 cm /sec (Fryberger et al., 1979). Some Ss4 are connected laterally to Ss3 and distributed as relatively tabular sheets with flat boundary to the underlain beds (see Figure 4.1; between section 5-6). Some of Ss3 and Ss4 are overlain by Ss1 and Ss2. Some Ss3 and Ss4 are overlain by interbedded sand-silt-clay and paleosols. Laterally, some of Ss3 and Ss4 change to Ss1,Ss2, ISS and paleosols. These vertical and lateral relationship may indicate the transition from fluvial to eolian. Although some sedimentary structures of these units are not unique to eolian origins, textures, stratigraphic relationships and geometries of type 3 and 4 sandstones can be used to interpreted that the type 3 and 4 sandstones are probably eolian deposits.

High permeability of these beds lets fluids (meteoric water) infiltrate and partially fill the pore space and then precipitate dissolved solids to produce concretions. In semiarid regions, atmospheric dust provides $CaCO_3$ to the soil which is remobilized by meteoric water (Gile et. al., 1981). Resulting calcite cements formed in the sediments, where vertical permeability is less than horizontal (Raiswell, 1971; Gluyas,1984).

The morphologies of concretions commonly follow the boundary of beds and have irregular elongated shapes. Organic matter and soil composition also influence calcite cement formation (Cerling, 1984; Quade, 1989; Pendall and Amundson, 1990; Mora et al., 1991).

5.1.3 Interbedded sand-silt-clay (ISS)

The interbedded sand-silt-clay can be interpreted as overbank deposits in a package of flood and fining upward deposits of wide-spread suspension load depositional systems (Davis, 1990, 1993; Lohmann, 1992; Gotkowitz, 1993). This interpretation is supported by the association of these lithofacies with sandstone type 2 (For example, see Figure 4.1; between section 5 and 6). This association shows that the sandstones type 2 may be fining upward to the overbank sediments and / or interfingering with overbank sediments, where overbank sediments are commonly deposited. I envision that this interbedded clay, silt, and sand are brought during large floods and settled as the discharge decreases. Horizontal lamination in silt-sands support decreasing intensity of discharge after large floods. Therefore, the possible depositional environment is overbank deposits.

5.2 Overall Depositional Sequences

General depositional sequences in the mapped area are similar to those mapped by Lohmann (1992) and Davis (1993), except the geometry of each differs locally. However, unlike the architectural elements that Lohmann (1992) and Davis (1993) used for describing the section, here I evaluate the section by lithofacies of the vertical sequences and lateral distribution of the deposits.

The stacking of each vertical section in my study area shows several sets of fining upward sequences (Gs-Ss-ISS-P). Generally my study area consists of 4 to 5 depositional sequences (Figure 5.4). Each sequence is commonly ended with soil at the top.

The first vertical sequence commonly consists of Gs-Ss1-Ss3-P-ISS-P, or Gs-Ss1-Ss3-P-Ss3-P. The second sequence is Ss2-Ss3-P-ISS-P, Ss2-ISS-P-ISS-P. The third sequences are dominated by fine-grained sands and clay such as, Ss4-ISS-Ss4-P, Ss2-Ss4-P-ISS-P, Ss2-Ss4-P1-ISS-Ss4-P. The fourth sequences are comprised of Ss4-ISS-Ss4-P, Ss1-ISS-Ss4-P, Ss2-Ss3-ISS-Ss4. The fifth sequence is similar to the fourth sequence, Ss4-ISS-P-Ss4-P, Ss4-ISS-P, but is thinner and discontinuous (see Figure 5.4 and Appendix II).

The whole sequence at the Bosque Site may be compared with Allen's (1974) facies models. Figure 5.5 shows the components of autocyclic and allocyclic depositional controls. Autocyclic controls on river movement are the results of changes in energy within the sedimentary basin, such as the results of channel avulsion, crevassing, and channel migration and cut-off. Allocyclic controls, on the other hand, originate in energy changes outside the sedimentary basin, such as shifts in the climatic and tectonic regimes. Changes in allocyclic controls result in overall changes in the discharge, load and slope of the stream.

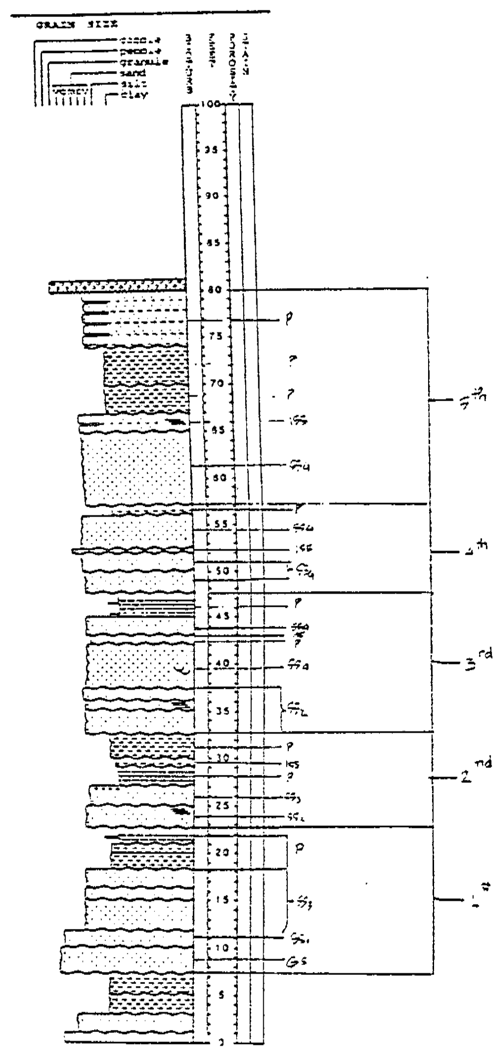

Figure 5.4 Graphical stacking of vertical sequences within my study area
(Numbers 1st , 2nd , 3rd , 4th and 5th indicate depositional sequences)

The first and fourth of Allen's six models are controlled by purely allocyclic factors, i.e. extreme climatic fluctuations (Figure 5.5). The second and third models are purely autocyclic, which are differentiated by the dominant of pattern of river movement

(Figure 5.6). The second and third models are differentiated by the amount of river avulsion as caused by lateral river movements and pedogenesis development. The third model develops more river avulsion and pedogenesis. The fifth and sixth models are controlled by both autocyclic and allocyclic factors. According to Figure 2.2, the study area is controlled by autocyclic deposition that is dominantly influenced by avulsion and channel migration of Rio Puerco or/and Rio San Jose. The channels migration and avulsion in study area are shown by the lateral continuity of gravelly sands and some type 1 and 2 sandstones.

The stack of Allan's model 3 deposits in the Figure 5.6 is similar to the stack of lithofacies within in my study area. Both of them are commonly end with soil development (pedogenesis). Vertical section in such models are often truncated due to large avulsive steps of the river and covered by eolian deposits. However, the meandering system in Allan's model 3 is not obvious as well as in the middle section of my study area. It is because thick eolian deposits occupy predominantly in the middle section of my study area. Since the study area is comprised of fining upward sequences with thick overbank deposits, crevasse splays of sandstones type 2, and pedogensis of eolian deposits (sandstones type 3) and sandy clay, therefore, the depositional systems in the mapped area can be similar to model 3 of Allen (1974). However, although depositional systems in the study area are controlled by autocyclic variations, climate also plays an important role as shown by soil development of orange eolian sands, calcite cements and carbonate nodules.

Imbrication in gravelly sands, trough cross-bedding in gravelly sands and sandstone type 2, and concretions in sandstone types 2 and 3 and in the boundary of sand-silt-clay found in the study area support the determination that the paleocurrent and depositional mechanisms are by fluvial systems derived from northwest of the study area.

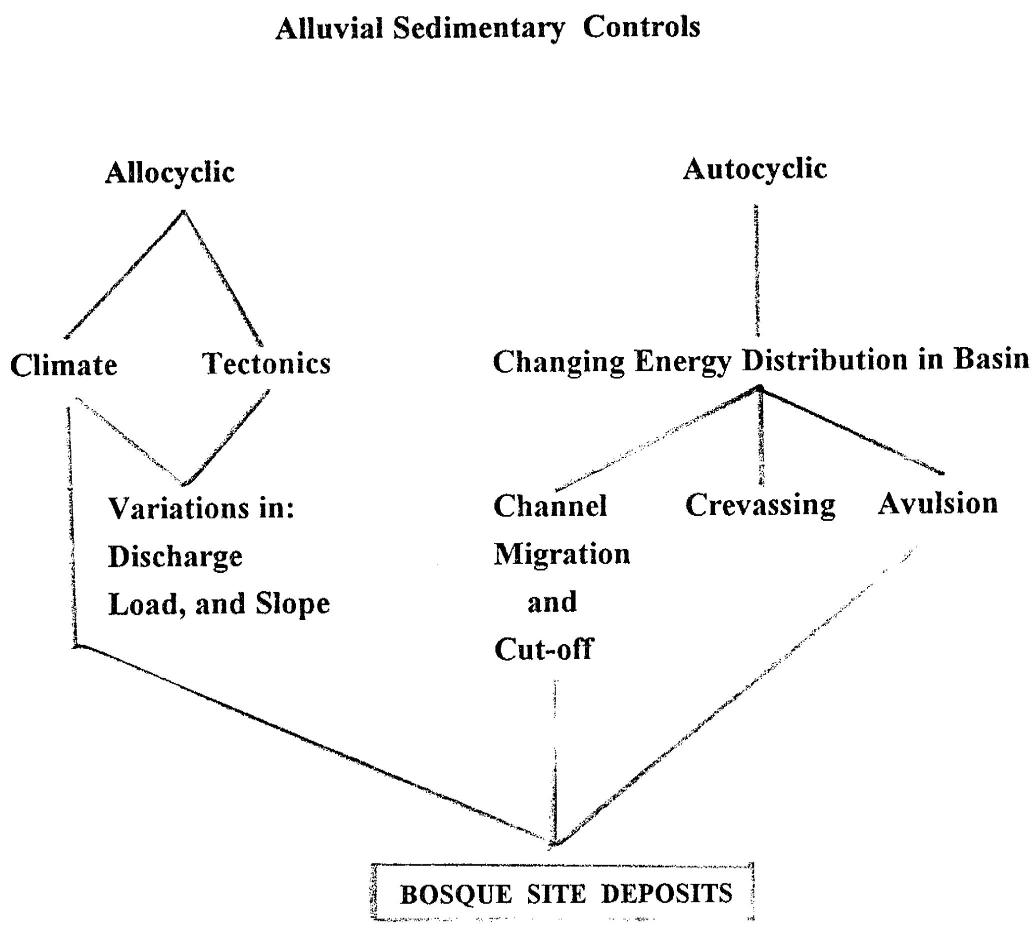

Figure 5.5. Autocyclic and allocyclic controls on deposition (Modified from Allen, 1974).

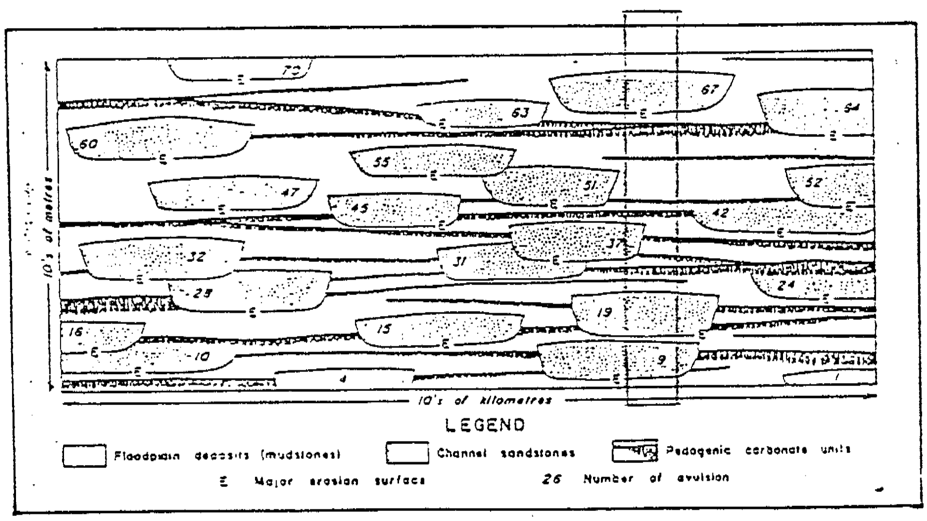

Figure 5.6. Theoretical two dimensional vertical profile normal to mean paleocurrent direction to illustrate the fluviatile sedimentation generated using Model 3 (Allen, 1974).

☐ = approximate scale of Bosque site cross section.

Judging from description above, the Bosque sediments are deposited under several types of channels and wind blown sand facies. The large braided channels occupy the bottom and the top of the section. Above the large basal braided channels, the deposition is controlled by eolian systems, other channels systems (crevasse splays and arroyos), overbank deposits, and soil development. The presence of local crevasse splays and thick overbank deposits indicate that the stream flooded periodically, and the stream channels migrated as in the meandering system. Finally, the large braided channels covered the top of the Bosque sediments (Figure 4.1 and 5.6). This fining upward sequences can be interpreted as products of meandering system.

There is also at least one period of time when eolian deposition replaced the fluvial system, as shown by the thick continuous sandstone type 4 in the middle of the section of study area.

5.3 Controls on Permeability Distribution

The objective of this section is to discuss the depositional system and its relation to the permeability distribution, including lateral and vertical distributions applied to petroleum migration. In order to address this goal, additional data, such as concretions and permeability values from the field and from previous work are also utilized.

In terms of petroleum migration, permeability is the most important property that allows fluid to flow within the deposits. Generally, permeability values increase by increasing the porosity. However, the porosity and permeability values are dependent upon the depositional systems that produce lithofacies. Different facies have different thicknesses, sedimentary structures, and composition.

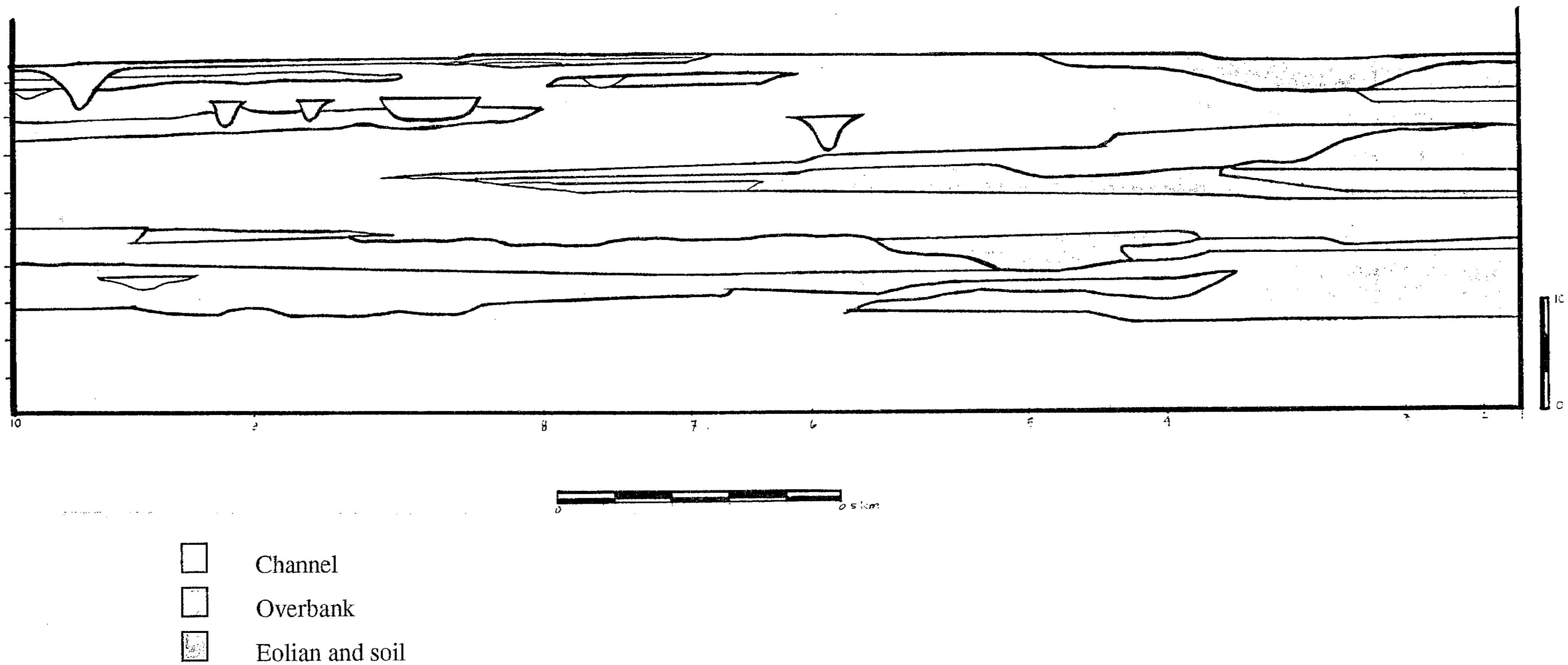

Figure 5.7. The interpretation of depositional environment of Bosque site deposits (Based on the lithofacies correlation).

5.3.1 Relation Depositional Systems and Permeability Distribution

As we described before (in Chapter 4), the mapped area consists of 4 lithofacies, gravelly sands, sandstones, interbedded sand-silt-clay, and paleosol, which were deposited originally from fluvial and eolian systems. Each lithofacies indicates each depositional system and shows different depositional mechanisms that work at the Bosque site. For example, gravelly sands and orange sandstones produced by fluvial and eolian processes respectively are distributed almost continuously along the mapped area from north to south with variable thickness. Some sandstones produced by fluvial processes form channel deposits, which are not distributed across the mapped area; some sandstones form tabular sands. This tabular sandstones are also not distributed continuously across the mapped area (Figure 4.1).

According to the Figure 5.8, the gravelly sands (Gs) of channel deposits have the highest permeability value followed by Ss2 of channels, Ss4 of eolian sands and ISS of overbank deposits respectively. Soils and clay deposits should have lower permeability.

Channel lithofacies Gs1, Ss1, Ss2 are categorized as high permeability ($k > 30$ darcies). Both eolian and overbank lithofacies (Ss3, Ss4, and ISS) have medium permeability ($1 < k < 30$ darcies). Clay-rich paleosols are categorized as low permeability ($k < 1$ darcies) (Figure 5.9). Although the general permeability distribution is easily recognized due to the partial cementation, discontinuity of vertical and lateral lithofacies distribution, and the heterogeneity of the deposits, the exact permeability distribution is variable (Table 5.2). In deposits partly cemented, for example, permeability measured now probably is different from the original permeability and probably will not useful for determining the permeability distribution in the future. If the arid condition keep continuing, the pore spaces will be completely cemented and/or influenced by ongoing diagenetic processes in the future as the atmospheric dust with high $CaCO_3$ keep dissolved by meteoric water. As a result, the permeability value can be either bigger or smaller.

Therefore, permeability distribution is controlled by depositional systems and post depositional processes.

5.3.2 Relation between Permeability Distribution and Petroleum Migration.

Hydrocarbon (oil and gas) is commonly controlled by its contact with surrounding water within rocks of variable permeability. This control is described by Hubbert's (1953) hydrodynamic equation:

$$\frac{\delta z_0}{\delta x} = \frac{\rho_w}{\rho_w - \rho_o} \frac{\delta h}{\delta x}$$

where $\delta z_o/\delta x$ = tilt of oil-water interface, $\delta h/\delta x$ = potentiometric surface gradient, ρw = density of water(g/cm3), and ρo= density of oil (g/cm3), and Hubbert's equation 41):

$$Eo = g + \frac{\rho^w}{\rho^o} (Ew - g) ,$$

where Eo = driving force of the oil (dynes), g = gravitational acceleration (cm/sec^2), and Ew = driving force of the water (dynes). Equation 4.1 shows that if density of water is the same as density of oil, the driving force of the oil will be equal with driving force of water. However, such a case is seldom found. Commonly density of oil is lighter than water. As a result, oil will be driven by driving force of water. Combination of these two equation indicate that besides permeability distribution, other parameters such as gradient is also significant to predict oil migration.

Paleoflow directions of the fluvial lithofacies are generally oriented S15^{0}E - S35^{0}E. Previous workers (Davis, 1991,1993; Lohmann, 1992) found that the permeability distribution at the north end of my study area is similar, S30^{0}E. This direction is indicative of the gradient for water in these underformed beds, especially under steady state flow, which is parallel to the potentiometric surface gradient (Davis, 1987).

PERMEABILITY VALUE AND LITHOFACIES RELATIONSHIP

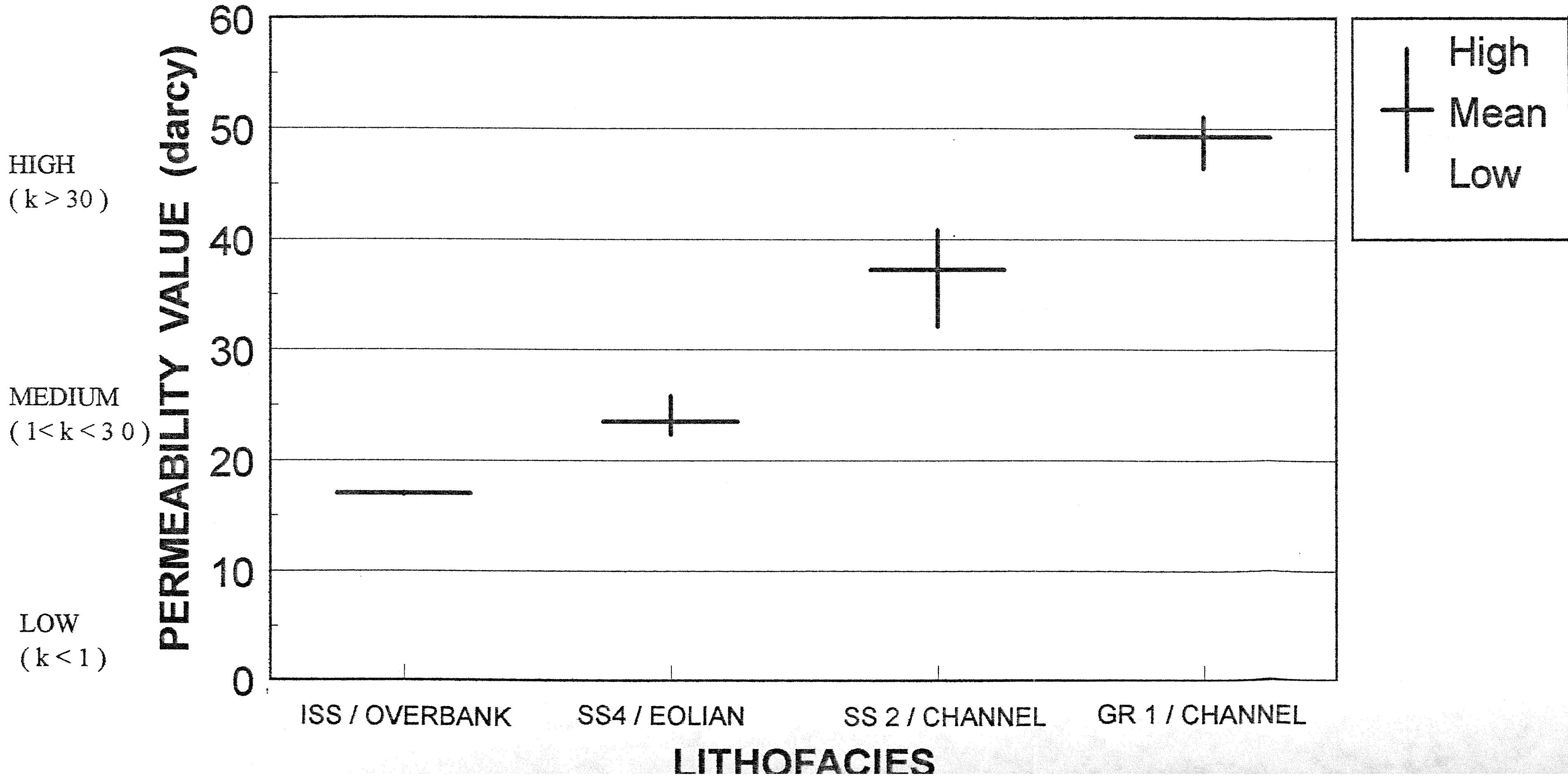

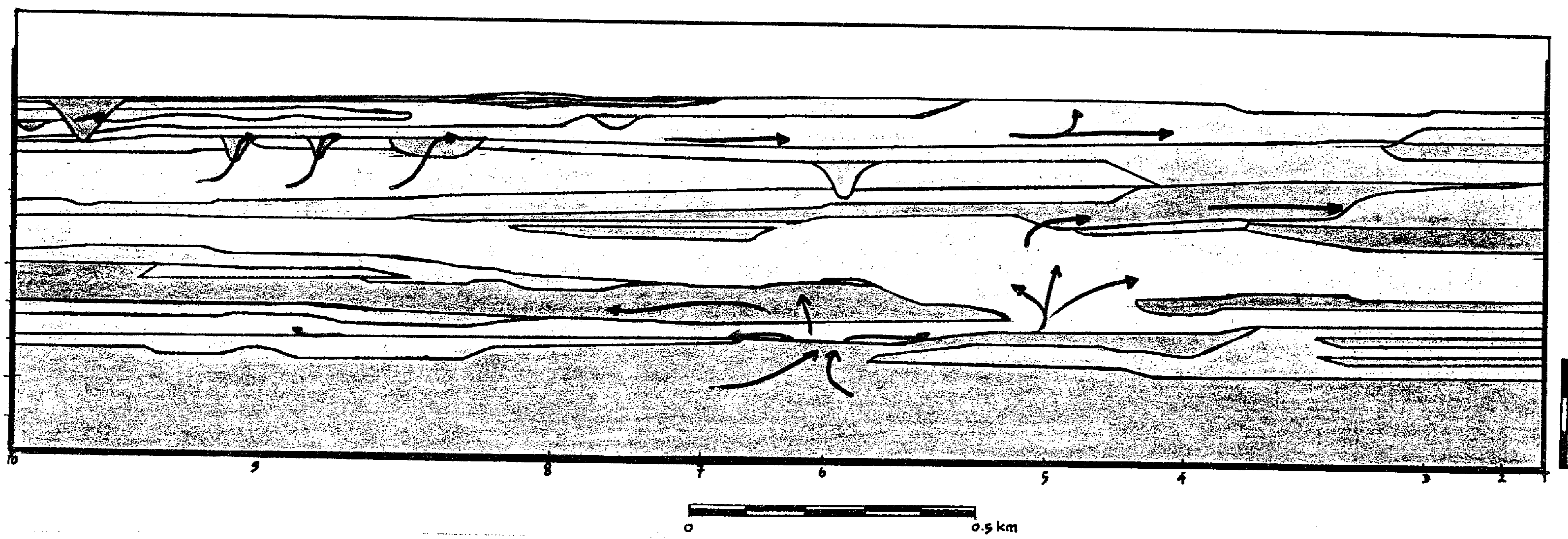

10
9
8
7
6
5
4
3
2
1
0
0.5 km
10'
0

●	= High Permeability	($k > 30$ darcy)
O	= Medium Permeability	($1 < k < 30$ darcy)
⊙	= Low Permeability	($k < 1$ darcy)

Figure 5.9. Interpretation of Permeability Distribution within Study Area
Arrows indicate the possible pathways of oil migration. These pathways are made with assumption of water drive.

Table 5.2 Relation of Permeability Value and Lithofacies

Lithofacies	Units	Description	Sedimentary Structures	Permeability (darcy)
Gravelly sands (Gs)	Gravelly sands (Gs)	Light gray, very coarse sand-cobles, poorly sorted, well rounded, well cemented.	Imbrication, trough cross-bedding, hz. lamination, graded, scoured	48.32
	Sandstone Type 1 (Ss-1)	Light gray, lower coarse-upper coarse sand with pebbles, well rounded, poorly sorted	Graded bedding	N/A
	Sandstone Type 2 (Ss-2)	Light gray-tan, upper medium-lower coarse sand, well rounded, med.sorted, cemented	Climbing ripples, low angle cross bedding, parallel lamiantion	32.65 - 40.89
Sandstones (Ss)	Sandstone Type 3 (Ss-3)	Light gray-tan, upper fine-upper medium sand, well rounded well sorted, concretions	Low angle trough cross bedding, climbing ripples, sand sheet	N/A
	Sandstone Type 4 (Ss-4)	Orange-reddish, upper fine-upper medium sand, well rounded, well sorted, med-well cemented, nodules	Relict tangential Cross-bedding	22.69 - 25.90
Interbedded Sand-Silt-Clay (ISS)	Interbedded Sand-Silt-Clay (ISS)	Dark brown - tan - whitish, upper fine sand-clay, well sorted and well rounded for sands.	Thin hz. lamination	17.17
	Clayey Sands (P-1)	Brown - reddish, churned, mud balls	N/A	N/A
Paleosols (P)	Sandstone Type 4 (P2/Ss-4)	Orange-reddish, upper fine-lower medium sand, nodules	Local faint tangential cross-bedding	(22.69 - 25.90)
	Clay (P-3)	Light brown - dark brown, red, churned, draping, nodules	N/A	N/A

Depositional sequences in Figure 4.1 and permeability distribution in Figure 5.9 show that there is a possibility that permeability might change direction due to lateral and/or vertical changes in lithofacies distribution. In terms of migration, light density of oil will always migrate to and accumulate at the highest point following the lithofacies pattern. Water having heavier density than oil, on the other hand, will always migrate downward and accumulate at the lowest point. Here, we need the overall inclination of the deposits. Once we know the regional inclination and permeability patterns, we can predict the direction of migration. Since the oil has a lighter density than water, oil will migrate in an opposite direction. Furthermore, the oil will migrate to the highest point. For example, in Figure 5.9, assuming units are undeformed as shown and under water drive, petroleum migrates upward from below through the permeability zones. (See the possible pathways of oil migration in Figure 5.9). The oil will migrate from high permeability to lesser permeability following the gradient of permeable zones. According to Figure 5.9, the change of oil to be accumulated in the trapping zones (place where reservoir zone is covered by impermeable zones or seal so oil are not able to move again) is very small and not prospective because the trapping zones are very small. As the result, oil keeps migrating through the leaking zone (area where oil are still able to move) out of the study area. Because this study performs only 2-D lateral and vertical distributions, the exact permeability patterns beyond this area (to the west) are hardly known.

CHAPTER 6 CONCLUSIONS

Based on lithofacies distribution and depositional environments interpretation, sedimentation processes in the Bosque site are controlled by meandering systems of Rio Puerco. Both fluvial and eolian processes aggrade the area in various sequences, such as stacked fluvial channels, eolian, and fluvial overbank-eolian deposition. The base and the top of the mapped area is controlled by an aggrading braided channel system.

Both allocyclic and autocyclic factors control the study area. Gravelly sands is the best indicator of autocyclic factors (channel avulsion and migration); continuous eolian sandstones are the best indicator for allocyclic factor (especially climatic) as the transition from fluvial to eolian systems in arid region. Discontinuity of other lithofacies show that local depositional energy and depositional mechanisms play an important role in aggradational processes at the Bosque site.

Fluvial channel and eolian lithofacies are the most significant units in estimating the permeability distribution. Paleoflow obtained from fluvial sedimentary structures and previous permeability measurements show that the general permeability distribution ranges from S15^{0}E - S35^{0}E. The opposite direction of this value can be used as the general trend of oil migration under present conditions.

Lateral permeability values of eolian sandstone lithofacies have relatively similar values at each of different sections from south to north in my study area. The small difference in permeability values is probably caused by heterogeneous texture of the lithofacies during sedimentation and the different intensity of local diagenesic processes.

Although there is no indication of oil in the study area, this study provides useful information for petroleum geologists who are developing or stimulating oil production in similar basinal settings about how depositional systems control the permeability distribution. However, since this study only describes lithofacies in 2-D, further study of permeability distributions to the west will produce better predictions regarding possible oil migration.

References

Allen, J. R. L., 1974, Studies in fluvialtile sedimentation : Implications of pedogenic carbonate units Lower Old Red Sandstone, Anglo-Welsh Outcrop: Geology Journal, vol. 9, pp. 181-208.

Allen, J. R. L., 1982, Studies in fluviatile sedimentation: bars, bar complexes and sandstone sheets (low-sinuosity braided streams) in the Brownstones (L. Devonian), Welsh Borders: Sedimentary Geology, v. 33, pp. 237-293.

Angevine, L. C. and Paola, C., 1990, Quantitative sedimentary basin modeling: American Association of Petroleum Geologists Course Note Series # 32, 120 p.

Berner, A. R., 1971, Principles of chemical sedimentology : Diagenesis of iron minerals: International Series in Earth and Planetary Science, McGraw-Hill, 197 p.

Berg, R. R., 1986, Reservoir sandstones, Prentice-Hall, Inc. New Jersey, 481 p.

Braester, C., Fligelman, H., and Kashai, E., 1991, Hydrocarbon accumulation on the Dead Sea Graben : A simulation approach: Journal of Petroleum Geology, v. 14, pp. 181-196.

Boggs, S. JR., 1995, Principles of sedimentology and stratigraphy, Prentice-Hall, Inc. New Jersey, 2nd ed. 773 p.

Cather, S. M., Chamberlin, M. R., Chapin, C. E., McIntosh C. W., 1994, Basins of the Rio Grade rift: Structure, Stratigraphy, and tectonic setting: Geological Society of America Special Paper 291, pp. 157-170.

Chamley, H, 1990, Sedimentology: Springer-Verlag, New York, 285 p.

Chapin C. E. and Seager, W. R., 1975, Evolution of the Rio Grande rift in Socorro and Las Cruses areas: New Mexico Geological Society Guidebook 26, pp. 297-321

Cerling, E. Thure, 1984, The stable isotopic composition of modern soil carbonate and its relationship to climate, Earth and Planetary Science Letters, v. 71, pp. 229-240.

Chapin, E. C. and Cather, S. M., 1994, Tectonic setting of the axial basin of the northern and central Rio Grande rift : Gelogical Society of America Special Paper 291. pp. 5-23.

Collinson, J .D and Thomson, B. D, 1982, Sedimentary Structures, George Allen and Unwin, Boston, 194 p.

Conybeare, C. E. B., 1979. Lithostratigraphic analysis of sedimentary basins. Academic Press, New York, 555 p.

Curtis, D. C., Coleman, L. M., and Love, G. L., 1986, Pore water evolution during sediment burial from isotopic and mineral chemistry of calcite, dolomite and siderite concretions: Geochimica et Cosmochimica Acta, v. 50, pp. 2321-2334.

Davis, M. J.,1990, An approach for the characterization of spatial variability of permeability in the Sierra Ladrones Formation, Albuquerque Basin, Central New Mexico: MS. Thesis, New Mexico Institute of Mining and Technology, Socorro. 128 p.

Davis, M. J., 1993. A conceptual sedimentological-geostatistical model of aquifer heterogeneity based on outcrops studies: Ph.D. Dissertation. New Mexico Institute of Mining and Technology , Socorro, 156 p.

Davis, M. J., Wilson, J. L., and Phillips, F. M., 1994. A portable air- minipermeameter for rapid in situ field measurements: Groundwater, v. 32, pp. 258 - 266.

Davis, W. R., 1987. Analysis of hydrodynamic factors in petroleum migration and entrapment: American Association of Petroleoum Geologists Bulletin, v. 71., pp. 643-649.

Dreyer, T., Scheie, A., and Walderhaug, O., 1990, Minipermeameter - based study of permeability trends in channel sand bodies, Water Resources Research, Vol. 26, pp. 163-164.

Fryberger, G. S., Ahlbrandt, S. T., and Andrews S., 1979, Origin, sedimentary features, and significance of low-angle eolian "Sand Sheet" deposits, great sand dunes National Monument and vicinity, Colorado: Journal of Sedimentary Petrology, vol. 49, pp. 733-746.

Gile L, H., Hawley, J. W., and Grossman, R.B. 1981, Soil and geomorphology in the basin and range area of southern New Mexico Guidebook to the Desert Project. New Mexico Bureau of Minerals Resources, Memoir 39, 222 p.

Gluyas, J. G., 1984, Early carbonate diagenesis within Phanerozoic shales and sandstones of the NW European shelf: Clay Mineralogy, v. 19, pp. 309-321.

Goggin, D. J., Chandler, M. A., Korcurek, G., and Lake, L. W., 1988, Patterns of permeability in eolian deposits: Page sandstones (Jurassic), northeastern Arizona: Society of Petroleum Engineer, Formation Evaluation. v. 3, pp. 297-306.

Gotkowitz, M., 1993, A study of the relationship between permeability distribution and small scale sedimentary features in a fluvial formation: MS. Thesis , New Mexico Institute of Mining and Technology 78 p.

Henriquez, A., Tyler, J. K., and Hurst, A., 1990, Characterization of fluvial sedimentology for reservoir simulation modeling, Society of Petroleum Engineer, Formation Evaluation, v. 5, pp. 211-216.

Hubert, M. K., 1953, Entrapment of petroleum under hydrodynamic conditions. American Association of Petroleum Geologists Bulletin, v. 37, pp. 1954-2026.

Hunter, R. E., 1977, Basic types of stratification in small eolian dunes: Sedimentology, v. 24, pp. 361-387.

Hunter, R. E., 1981, Stratification styles in eolian sandstones - some Pennsylvanian to Jurassic example from the western interior U.S.A., in non -marine depositional environments-models for exploration : Society of Economic Paleontologists and mineralogist Special Publications No. 31, pp. 315-329.

Keller, R. G. and Cather, M. S., 1994, Basin of the Rio Grande Rift : Structures , Stratigraphy, and Tectonic Setting: Geological Society of America Special Paper 291, 251 p.

Kocurek, G. and Dott, H. R. Jr., 1981, Distinction and uses of stratification types in the interpretation of eolian sand: Journal of Sedimentary Petrology, v. 51, pp. 579-595.

Koster, H. E. and Steel, J. R., 1984, Sedimentology of gravels and conglomerates: Canadian Society of Petroleum Geologists, Memoir 10, 441 p.

Leeder, M. R., 1982, Sedimentology : Process and product. London, 338 p.

Lohman, C. R., 1992, A sedimentological approach to hydrologic characterization: a detailed three-dimensional study of an outcrop of the Sierra Ladrones Formation, Albuquerque Basin: MS. Thesis, New Mexico Institute of Mining and Technology 97 p.

Love, D. W., and Young, D. J., 1983, Progress report on the Late Cenozoic evolution of the Lower Rio Puerco: New Mexico Geological Society Guidebook, 34th Field Conference, Socorro Region II, pp. 277-284.

Lozinsky, R. P., 1988, Stratigraphy, sedimentology and sands petrology of the Santa Fe Group and pre-Santa Fe Tertiary deposits in the Albuquerque Basin, Central New Mexico: Ph. D. Disertation, New Mexico Institute of Mining and Technology, Socorro, New Mexico, 298 p.

Lozinsky, R. P., Hawley, J. W., and Love, D. W., 1991, Geologic overview and Pliocene-Quaternary history of the Albuquerque Basin, Central New Mexico, in J. W. Hawley and D. W. Love (eds.), Quaternary and Neogene landscape evolution: A transect across the Colorado plateau and asin and range province in the west-central and central New Mexico: New Mexico Bureau of Mines and Mineral Resources Bulletin 137, pp. 157-162.

Lozinsky, R. P., 1991, Geology and paleontology of the Santa Fe Group, southwestern Albuquerque Basin, Valencia County, New Mexico: New Mexico Bureau of Mines and Mineral Resources Bulletin 132, 86 p.

Lundegard, D. P. and Trevena, S. A., 1990, Sandstone diagenesis in the Pattani Basin (Gulf of Thailand): History of water-rock interaction and comparison with the Gulf of Mexico: Applied Geochemistry, v. 5, pp. 669-685.

Mack, H. G, and Seager, R. W., 1990, Tectonic control on facies distribution of the Camp Rice and Palomas Formations (Pliocene-Pleistocene) in the southern Rio Grande rift: Geological Society of America Bulletin, v. 102, pp. 45-53

Mack, H. G., James, C. W., Monger, C. H., 1993, Classification of paleosols: Geological Society of America Bulletin, v. 105, pp. 129-136

Mack, H. G., Seager, R. W., Kieling, J., 1994, Late Oligocene and Miocene faulting and sedimentation, and evolution of the Rio Gande rift, New Mexico, USA: Sedimentary Geology, vol. 92, pp. 79-96.

McKee, E. D., 1965, Experiments on ripple lamination. In : Middleton, G. V., ed. Primary sedimentary structures and their hydrodynamic interpretation: Society of Economic Paleontologists Mineralogists Special Publicaton 12, pp. 66-83.

McKee, E. D., Crosby, J. E, and Berryhill, L. H. Jr., 1967, Flood deposits, Bijou Creek, Colorado, June 1965: Journal of Sedimentary Petrology, v 37, pp. 829-851

Miall, D. A., 1978, Lithofacies types and vertical profile models of braided river deposits: a summary in Miall, D. A. (ed), Fluvial sedimentology: Canada Sociey of Pertoleum Geologists, Memoir 5, pp. 597-604.

Miall, D. A., 1981, Sedimentation and tectonics in alluvial basins: Geological Association of Canada, Johanns Graphics, Waterloo, Ontario, Canada, 272 p.

Miall, D. A, 1985, Architectural element analysis: A New method of facies analysis applied to fluvial deposits: Earth Science Review, v. 22, pp. 261-308.

Miall, D. A, 1988, Facies architecture in clastic sedimentary basin: Springer-Verlag, New York, 452 p.

Middleton, V. G, 1977, Sedimentary Processes: Hydraulic interpretation of primary sedimentary structures: Society of Economic Paleontologist and Mieralogist Series No. 3, 285 p.

Mora, I. C., Driese, G. S., Seager, G. P., 1991, Carbon dioxide in the Paleozoic atmosphere: Evidence from carbon-isotope composition of pedogenic carbonate: Geology, v. 19, pp. 1017-1020.

Pendall, E. and Amundson, R., 1990, The stable isotope chemistry of pedogenic carbonate in an alluvial soil from the Punjab, Pakistan.: Soil Science, v. 149, pp. 199-211.

Picard, M. D., and High, R. L., 1973, Developments in sedimentology 17: Sedimentary Stuctures of Ephemeral Streams: Elsevier Scientific Publishing Co. New York, 233 p.

Potter, P. E., and Pettijohn, F. J., 1977, Paleocurrent and basin analysis, 2nd ed.: Springer-Verlag, New York, 460p.

Pratch, C. J., 1991, Vertical hydrocarbon migration: Journal of Petroleum Geology, v. 14, pp. 429-444.

Potter, P.E. and Pettijohn, F.J., 1977, Paleocurrents and Basin Analysis, Springer-Verlag Berlin Heidelberg, New York, 425 p.

Prior, A. W, 1973, Permeability-porosity pattern and variations in some Holocene sand bodies: American Association of Petroleum Geologists Bulletin, v. 57, pp. 162-189.

Quade, J., Cerling, E. T., Bowman, R. J., 1989, Systematic variations in the carbon and oxygen isotopic composition of pedogenic carbonate along elevation transects in the southern Great Basin, United States: Geological Society of America, Bulletin v. 101, pp. 464-475.

Raiswell, R., 1971, The growth of Cambrian and Liassic concretions: Sedimentology, v. 17, pp. 147-171.

Ravene, C., Eschard, R., Galli, A., Mathieu, Y., Montadert, L., and Rudkiewicz, L. J., 1989, Heterogeneities and geometry of sedimentary bodies in fluvio-deltaic reservoir: Society of Petroleum Engineer, Formation Evaluation, v. 4, pp. 239-246.

Reading, H. G., 1986, Facies, in Reading, H. G. (ed.): Sedimentary environments and facies: Srpinger-Verlag, New York 615 p.

Reineck, E. H and Singh. B. I, 1980, Depositional sedimentary environments, Srpinger - Verlag, New York, 549 p.

Rubin, M. D. and Hunter, E. R., 1987, Field guide to sedimentary structures in the Navajo and Entrada sandstones in Southern Utah and Nothern Arizona, pp. 126-139, in Geologic diversity of Arizona and its margins : Excursions to choise areas: Arizona Bureau of Geology and Mineral Technology Geological Survey Branch Special Paper 5.

Schere, M., 1987, Parameter influencing porosity in sandstones : a model for sandstones porosity prediction : American Association of Petroleum Geologists Bulletin, v. 71, pp. 485-491.

Seager, W. R., Shafiqullah, M., Hawley, J. W., and Marvin, R., 1984, New K-Ar dates from basalt and evolution of the southern Rio Grande rift: Geological Society of America Bulletin, v. 95, pp. 87-99.

Sheperd, G. R and Macke, L. D, 1978, Discrimination of fluvial and eolian deposits by number -frequency analysis of sediments of sands trough silt size from a point bar, Rio Puerco, New Mexico, Journal Research U.S. Geological Survey, v. 6, pp. 499-504.

Simon, E. V. and Nordin. C. F. Jr., 1965, Sedimentary structures generated by flow in alluvial channels in G.F. Middleton, editor, Primary structures and their hydrodynamic interpretation : Society of Economic Paleontologists and Mineralogists Special Publication 12, pp. 34-52.

Smith, L. and Schartz, W. F., 1980, Mass Transport 1. A Stochastic analysis of macroscopic dispertion, Water Resources Research, v. 16, pp. 303-313.

Stephens, D.B., Cox, W., and Havlena, J., 1988, Field study of ephemeral stream infiltration and recharge, New Mexico Water Resources Research Institue Technical Completion Report, Project Numbers 1423655, 1423658, 188 p.

Sundborg, A., 1956, the River Klarälven, a study of fluvial processes: Geograf. Annaler, v. 38, pp. 125-316.

Surdam, C. R., and Moraes, A. S. M., 1993, Diagenetic heterogeneity and reservoir quality: Fluvial, deltaic and turbiditic sandstone reservoirs, Potiguar and Reconcavo Rift Basins, Brazil: American Association of Petroleum Geologists Bulletin, v. 77, pp. 1142-1158.

Van de Graaff, W. J., and Ealey J. P., 1989, Geological Modeling for Simulation Studies, American Association of Petroleum Geologists Bulletin, v. 73, p. 1436-1444.

Walker, T. R, 1971, Formation of red beds in modern and ancient desert, Geological Society of America Bulletin, v. 78, pp. 353-368.

Walker, G. R. and James, P. N., 1992. Facies Models : Resposnse to sea level changes: Geological Association of Canada, 409 p.

Wilkinson, M. and Dampier, D.M., 1990, Growth of Calcite Concretion in Sandstones, Geochimica et cosmochimica Acta., v. 54, pp. 3391-3399.

Wright, H. E. Jr., 1965. Tertiary and Quaternary geology of the Lower Rio Puerco Area, New Mexico, Geological Society of America Bulletin, v. 57, pp. 383-456.

Young , J. D., 1982. Late Cenozoic geology of the lower Rio Puerco, Valencia and Socorro Counties, New Mexico: M. S. Thesis, New Mexico Institue of Mining and Technology, Socorro, 126 p.

APPENDICES

APPENDIX I

MEASURED GEOLOGIC SECTIONS

Section 1 1993

(ft)

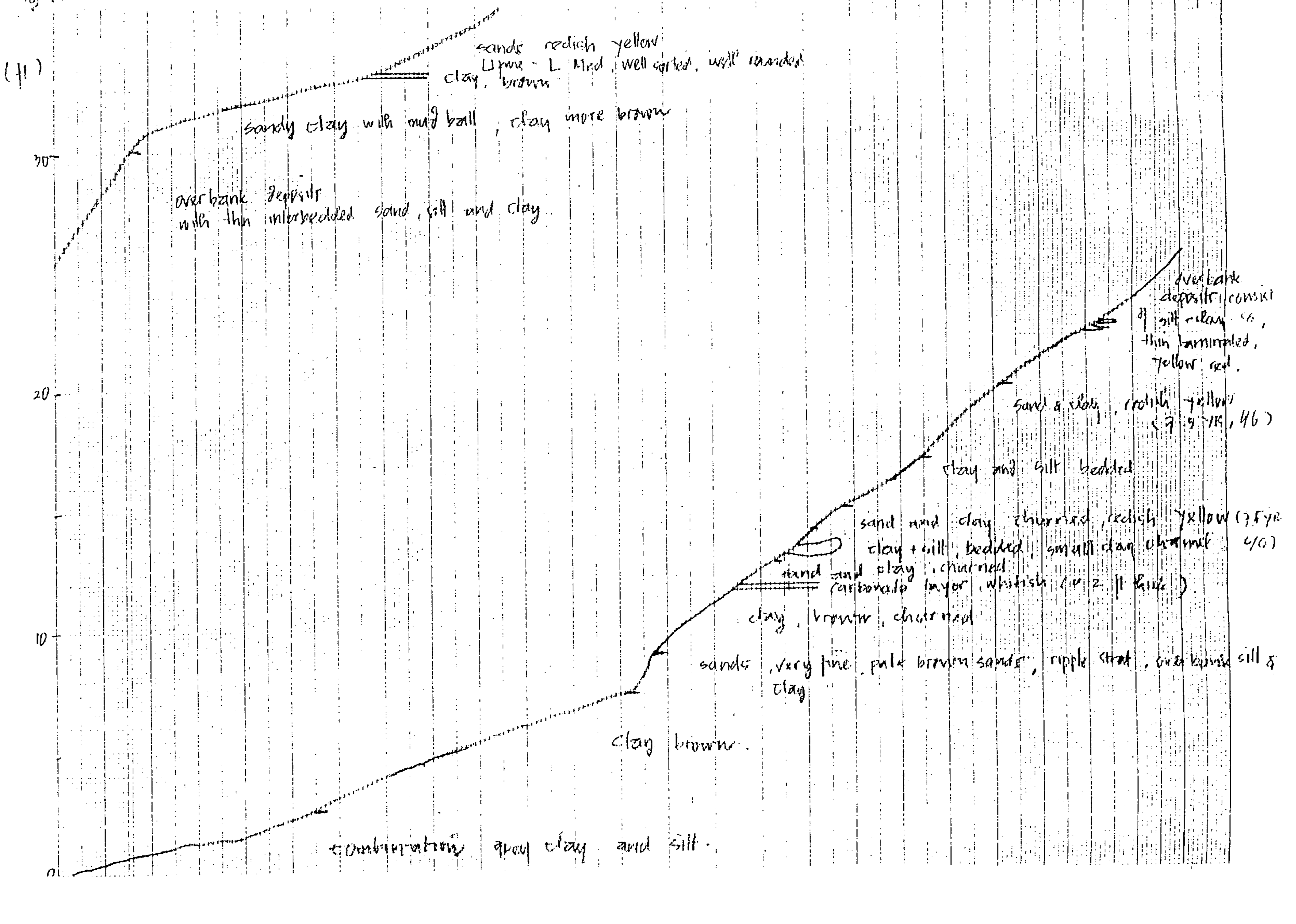

Section 1.

1993

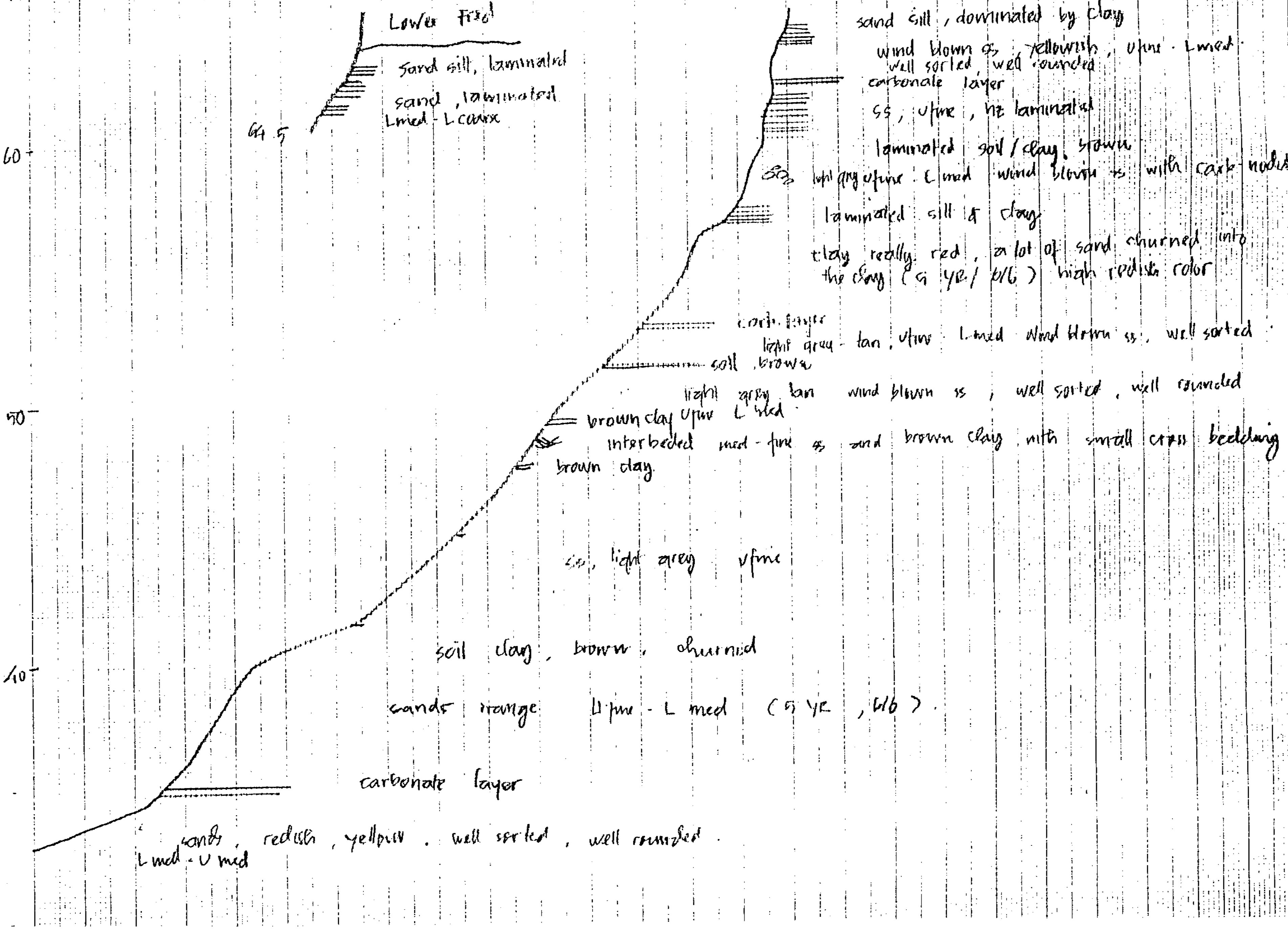

July 20/94 D 15/XV

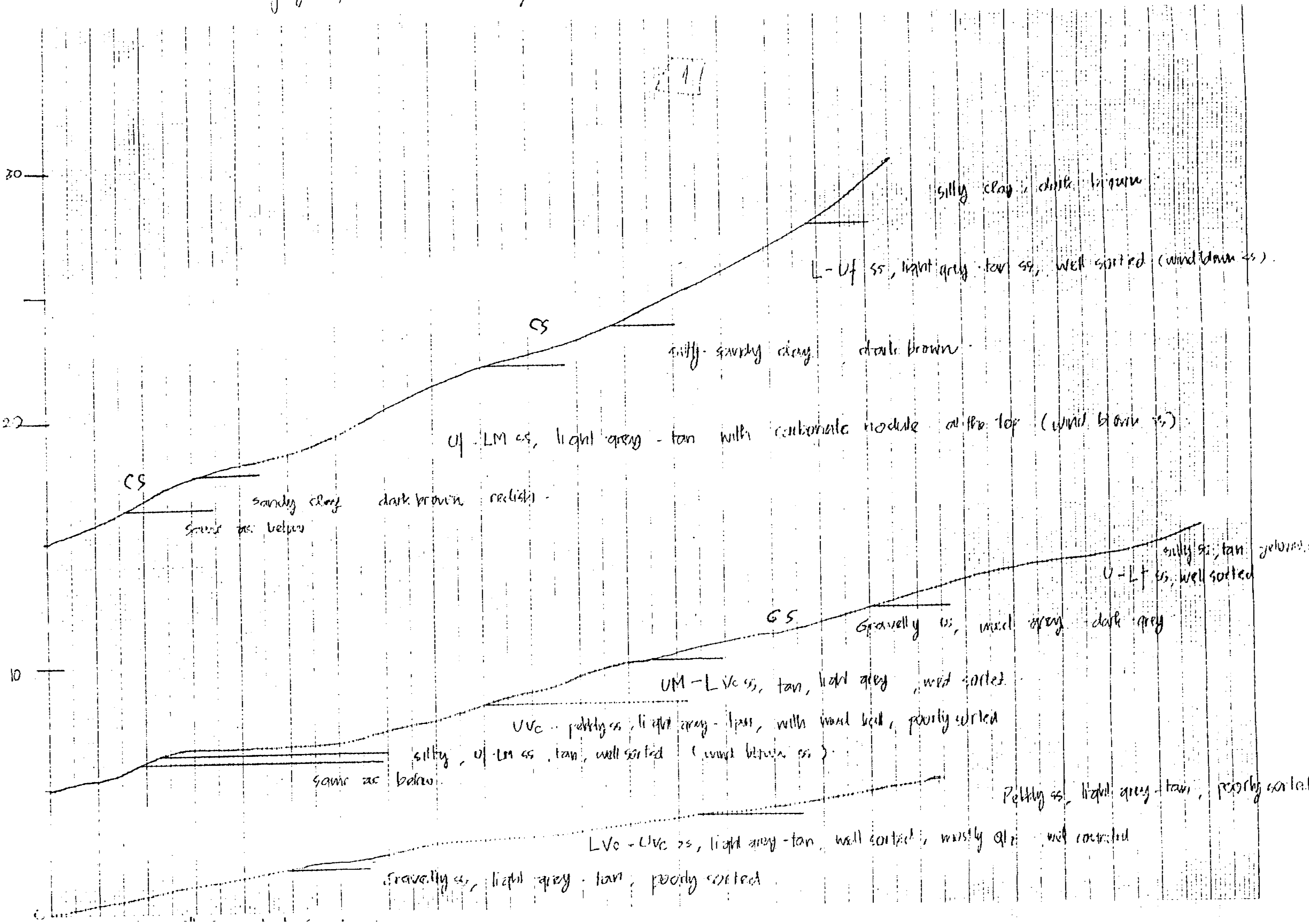

July 20/94 (2)

4)

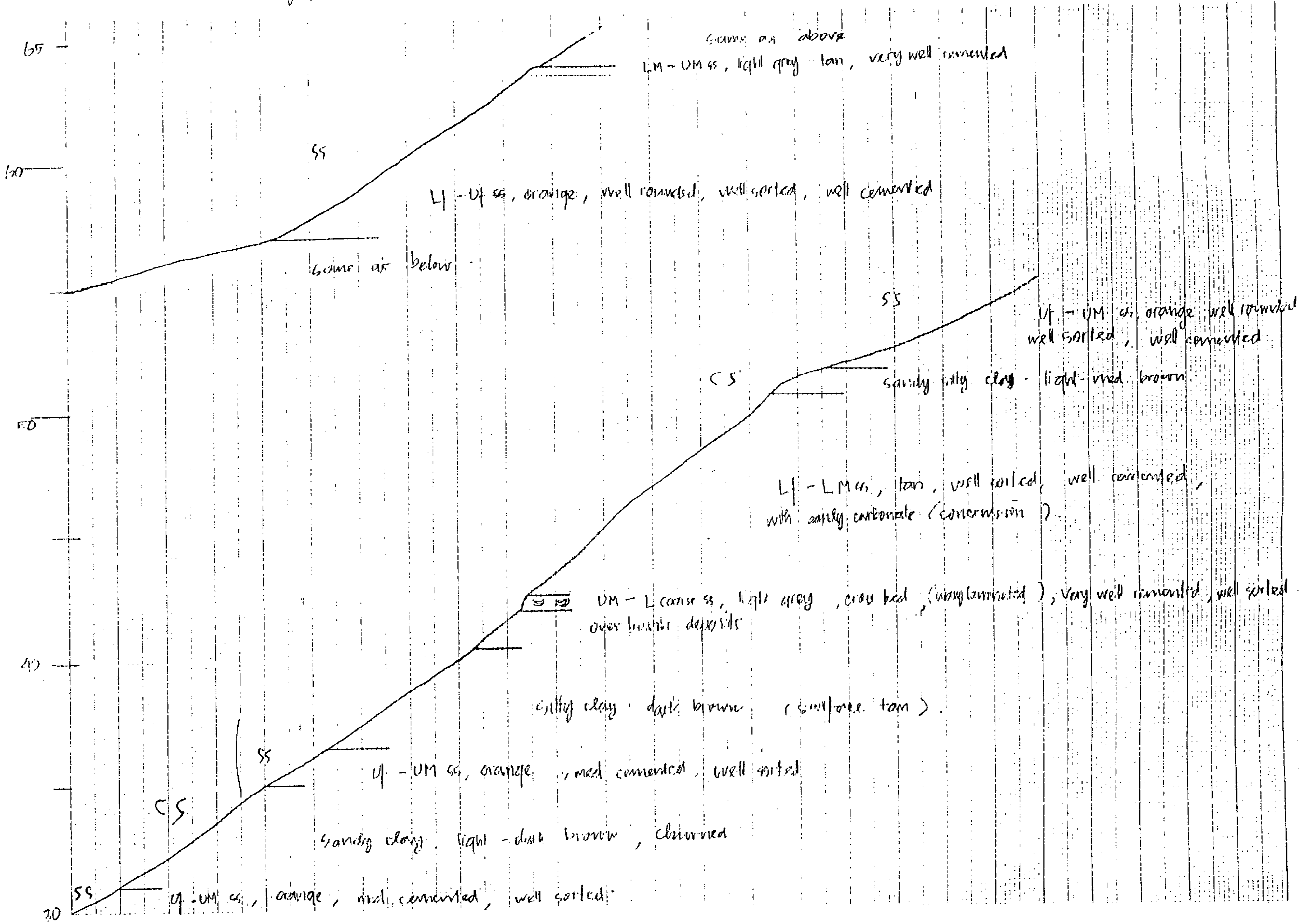
65
60
50
40
30
Same as above
LM - UM ss, light grey - tan, very well cemented
SS
LI - UI ss, orange, well rounded, well sorted, well cemented
Same as below
SS
UI - UM ss, orange, well rounded, well sorted, well cemented
CS
Sandy silty clay - light - med. brown
LI - LM ss, tan, well sorted, well cemented, with early carbonate (concretion)
UM - L coarse ss, light grey, cross bed, (ubig laminated), very well cemented, well sorted
over lunate deposits
silty clay - dark brown (surface tan)
SS
UI - UM ss, orange, med cemented, well sorted
CS
Sandy clay, light - dark brown, churned
SS
UI - UM ss, orange, med. cemented, well sorted

July 20/99 (3)

(2)

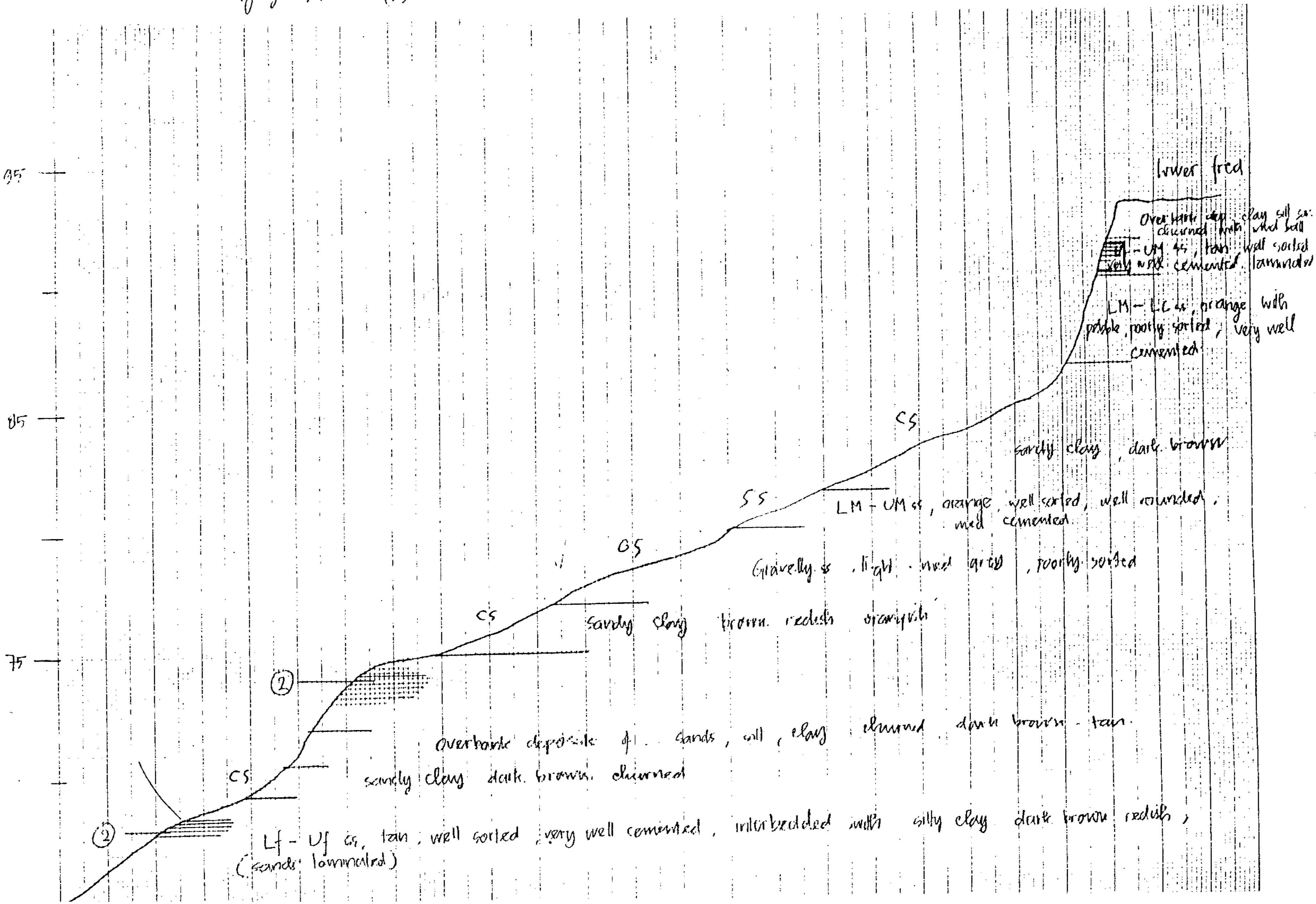
95
85
75
lower fred
Overbank dep. clay silt ss. churned with mud ball
LM - UM ss, tan, well sorted, very well cemented, laminated
LM - LC ss, orange with pebble, poorly sorted, very well cemented
CS
sandy clay, dark brown
SS
LM - UM ss, orange, well sorted, well rounded, med cemented
OS
Gravelly ss, light - med grey, poorly sorted
CS
sandy clay brown reddish orangish
(2)
Overbank deposits of sands, silt, clay churned dark brown - tan
CS
sandy clay dark brown churned
(2)
Lf - Uf ss, tan, well sorted, very well cemented, interbedded with silty clay dark brown reddish,
(sands laminated)

June 27 /94

①

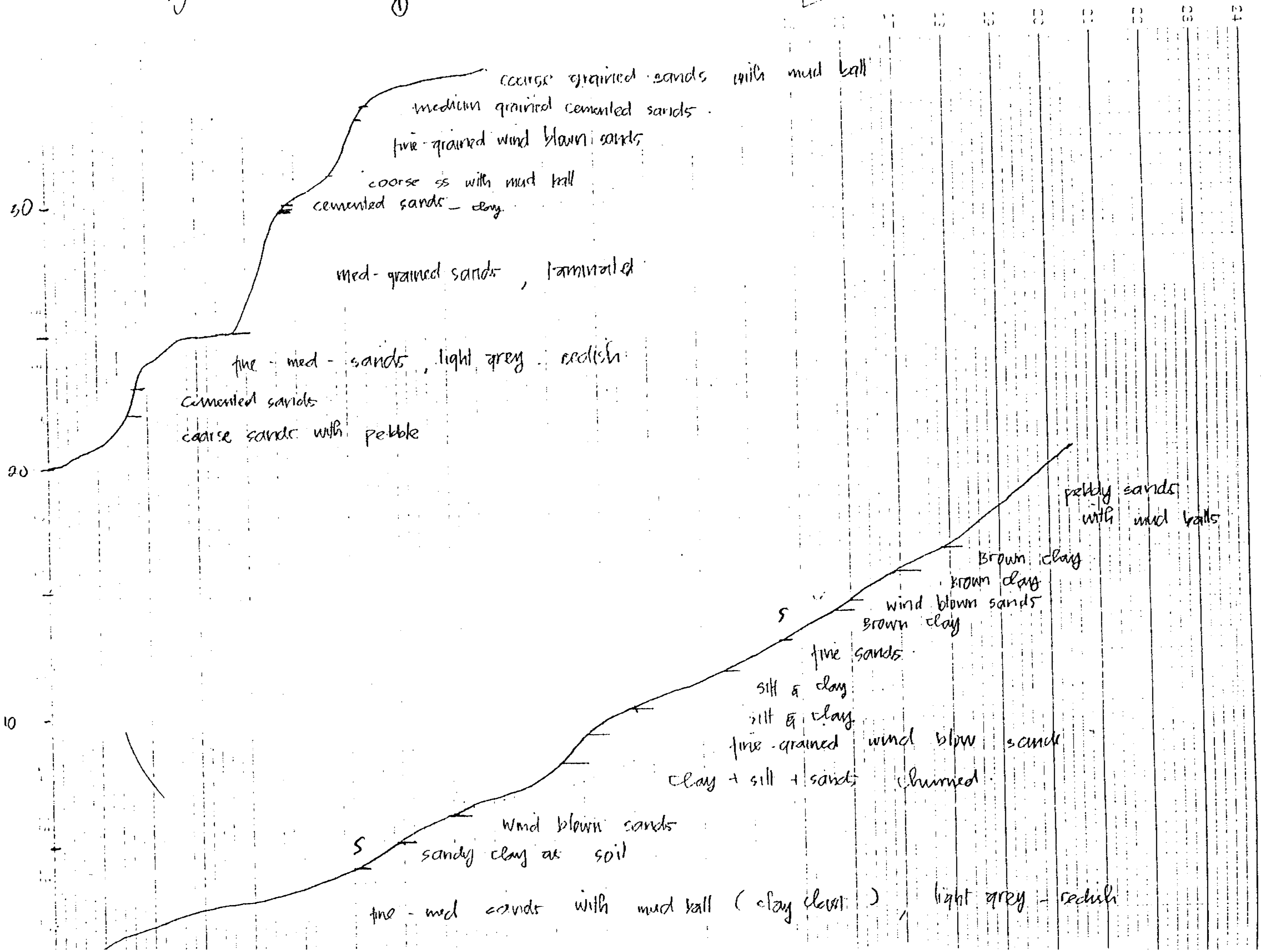
coarse grained sands with mud ball
medium grained cemented sands
fine grained wind blown sands
coorse ss with mud ball
cemented sands _ clay
30
med - grained sands , laminated
fine - med - sands , light grey . redish
cemented sands
coarse sands with pebble
20
pebbly sands with mud balls
Brown clay
brown clay
wind blown sands
Brown clay
fine sands
silt & clay
silt & clay
fine - grained wind blow sands
clay + silt + sands churned
10
wind blown sands
sandy clay as soil
fine - med sands with mud ball (clay clast) , light grey - redish

June 27 /94

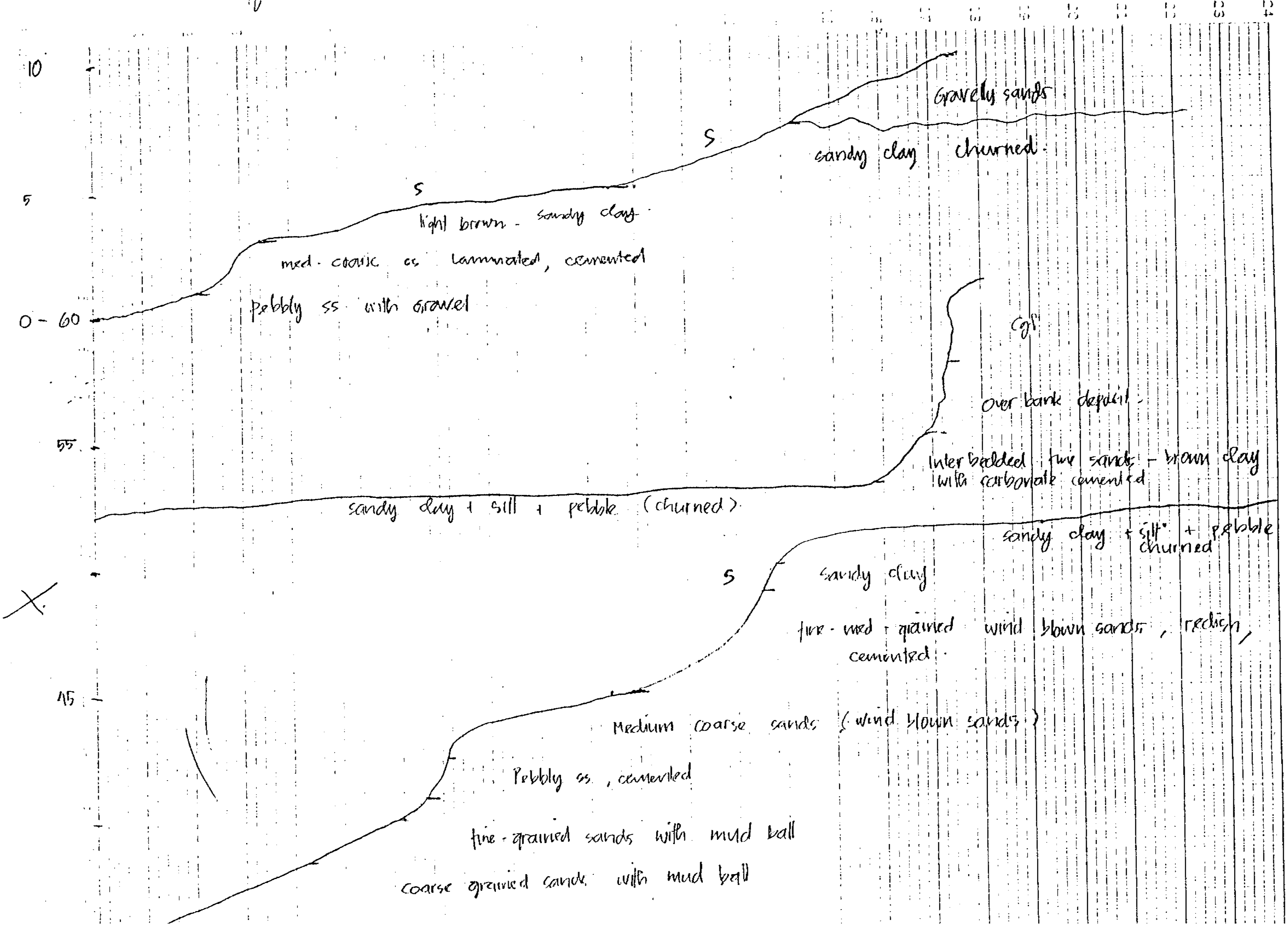
10
5
0 - 60
55
45
Gravely sands
sandy clay churned
light brown - sandy clay
med - coarse ss laminated, cemented
Pebbly ss with gravel
Cgl
Over bank deposit
Interbedded fine sands - brown clay
with carbonate cemented
sandy clay + silt + pebble (churned)
sandy clay + silt + pebble
churned
sandy clay
fine - med - grained wind blown sands, redish,
cemented
Medium coarse sands (wind blown sands)
Pebbly ss, cemented
fine - grained sands with mud ball
coarse grained sands with mud ball

June 27. (3)

section 3

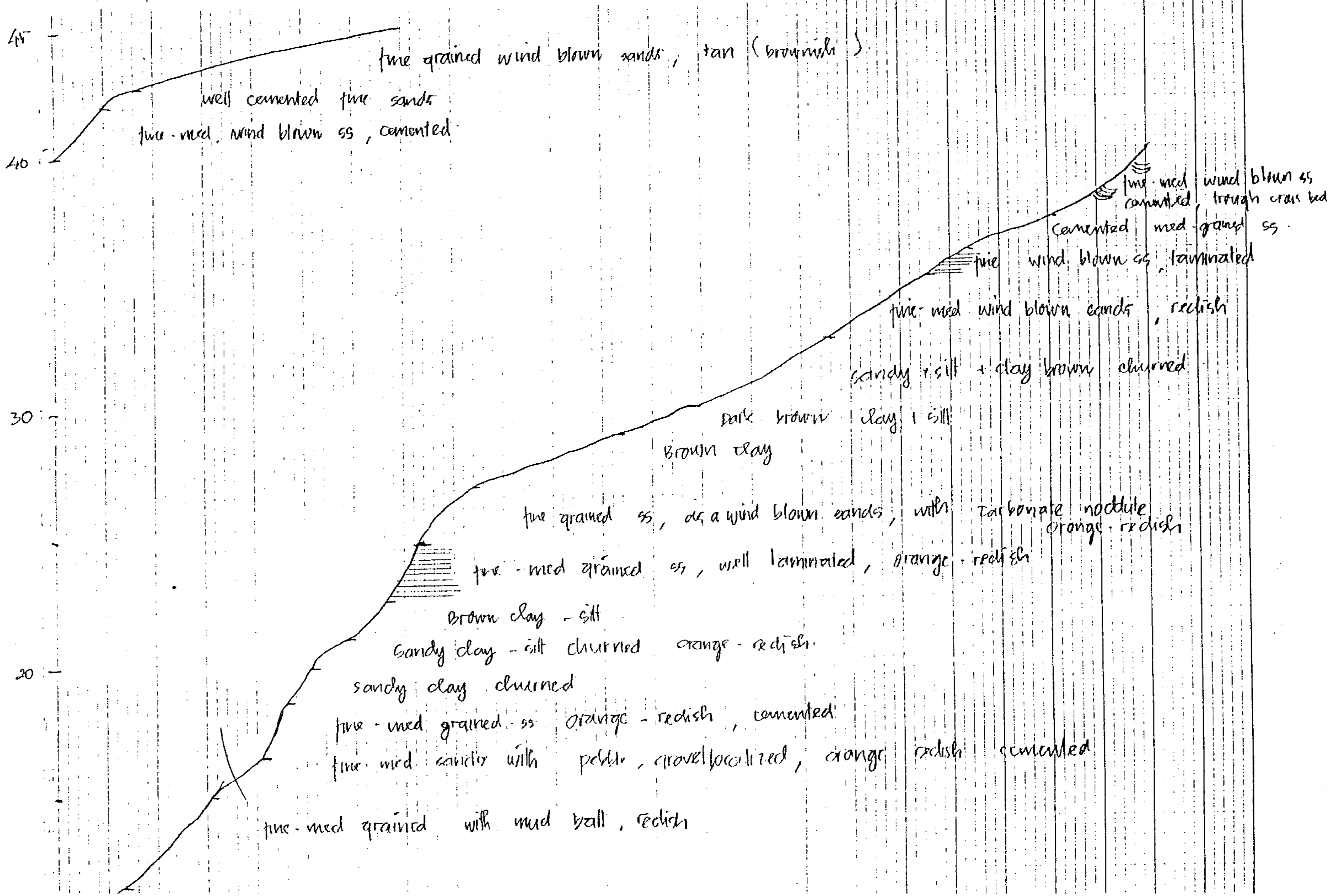

pg. 4 · June 27 section 3

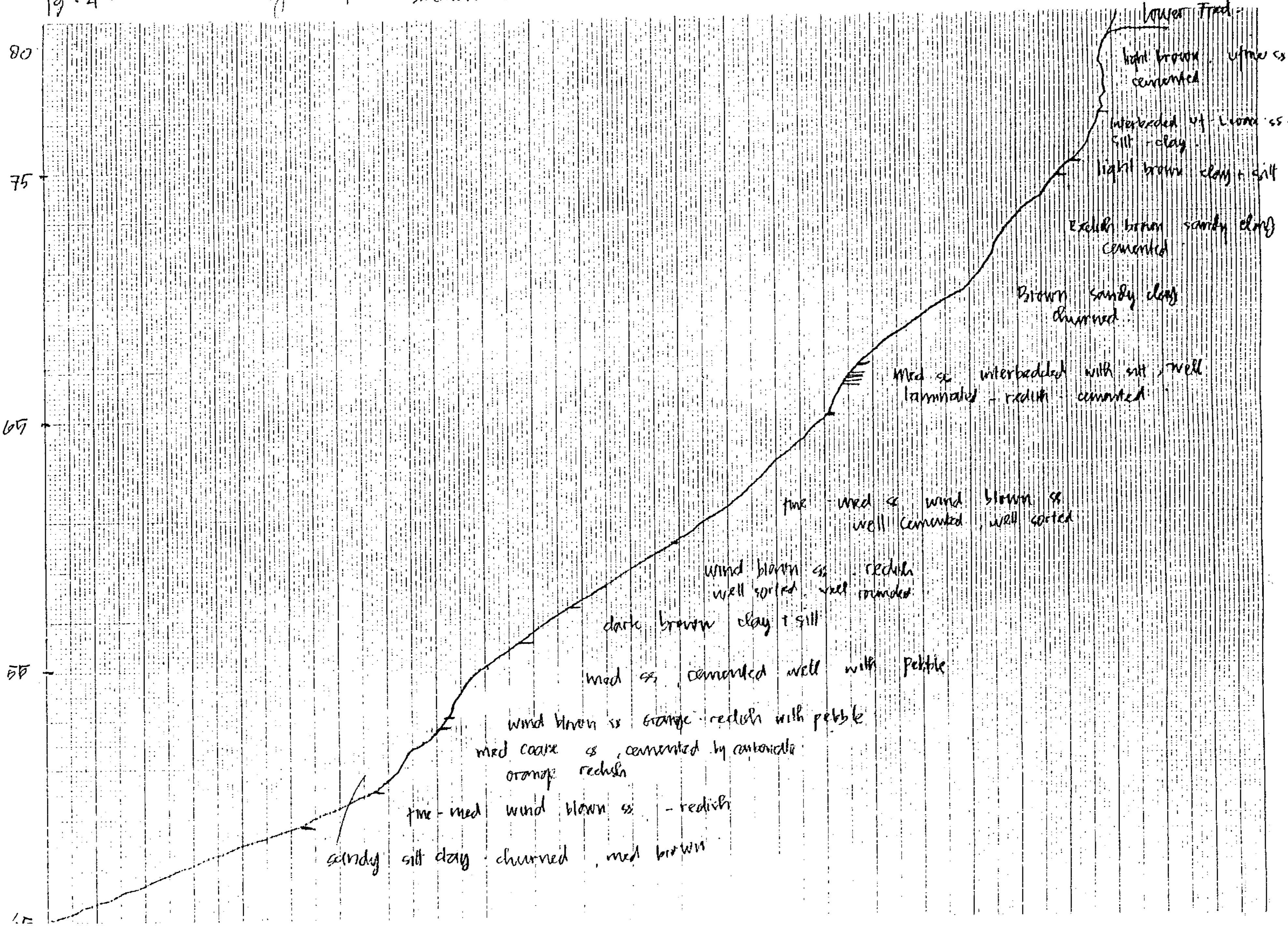

pg. 1. Section 4 1993.

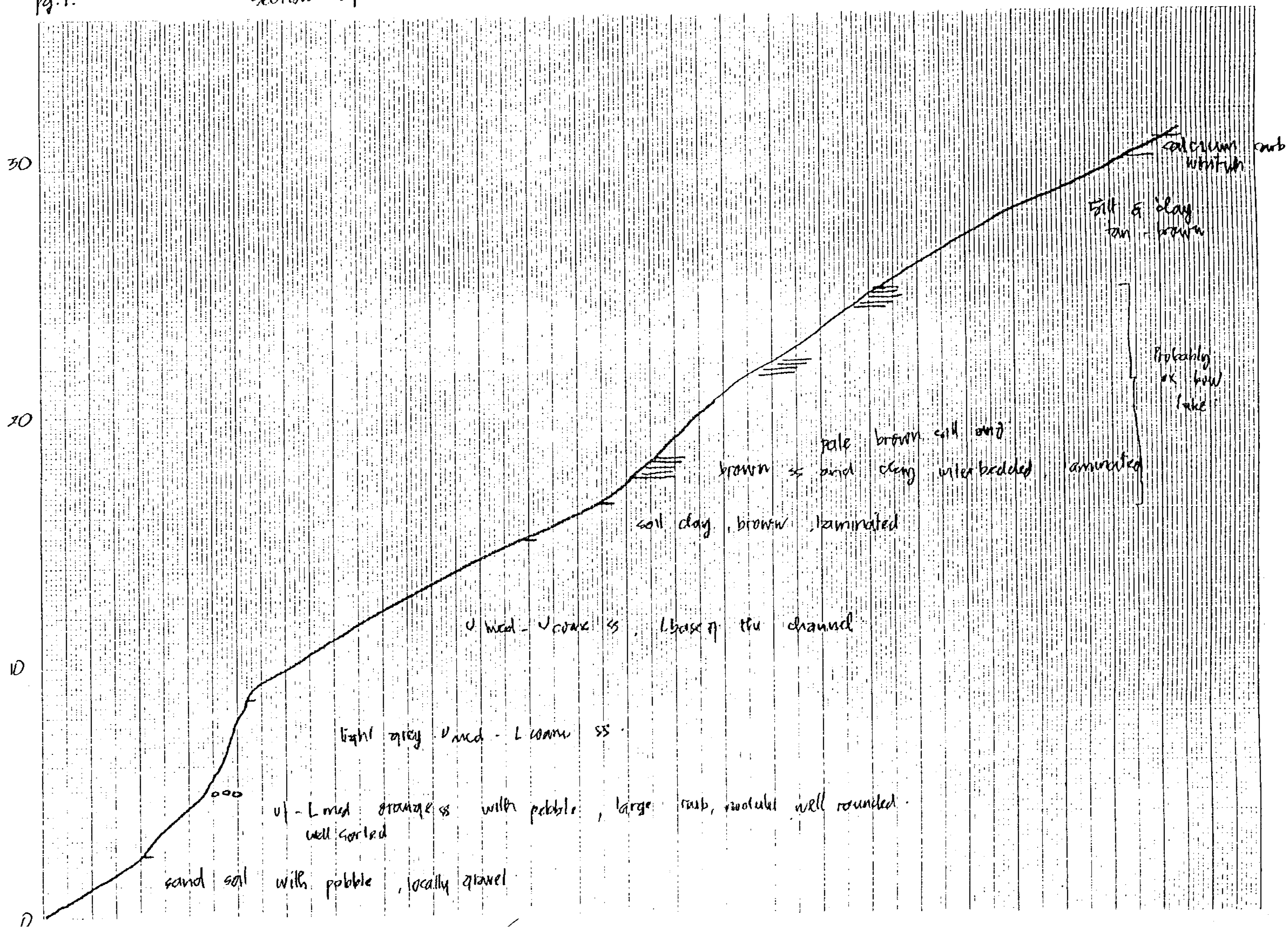

pg. 2. section 4

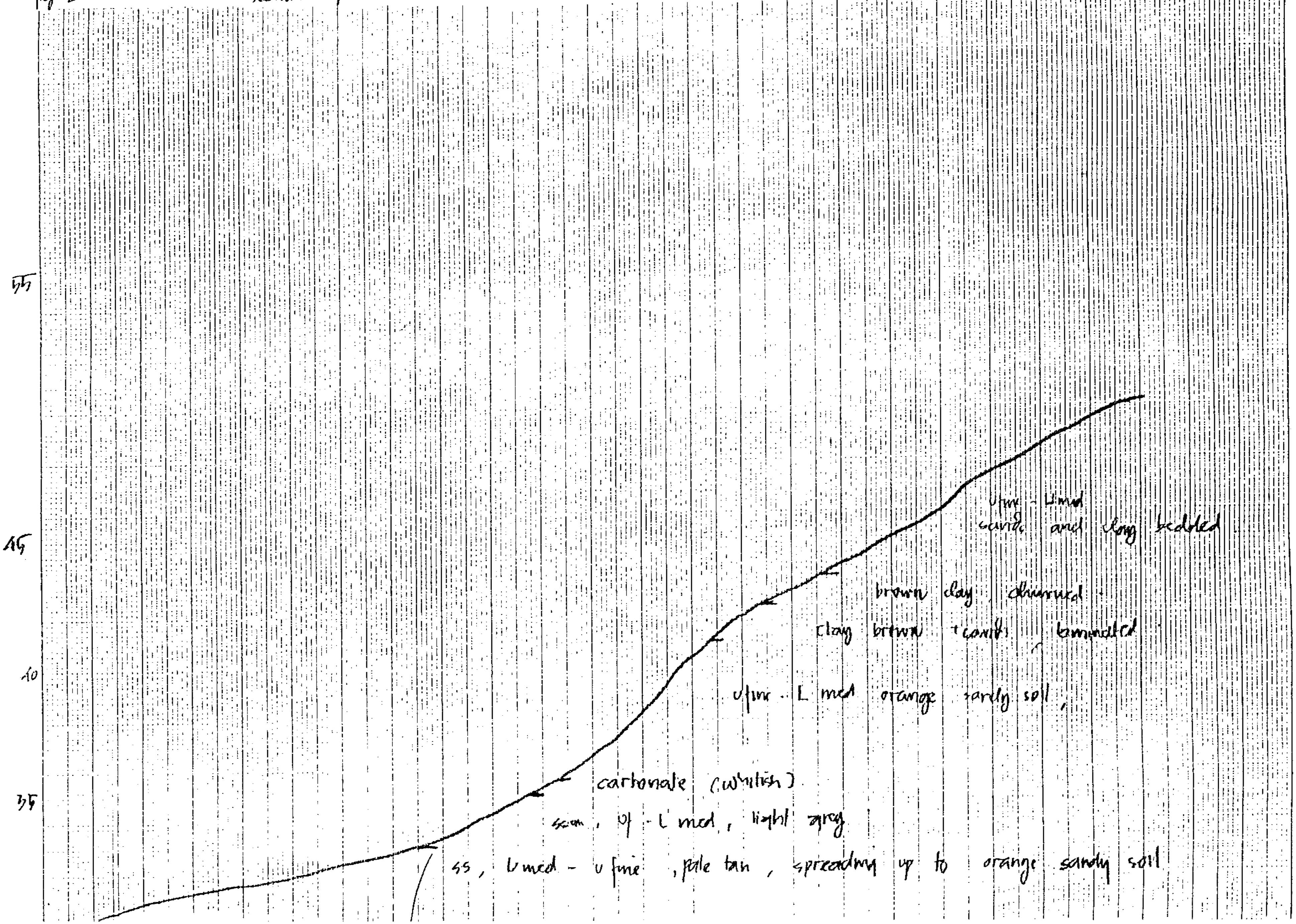

pg-3. Section 4. 1993

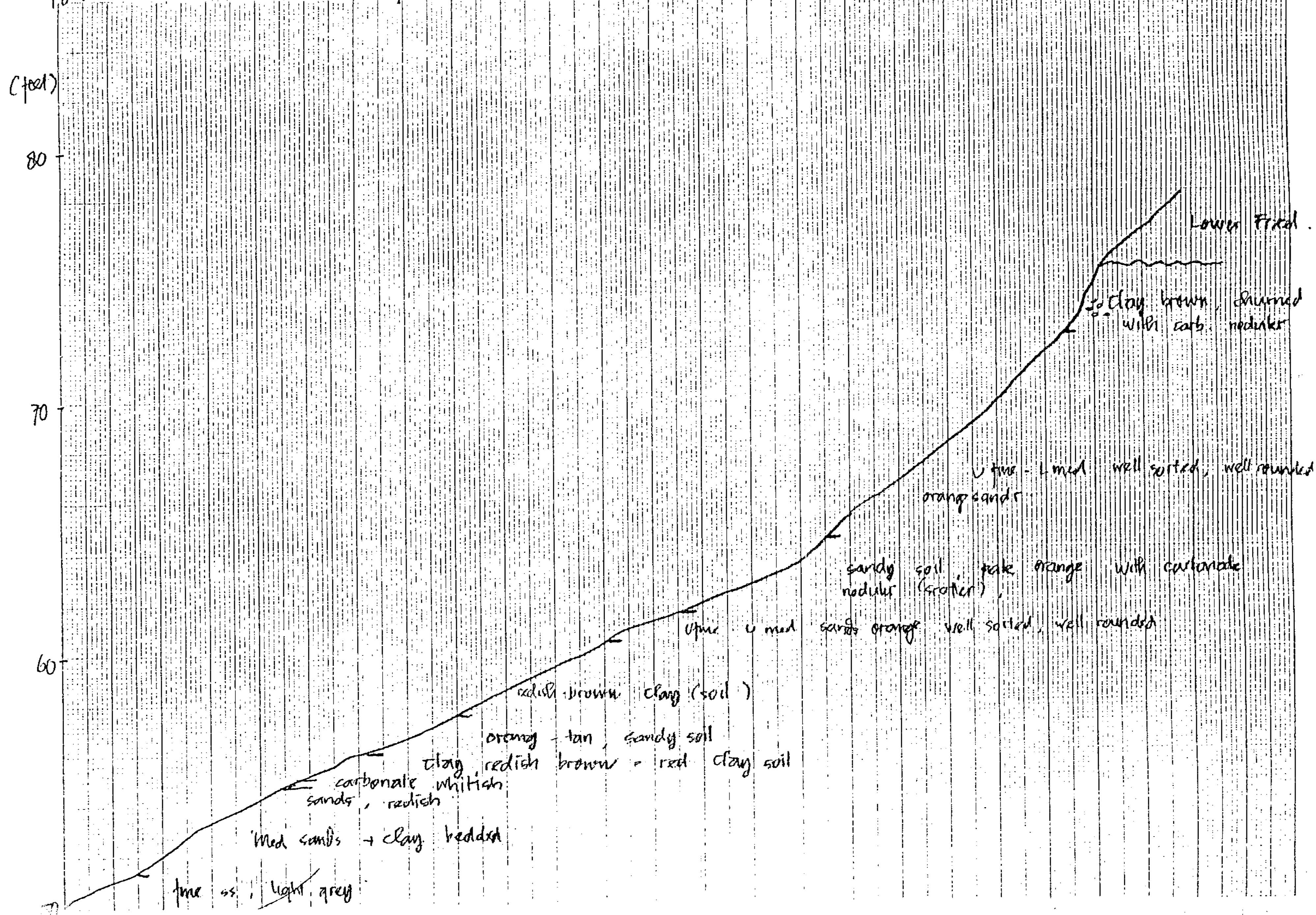

July 10/94 ① XIV

5

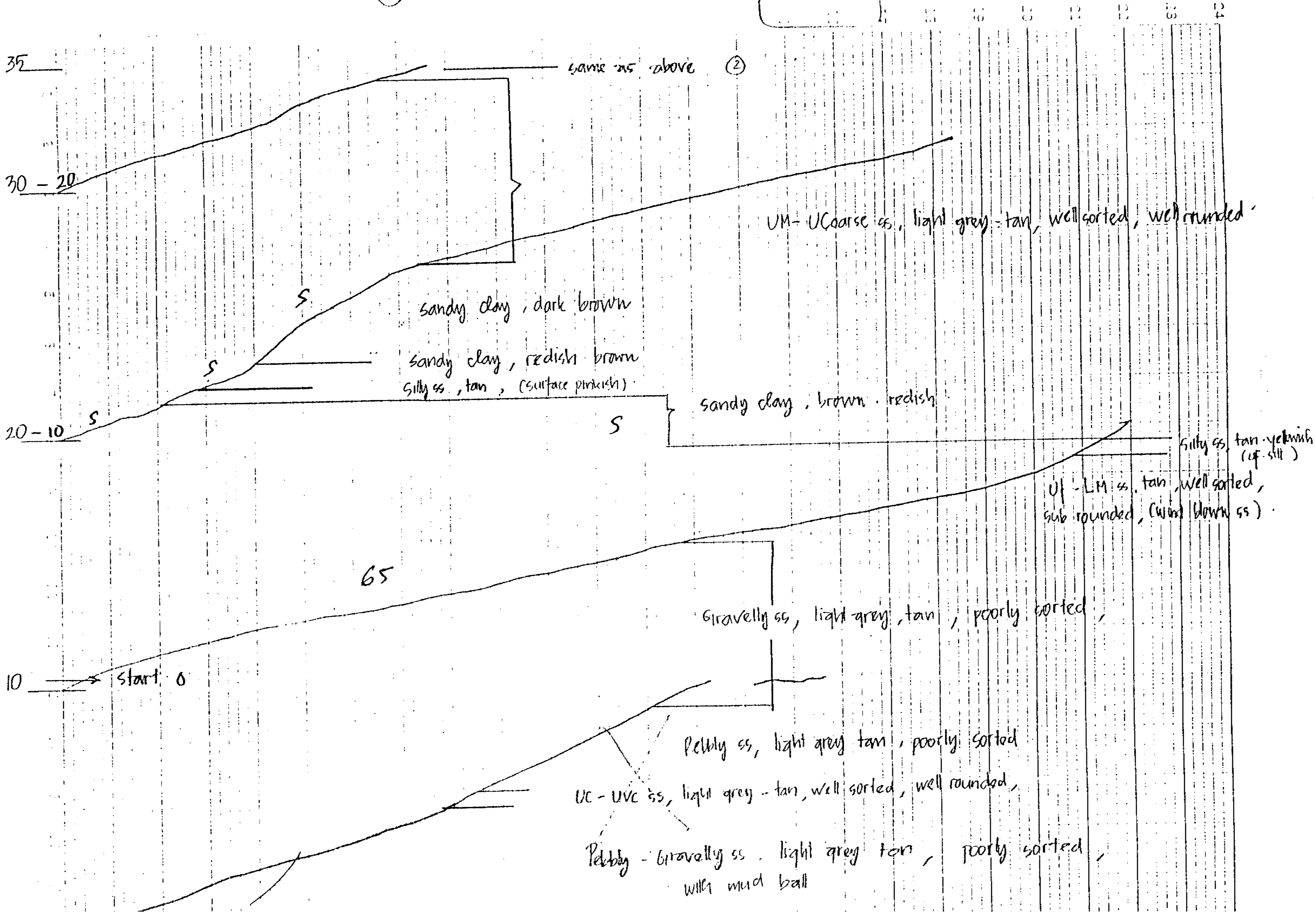

July 18/'91 (2) XIV

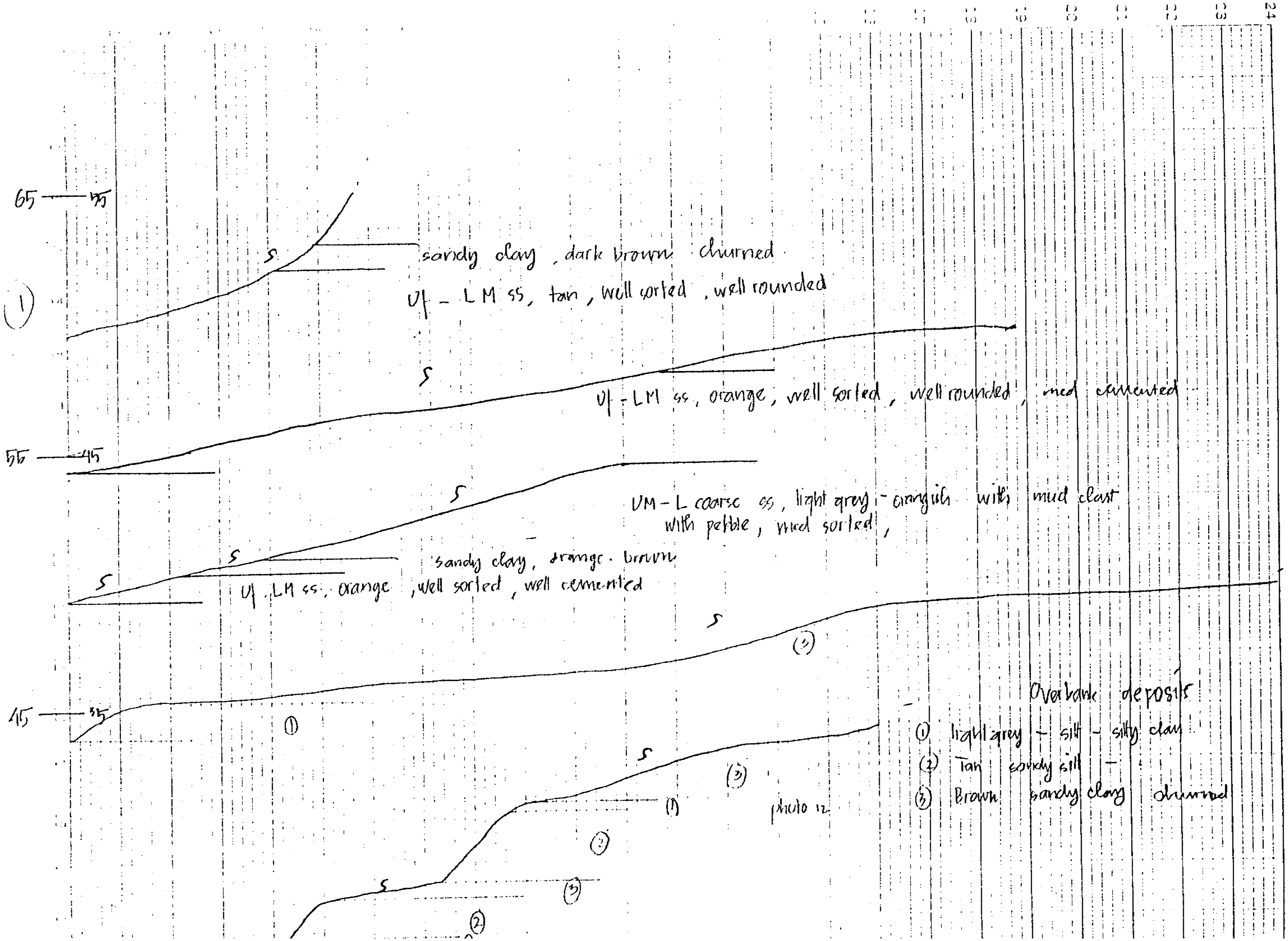

July 18/94 (3)

5

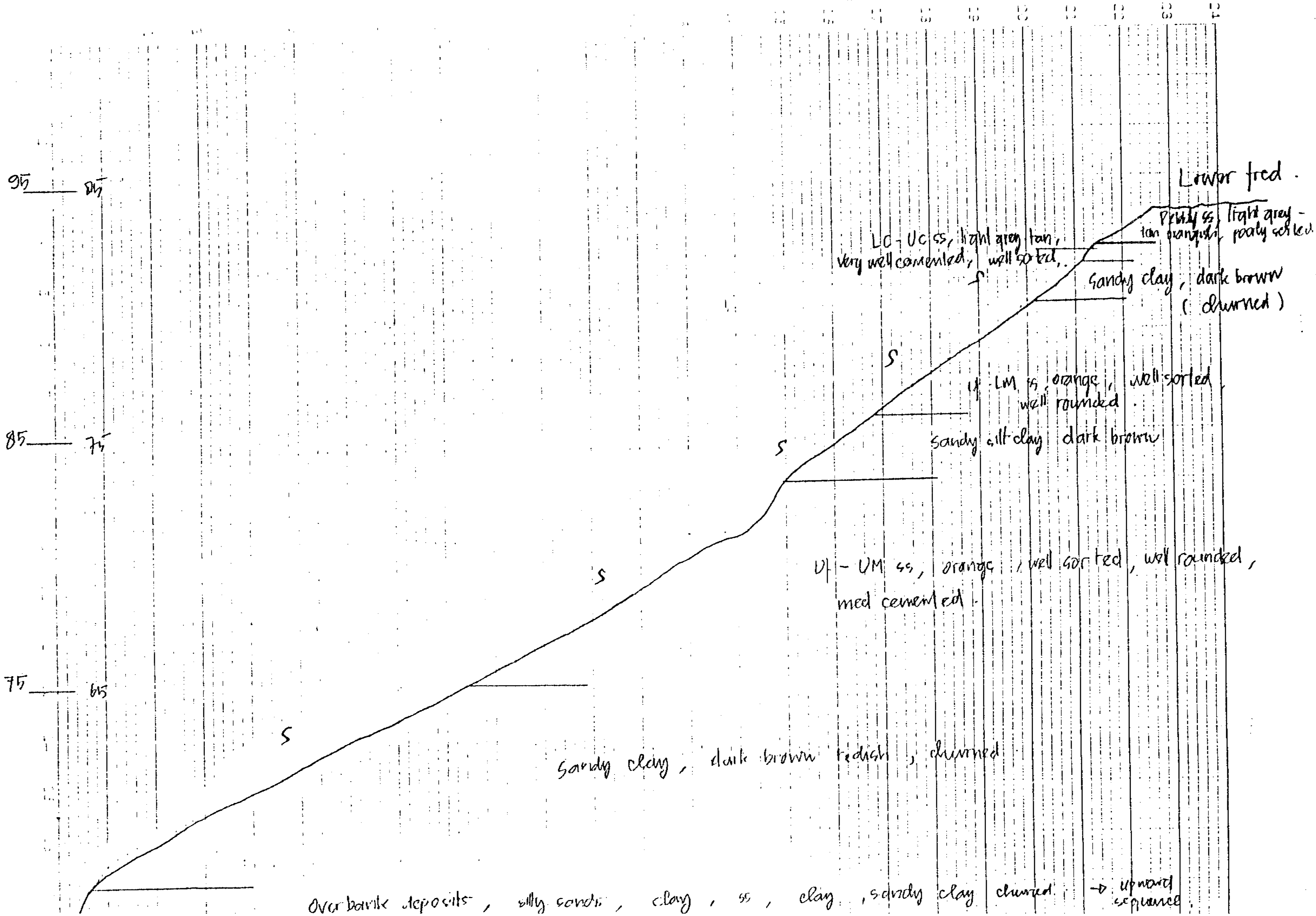

95 — 85
85 — 75
75 — 65
Lower fred.
Pebbly ss, light grey - tan orangish, poorly sorted
LC - UC ss, light grey tan, very well cemented, well sorted,
Sandy clay, dark brown (churned)
UF - LM ss, orange, well sorted, well rounded.
Sandy silt-clay dark brown
UF - UM ss, orange, well sorted, well rounded, med cemented.
Sandy clay, dark brown reddish, churned
Over bank deposits, silty sands, clay, ss, clay, sandy clay churned → upward sequence.

Pg 1. Section 6 Feb 19, 1994

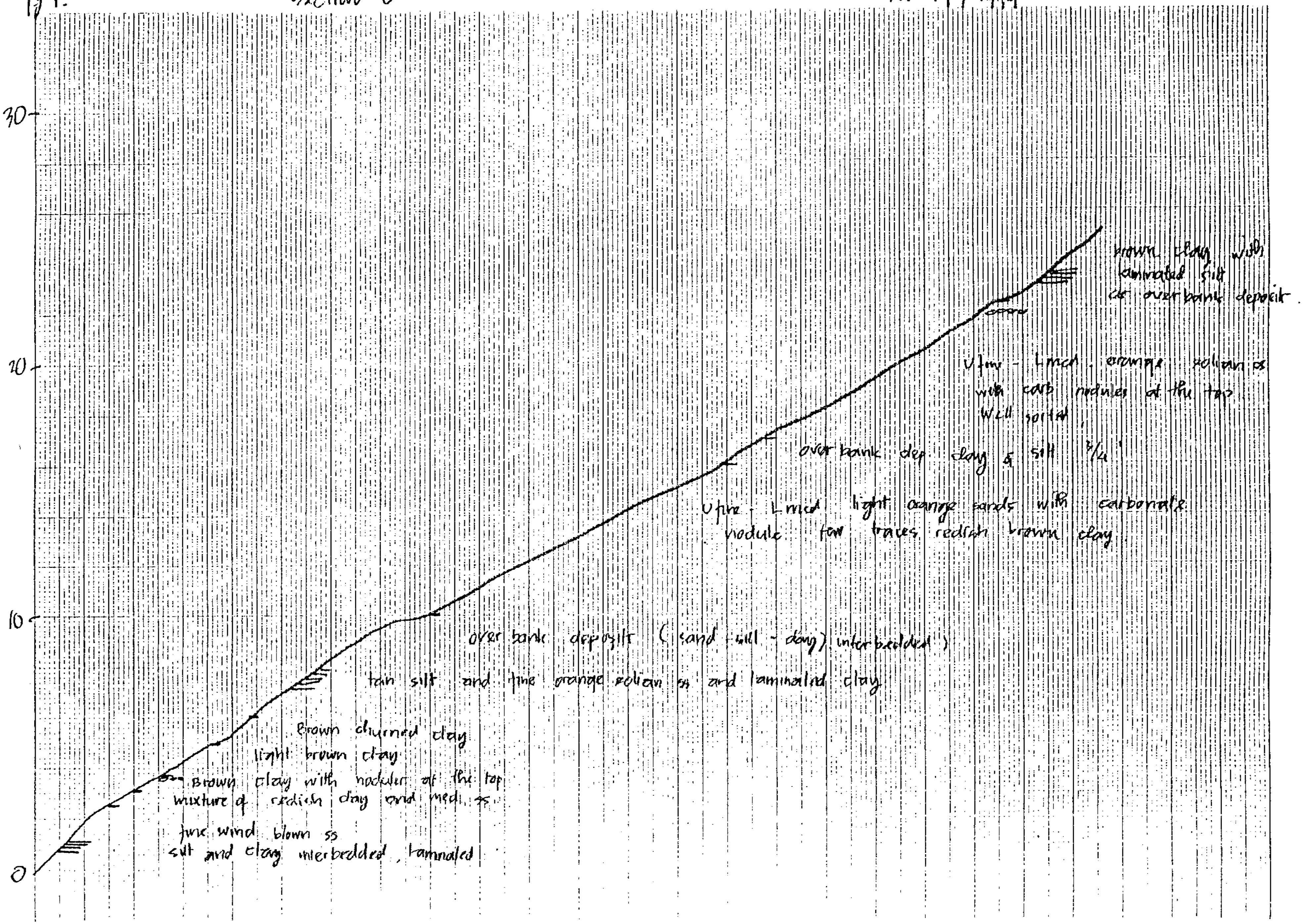

Fig. 2. Section C Feb 19, 1994

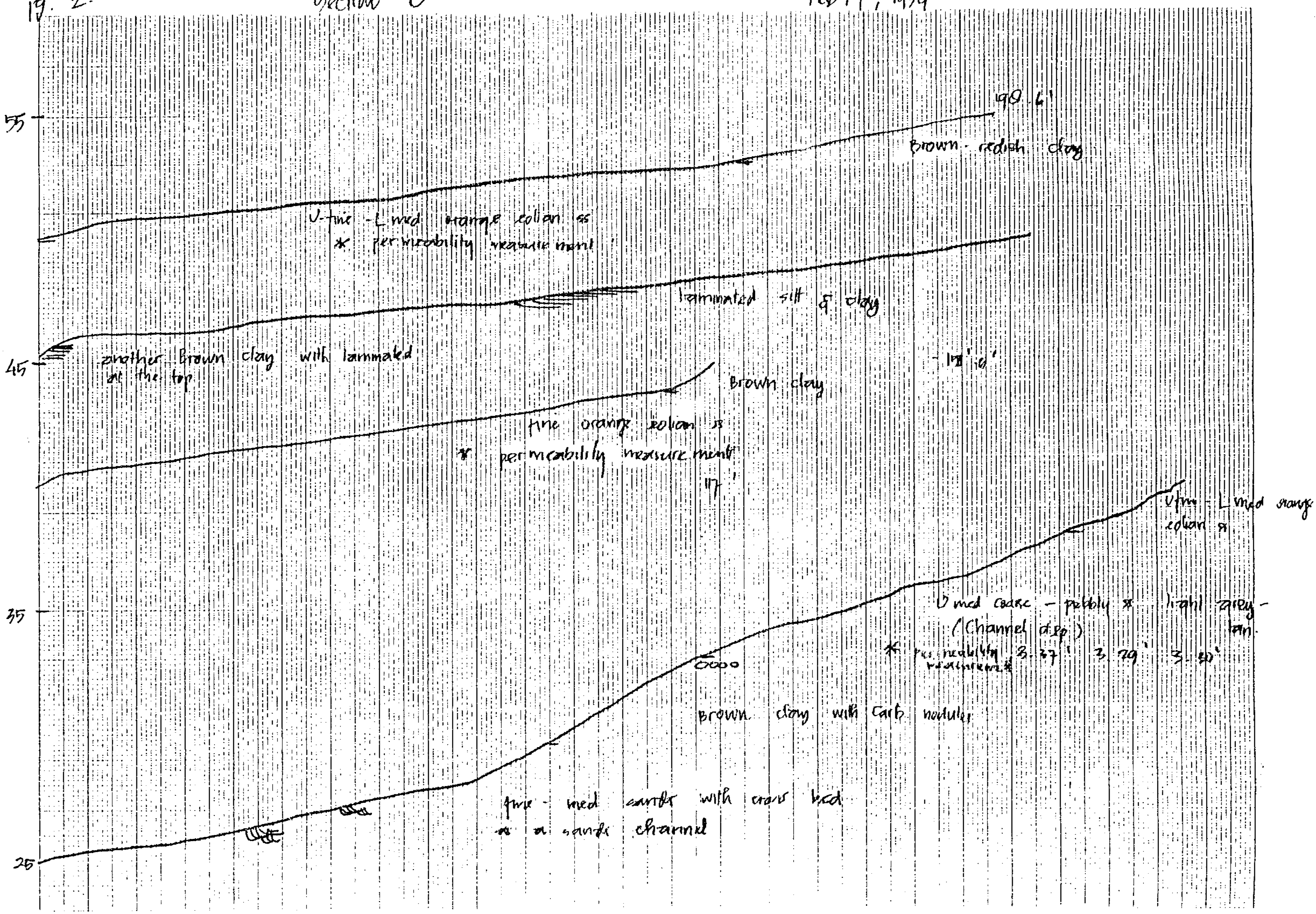

Pg-3 Section 6 Feb 19 1994

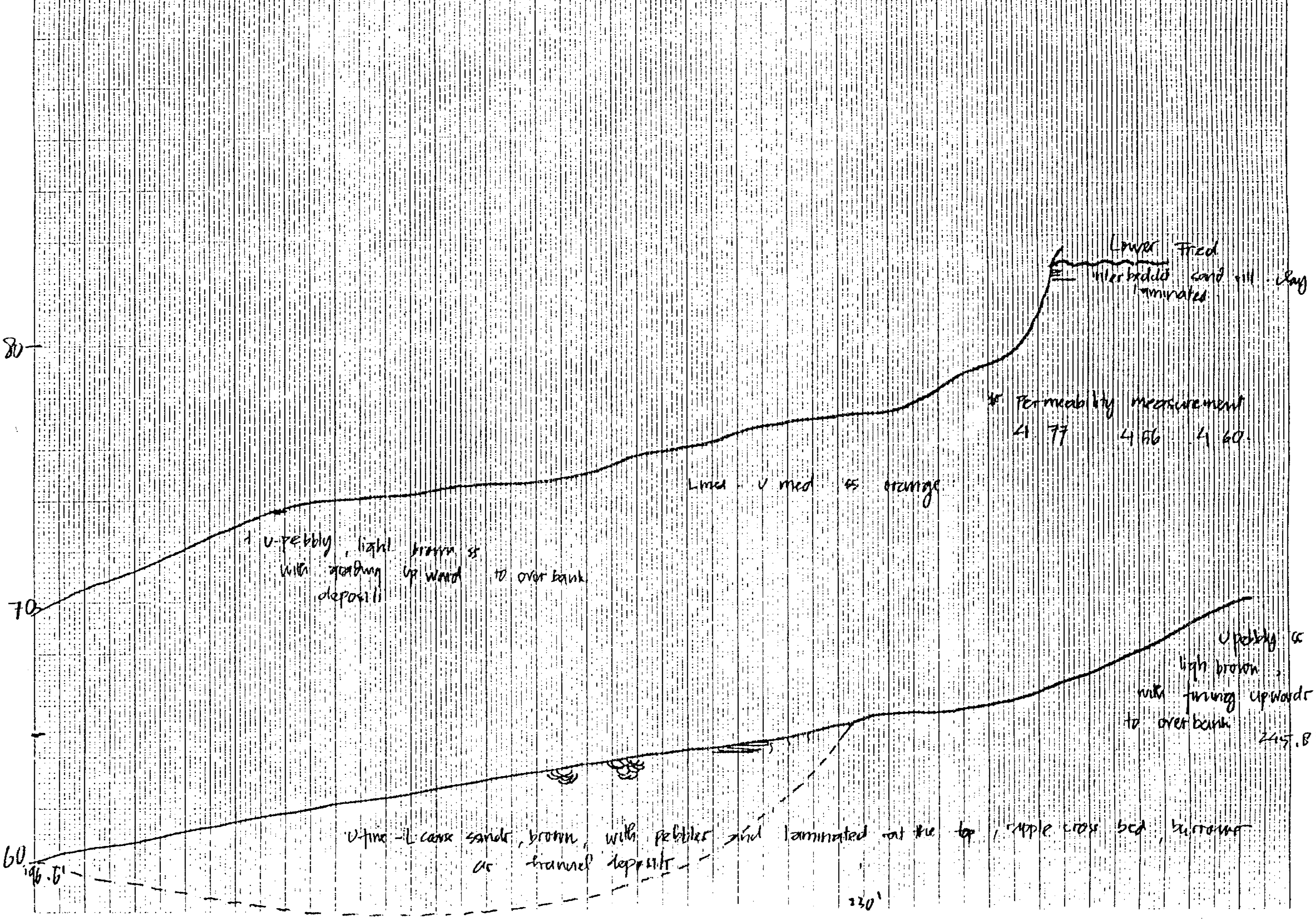

IV

① June 22/94 Section 7

(7)

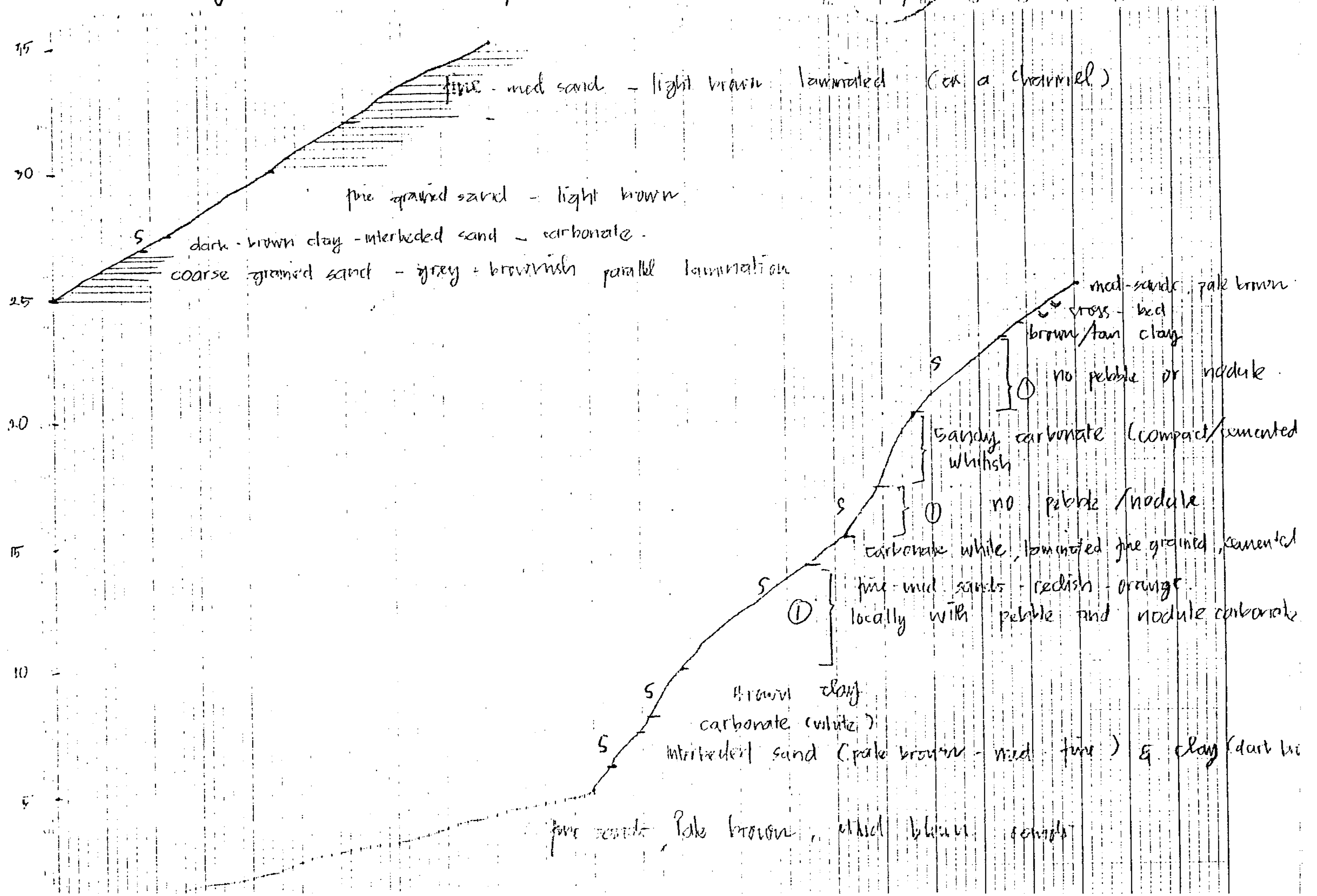

(2) June 22/94

Section 7

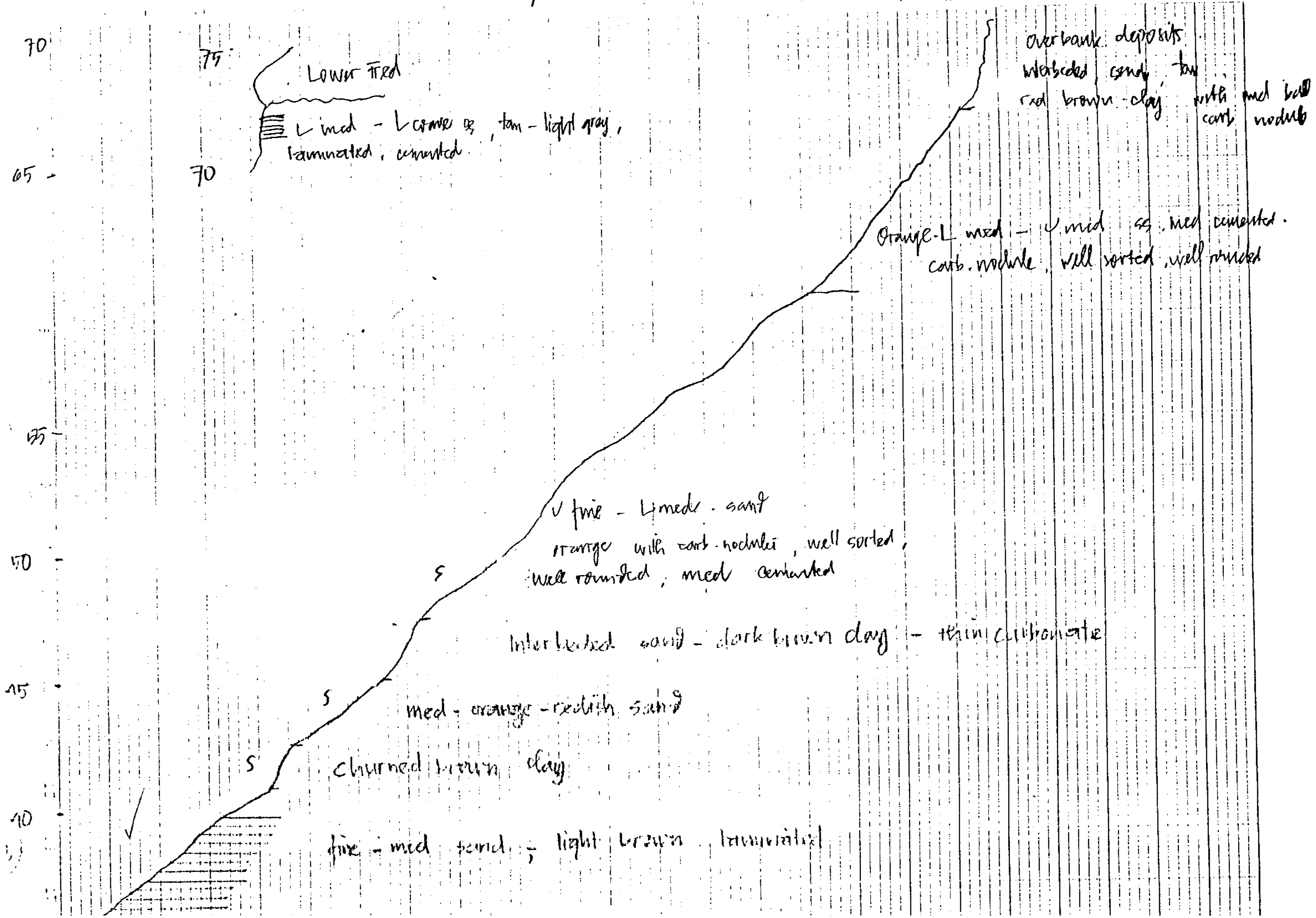

VII

June 20/94 ①

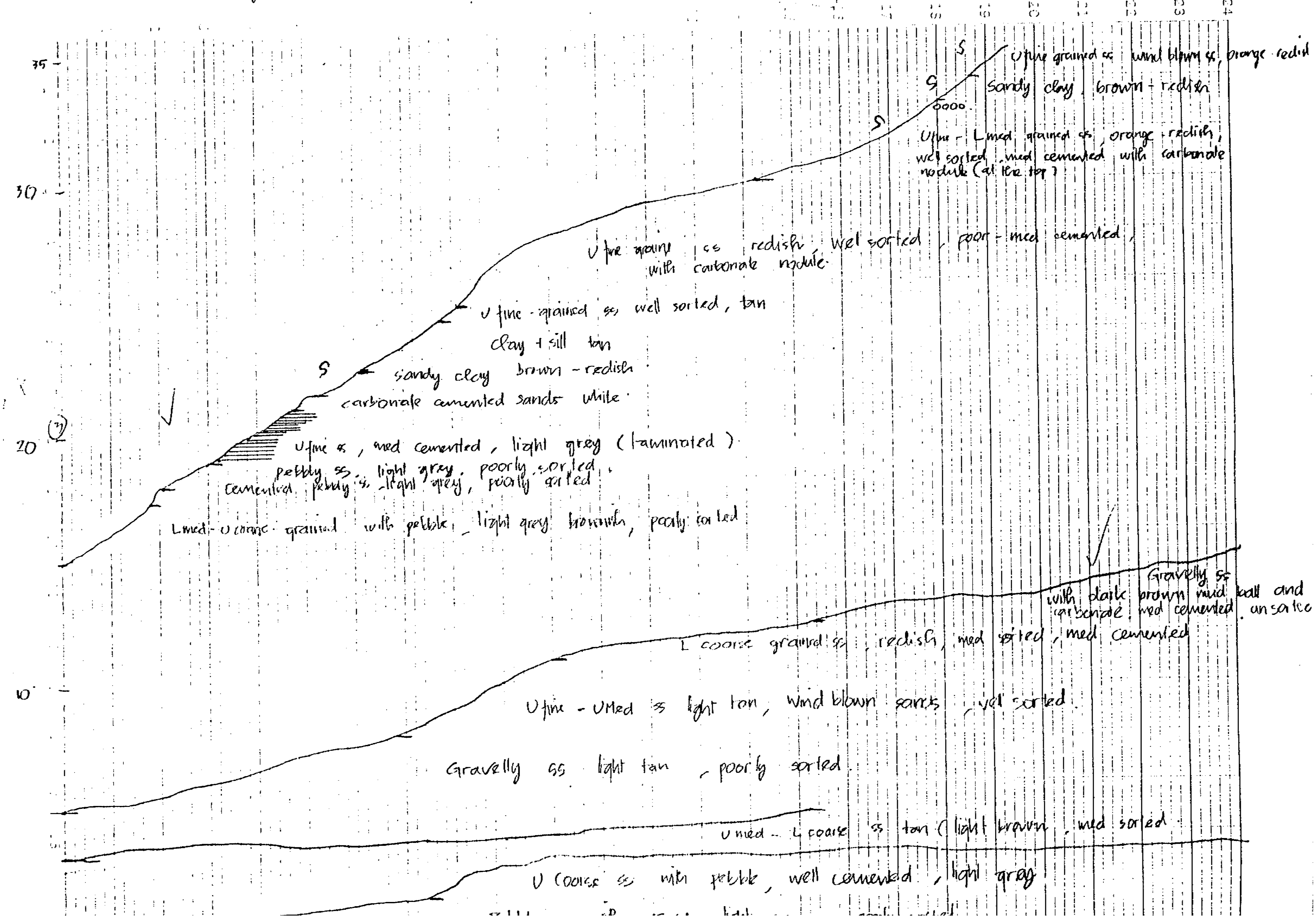

June 29/94 (2)

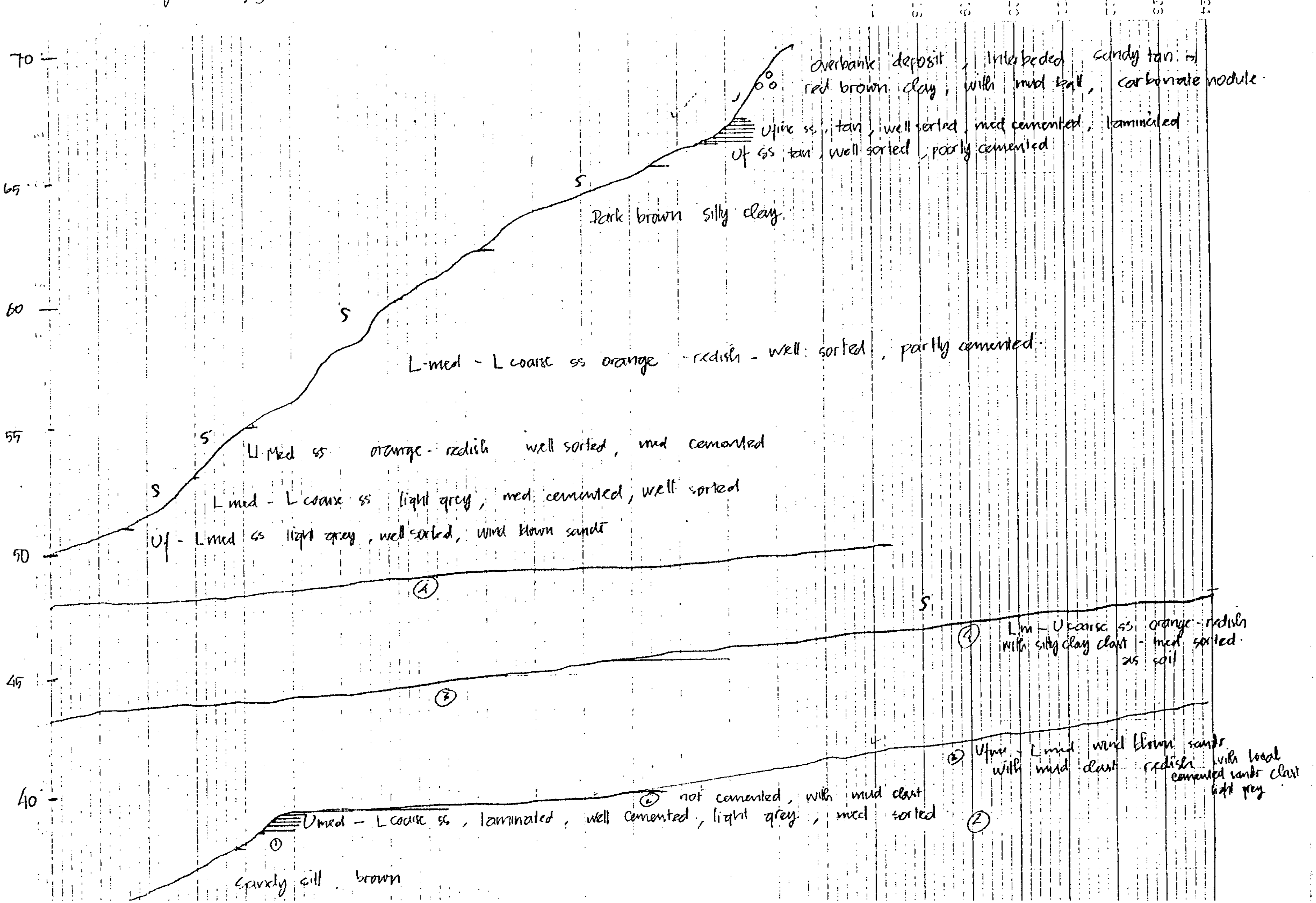
70
65
60
55
50
45
40
Overbank deposit, Interbeded sandy tan ~ red brown clay, with mud ball, carbonate nodule.
Ufine ss, tan, well sorted, med cemented, laminated
Uf ss tan, well sorted, poorly cemented
S
Dark brown silty clay.
S
L-med - L coarse ss orange - redish - well sorted, partly cemented.
S
U Med ss orange - redish well sorted, med cemented
S
L med - L coarse ss light grey, med cemented, well sorted
Uf - Lmed ss light grey, well sorted, wind blown sandt
A
S
4
Lm - Ucoarse ss orange - redish with silty clay clast - med sorted.
ss soil
3
3
Ufine - Lmed wind blown sandr with mud clast redish with local cemented sandr clast light grey
c
not cemented, with mud clast
Umed - L coarse ss, laminated, well cemented, light grey, med sorted
2
1
Sandy cill, brown

June 29/94 (3)

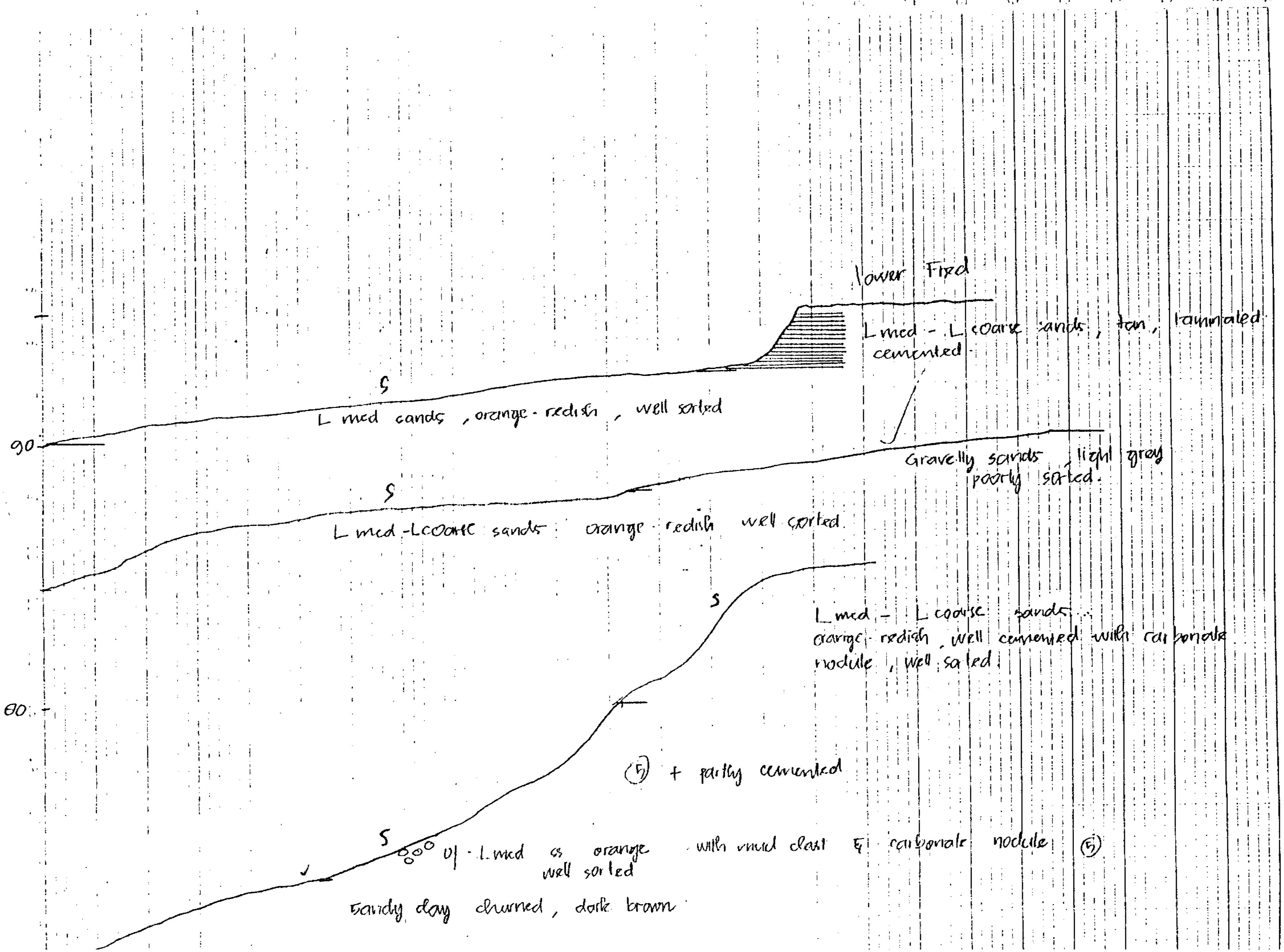
lower Fred
L med - L coarse sands, tan, laminated
cemented
L med cands, orange-redish, well sorted
90
Gravelly sands light grey
poorly sorted.
L med - L coarse sands orange redish well sorted
L med - L coarse sands
orange redish, well cemented with carbonate
nodule, well sorted
80
(5) + partly cemented
of L med cs orange
well sorted
with mud clast & carbonate nodule (5)
Sandy clay churned, dark brown

july 5/94 (4)

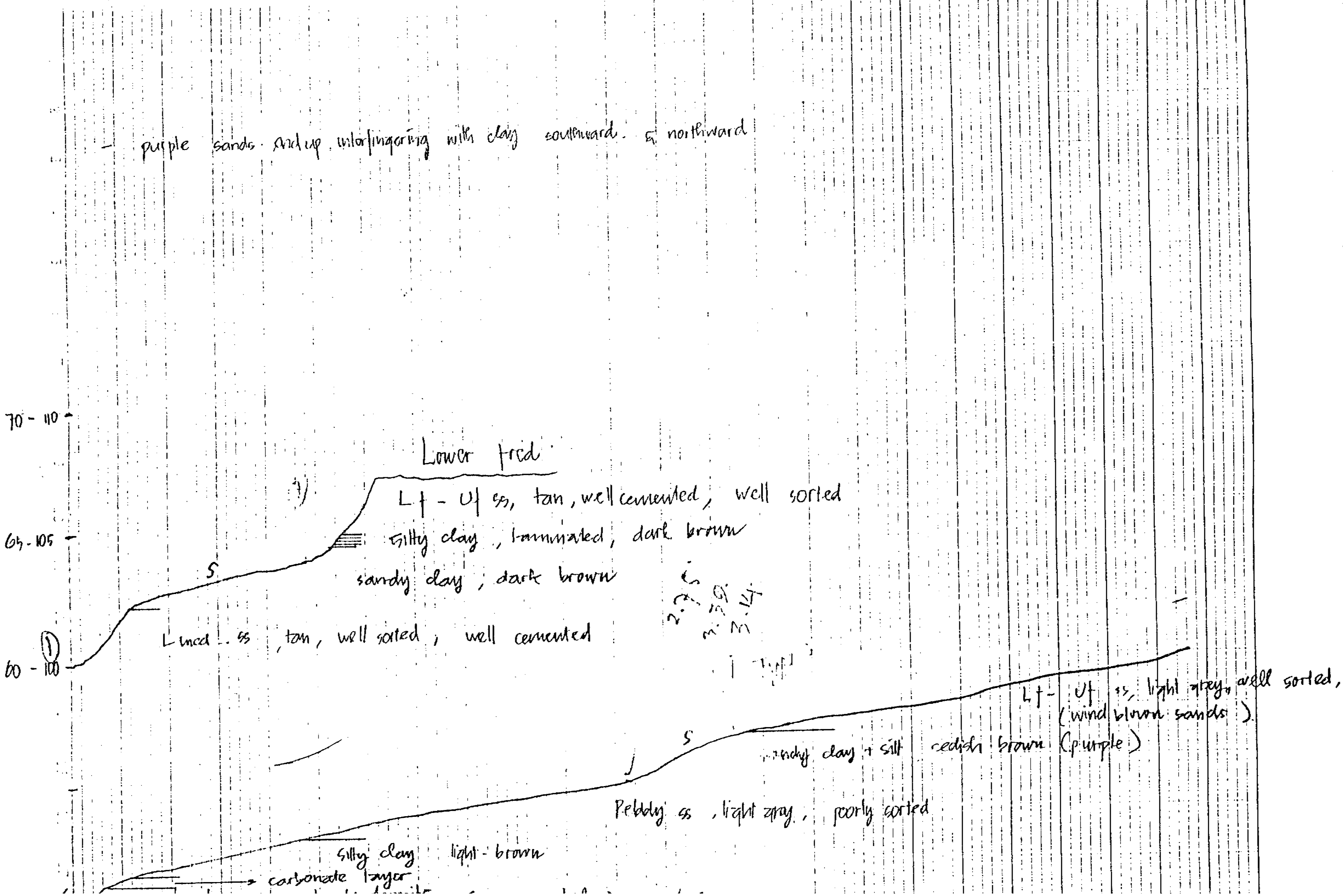
purple sands and up interfingering with clay southward. ss northward
70 - 110
65 - 105
60 - 100
(1)
Lower fred
Lf - Uf ss, tan, well cemented, well sorted
Silty clay, laminated, dark brown
sandy clay, dark brown
S
L med . ss, tan, well sorted, well cemented
Lf - Uf ss, light grey, well sorted,
(wind blown sands)
sandy clay + silt reddish brown (purple)
S
Pebbly ss, light gray, poorly sorted
Silty clay light - brown
carbonate layer

9

gale 1/94 (1)

VIII

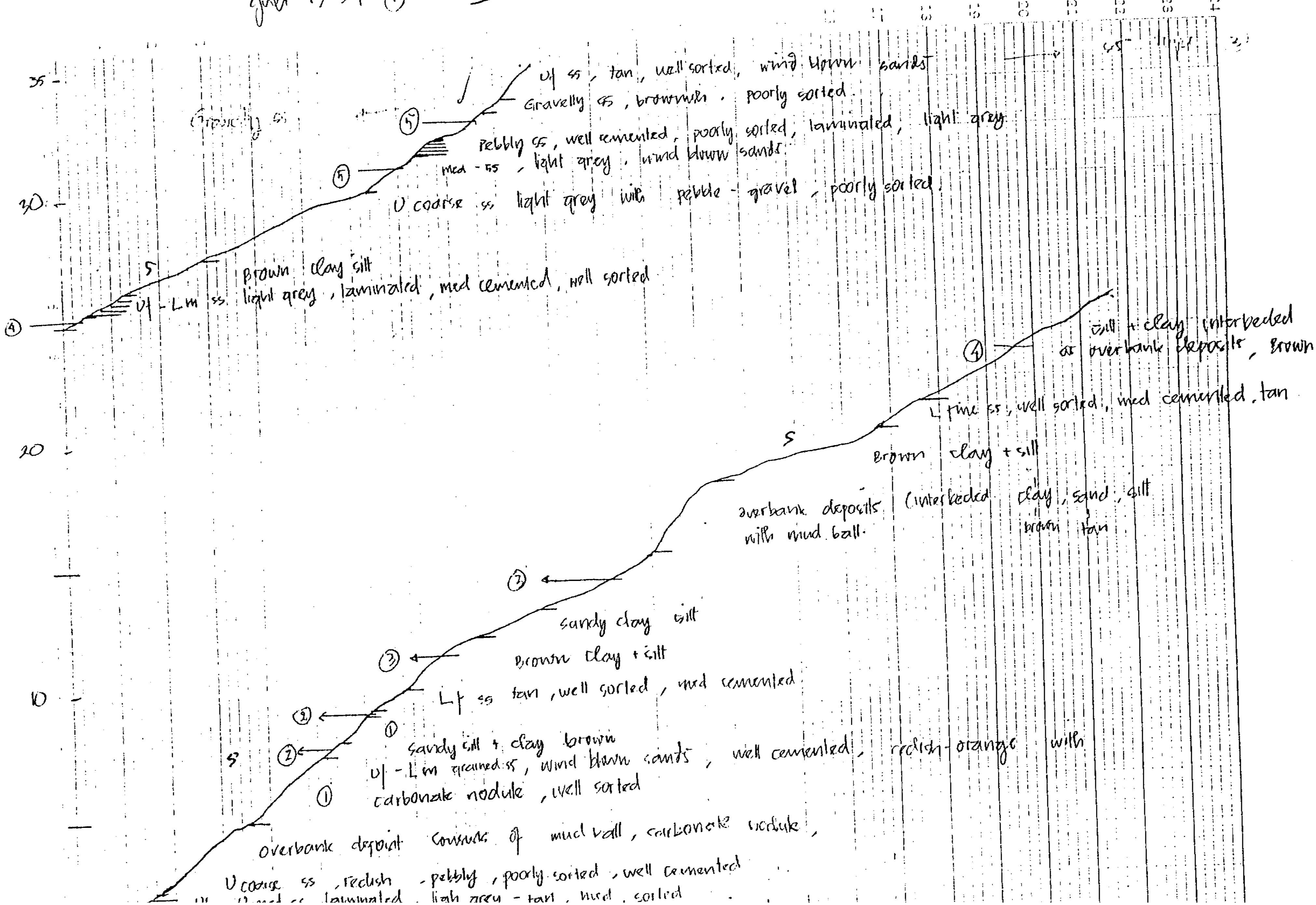

July 1/94 (3)

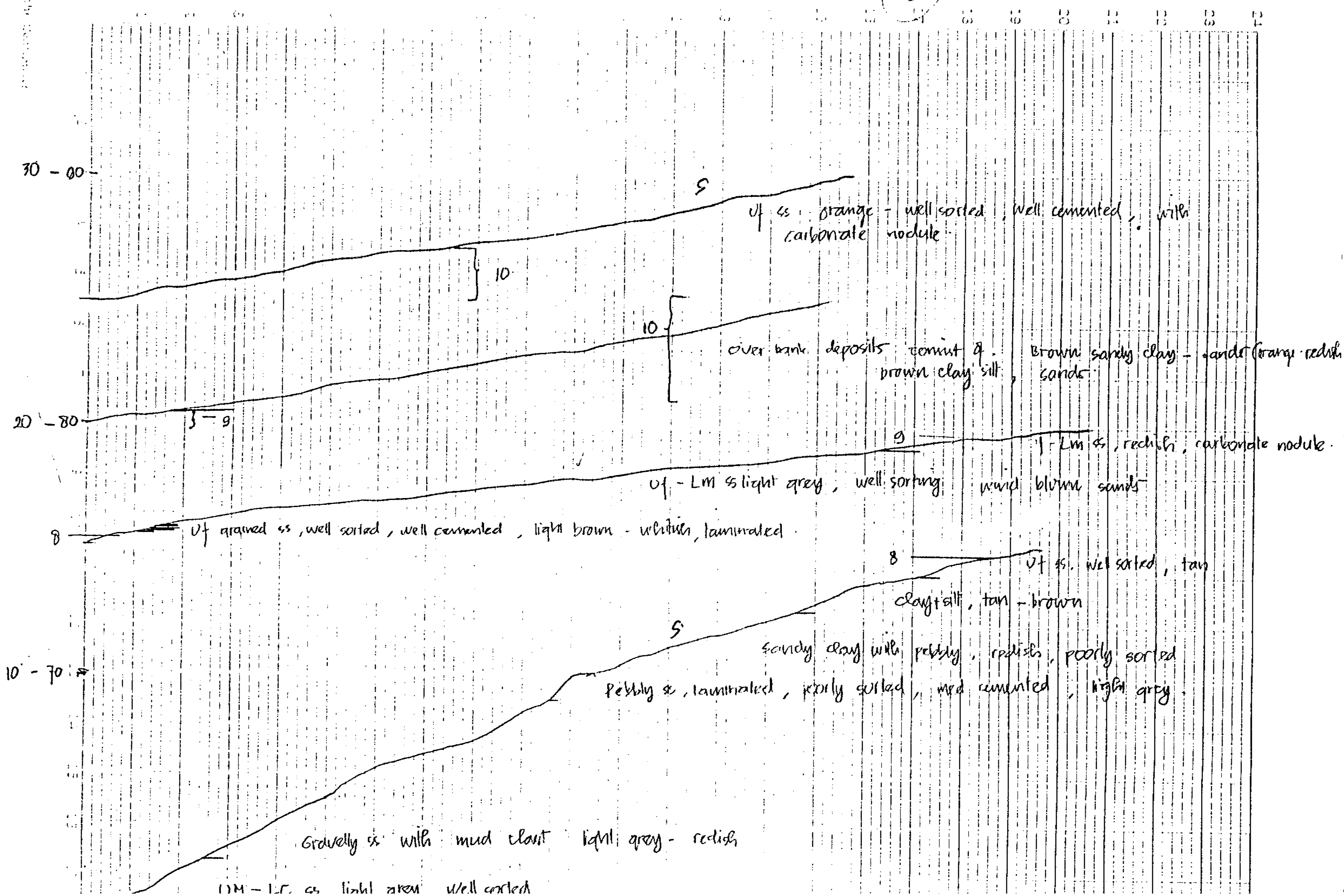
30 - 00
20 - 80
8
10 - 70
5
10
Uf ss orange - well sorted, Well cemented, with carbonate nodule
over bank deposits consist of brown clay silt, Brown sandy clay - sands (orange reddish sands
9
Uf - Lm ss, reddish, carbonate nodule
Uf - Lm ss light grey, well sorting, wind blown sands
Uf grained ss, well sorted, well cemented, light brown - whitish, laminated
8
Uf ss. well sorted, tan
clay+silt, tan - brown
Sandy clay with pebbly, reddish, poorly sorted
Pebbly ss, laminated, poorly sorted, med cemented, light grey
Gravelly ss with mud clast light grey - reddish
UM - LC ss light grey well sorted

July 1/94 (4)

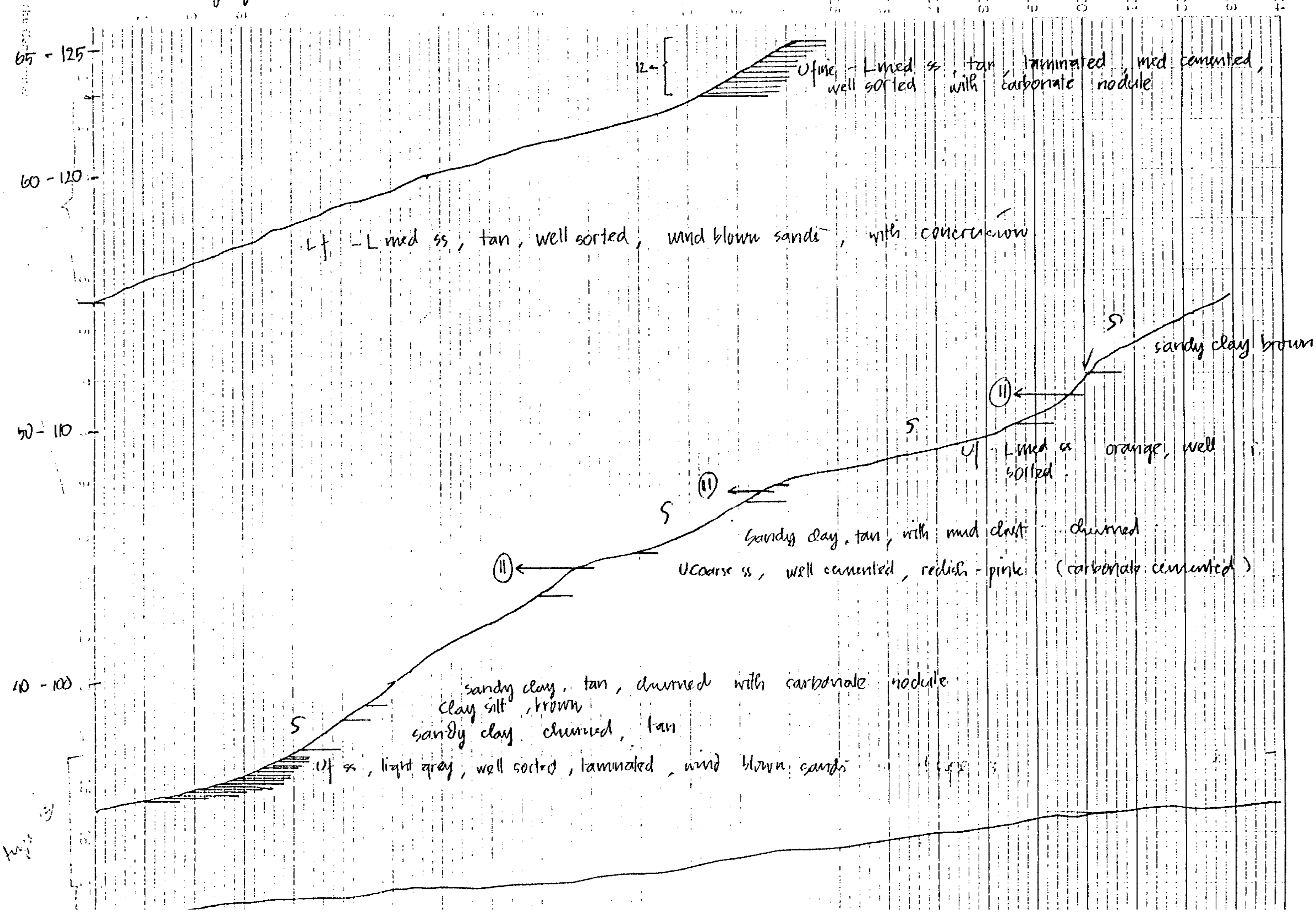
65 - 125
60 - 120
50 - 110
40 - 100
12
Ufine - L med ss, tan, laminated, med cemented, well sorted with carbonate nodule
L f - L med ss, tan, well sorted, wind blown sands, with concrecion
S
sandy clay brown
11
S
U f - L med ss orange, well sorted
11
S
Sandy clay, tan, with mud clast churned
11
U coarse ss, well cemented, redish - pink (carbonate cemented)
sandy clay, tan, churned with carbonate nodule
clay silt, brown
sandy clay churned, tan
S
U f ss, light grey, well sorted, laminated, wind blown sands

July 1/94 (5)

9

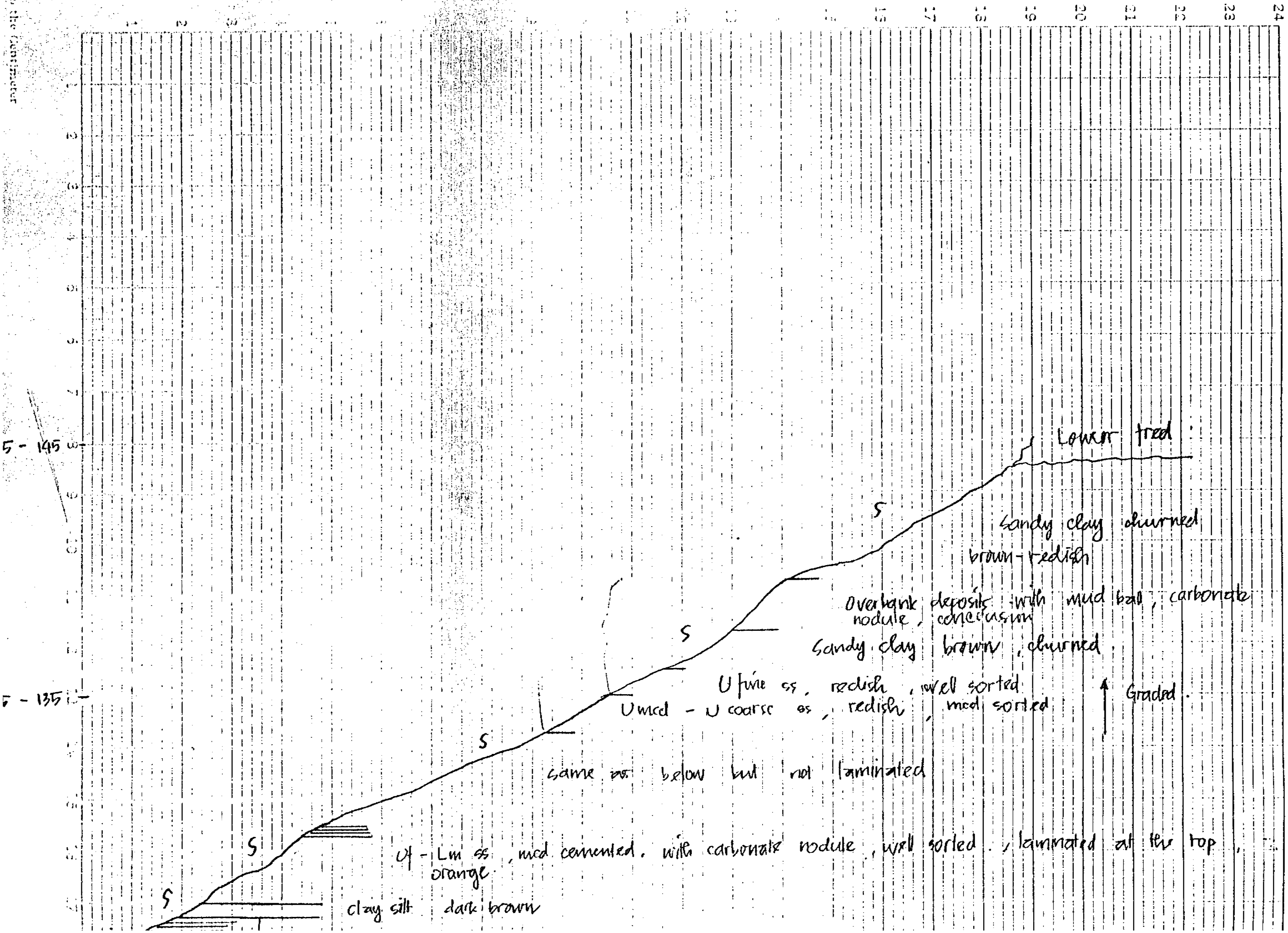

Squares to the Centimeter

July 5 /94 (1) IX

10

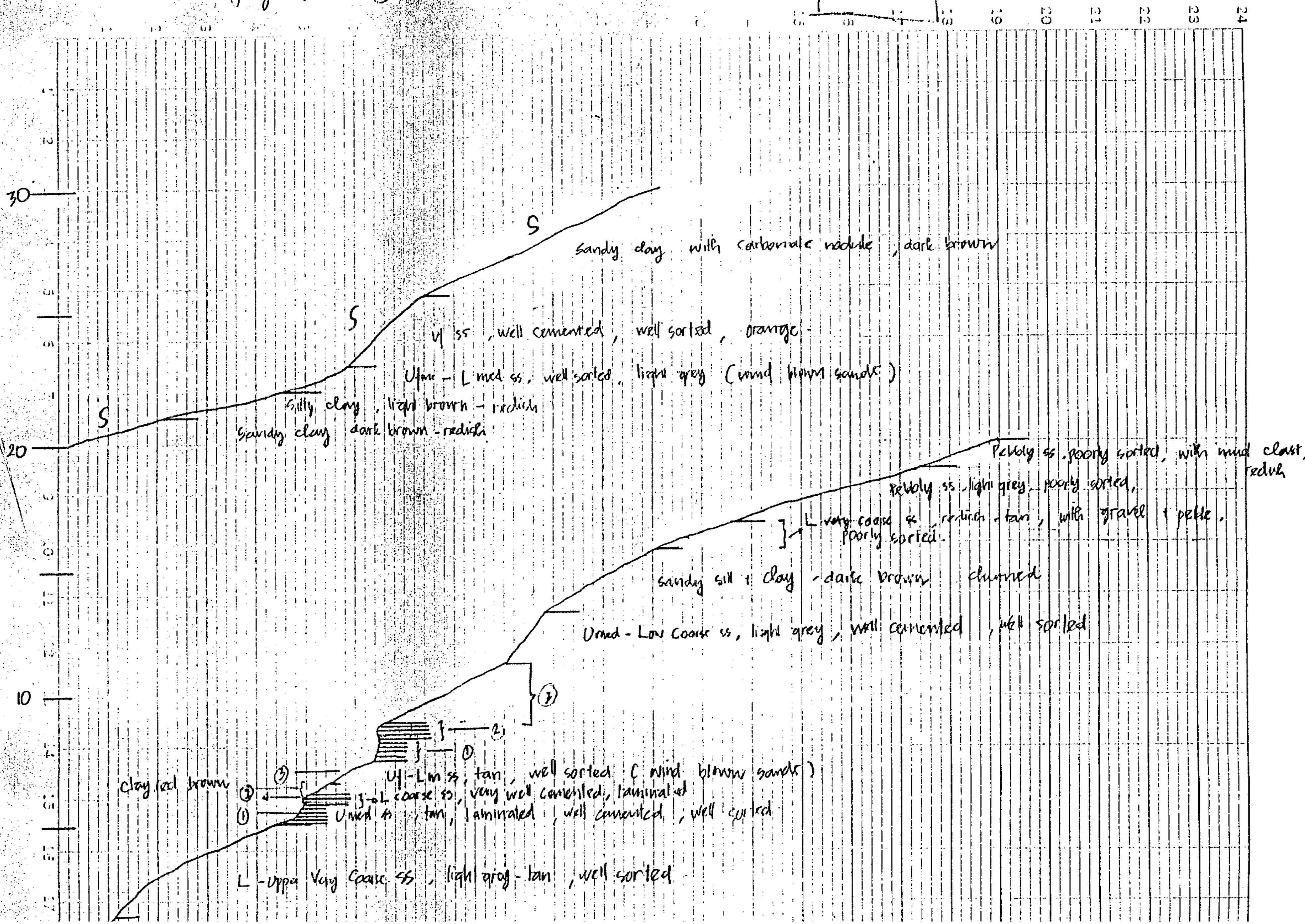

Squares to the Centimeter

July 5/94 (2)

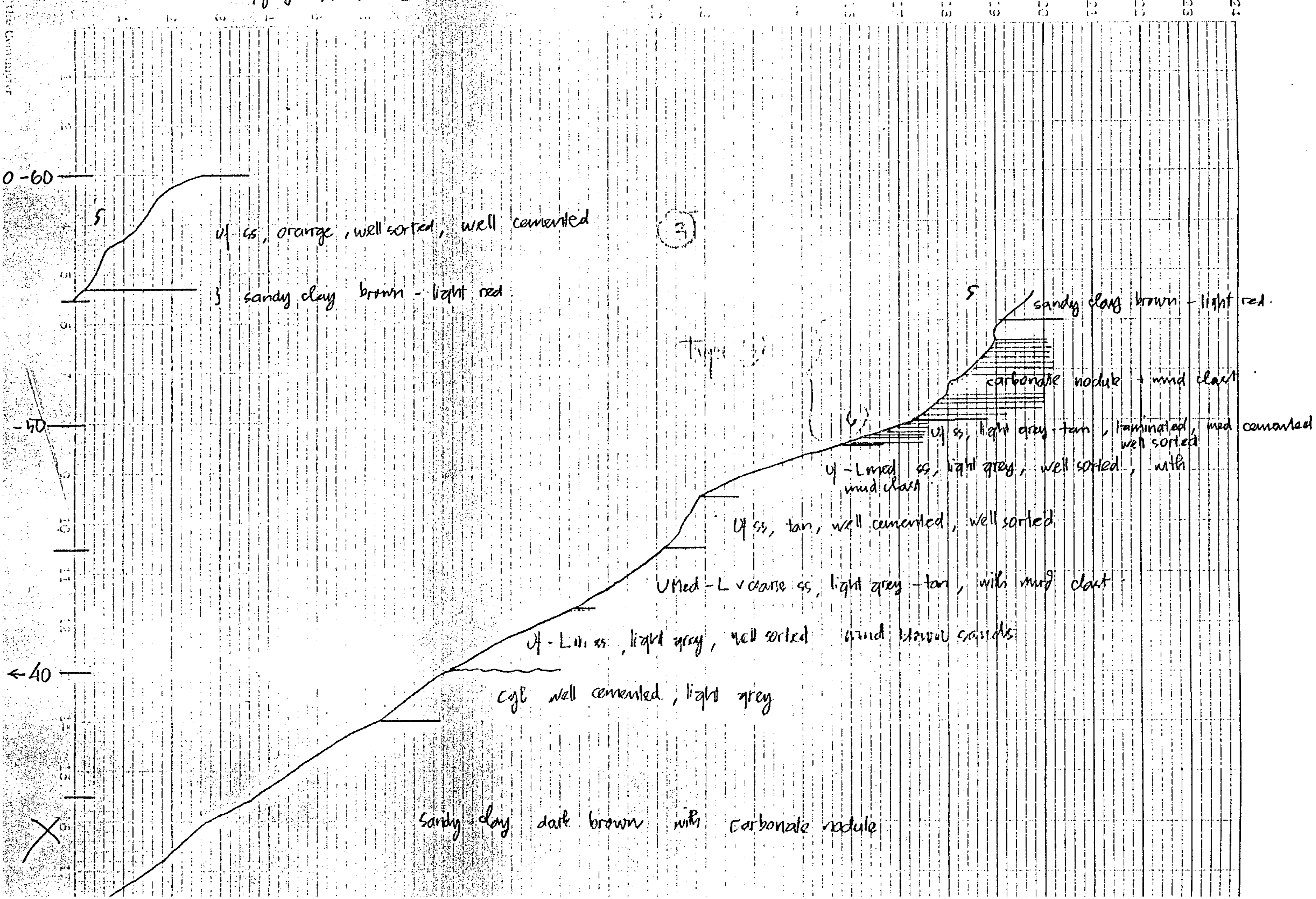

0-60
-50
←40
Uf ss, orange, well sorted, well cemented
sandy clay brown - light red
sandy clay brown - light red.
carbonate nodule + mud clast
Uf ss, light grey - tan, laminated, med cemented, well sorted
Uf - Lmed ss, light grey, well sorted, with mud clast
Uf ss, tan, well cemented, well sorted
UMed - L v coarse ss, light grey - tan, with mud clast
Uf - Lm ss, light grey, well sorted
Cgl well cemented, light grey
Sandy clay dark brown with carbonate nodule

July 5/99, 3

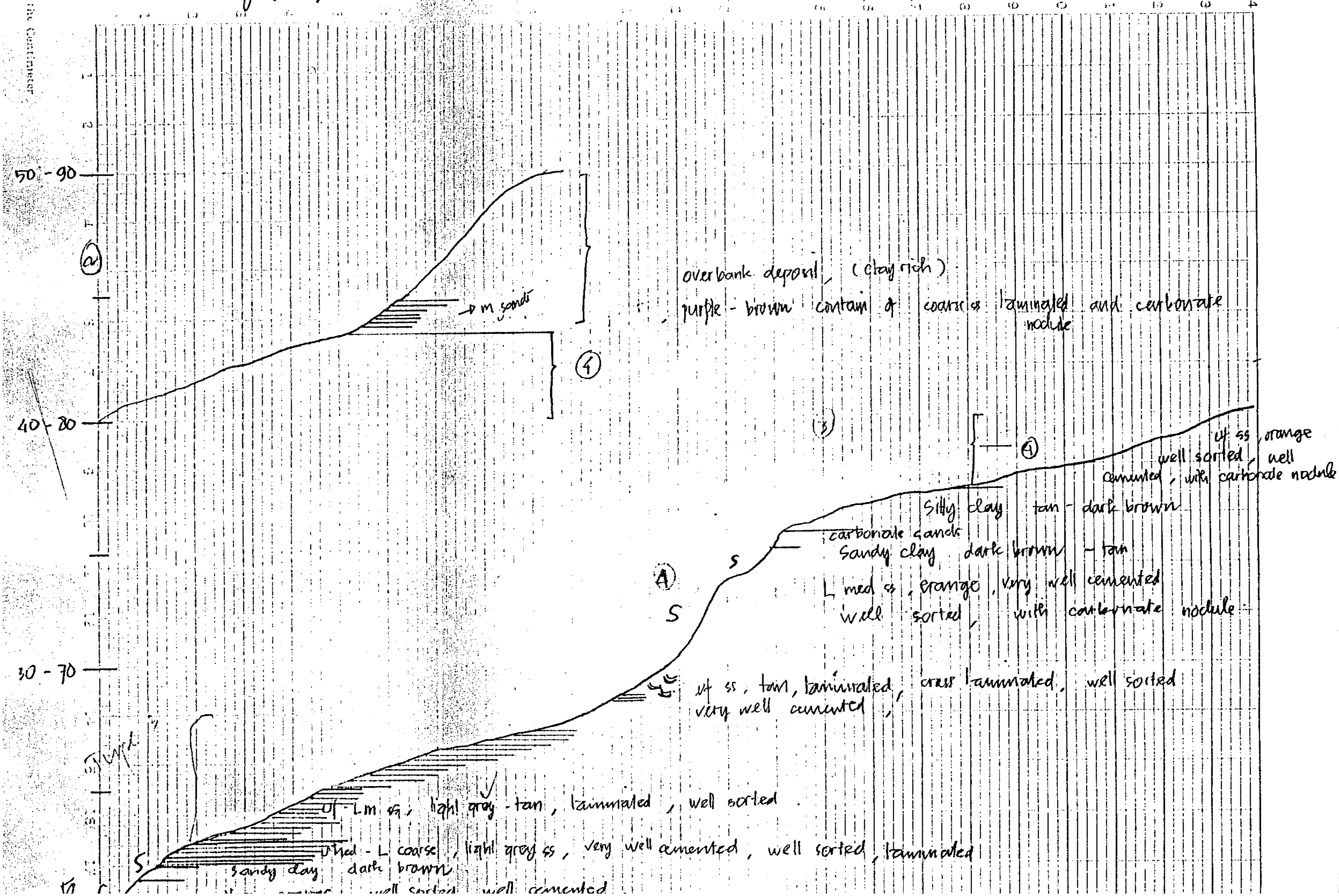
50 - 90
40 - 80
30 - 70
a
→ m sand
4
overbank deposit, (clay rich)
purple - brown contain of coarse ss laminated and carbonate nodule
3
4
A
S
S
vf ss, orange
well sorted, well cemented, with carbonate nodule
Silty clay tan - dark brown
carbonate sands
Sandy clay dark brown - tan
L med ss, orange, very well cemented
well sorted, with carbonate nodule
vf ss, tan, laminated, cross laminated, well sorted
very well cemented,
vf - L m ss, light grey - tan, laminated, well sorted.
med - L coarse, light grey ss, very well cemented, well sorted, laminated
Sandy clay dark brown
well sorted well cemented
S

APPENDIX II

LITHOFACIES CORRELATION

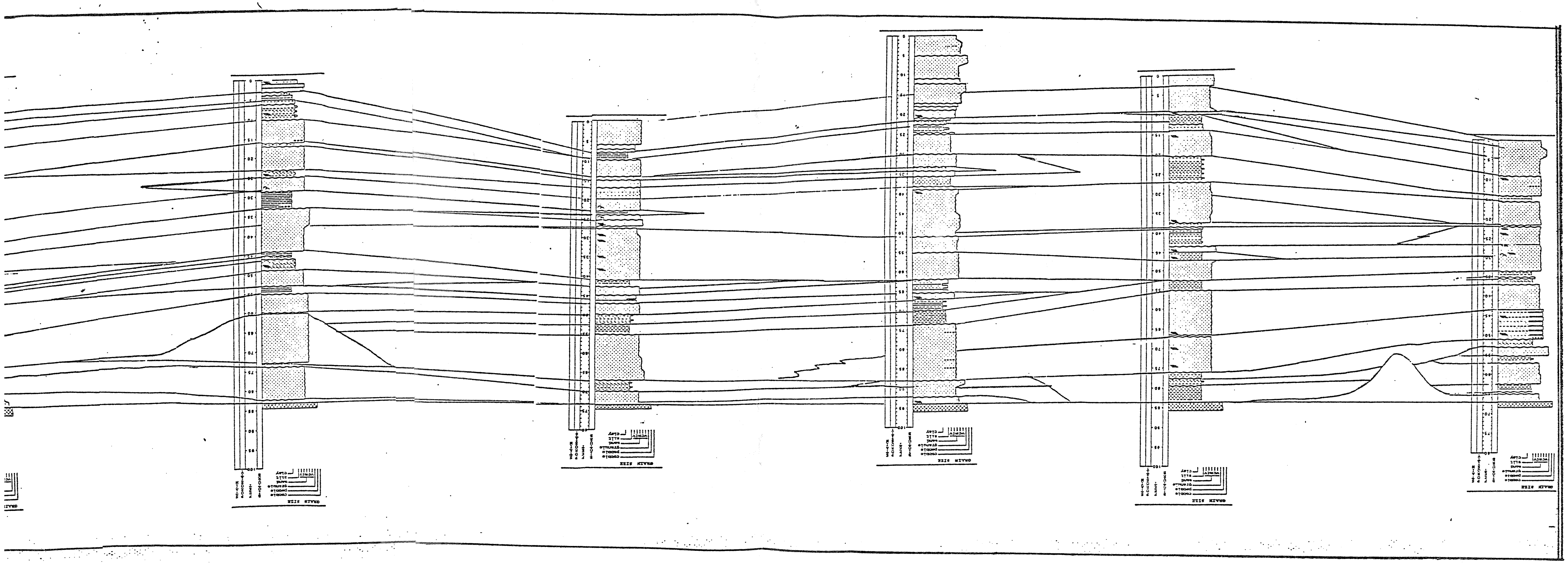

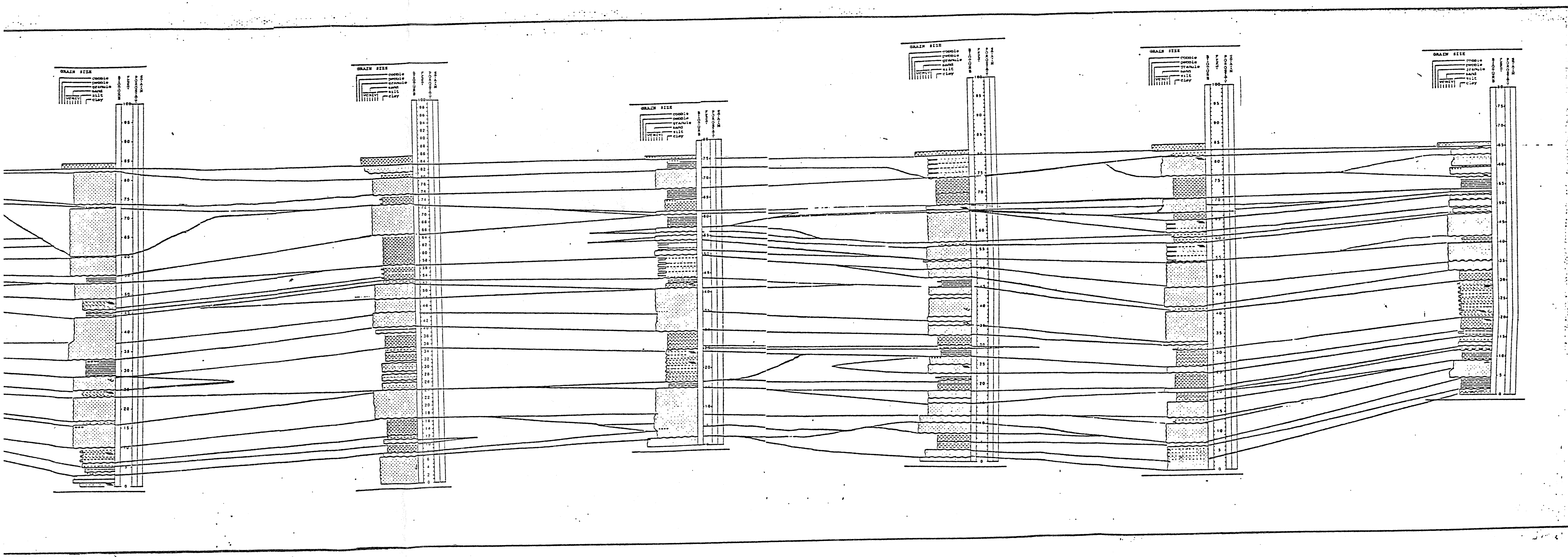
GRAIN SIZE
cobble
pebble
granule
sand
silt
clay

APPENDIX III

Example of Mini AirPermeameter Calibaration

Formula $k = \dfrac{2\,\mu q\,P1}{a\,Go(bD)\,(P1^2 - P0^2)}$

(μ)	Viscosity of air [Pa S]	$= 1.745 \times 10^{-5}$
(q)	Vol. Flow Rate [m3/s]	= volume / time = 5.5×10^{-5} / time
(P1)	Press. at Tip Pa]	= P1 = Po + Pn , where Pn is the net pressure.
(Po)	Atm. Press. [Pa]]	= 85.622
(a)	Radius of Tip [m]	= 0.002 m
(Go bD)	Geometric Factor	= 4.5
(m)	Mass piston	= 0.178 kg
(A)	Area Piston	= 0.00101 m^2

$$Pg = \frac{Fg}{A} = \frac{mg}{A}$$

Ff $= \beta v^2 = 0.1 + 155\,v^2$; v $= q / A$

q = Vol. / time ; $\Delta P = \alpha q - b$

P1 = Po + Pn , where Pn is the net pressure.

$$Pn = \frac{Fg}{A} - \frac{Ff}{A} - \Delta P = \frac{mg}{A} - \frac{\beta v^2}{A} - \alpha q - b$$

Example :

For Gravelly sands (GR1) sec. 6

Time = 2.88 sec.

q $= 5.5 \times 10^{-5} / 2.88 = 1.909 \times 10^{-5}$; v $= 1.909 \times 10\text{-}5 / 0.00101 = 0.0189$

Ff $= 0.1 + 155\,v^2 = 0.1 + 155 \times 0.0189^2 = 0.155$; Fg $= mg = 0.178 \times 9.8 = 1.7444$

$\Delta P = (8.3 \times 10^6 \times 1.909 \times 10^{-5}) - 50 = 108.447$; Pn $= (0.155 / 0.00101) + (1.7444 / 0.00101) - 108.447 = 1464.8$

P1 $= 85.622 + 1464.8 = 1550.42$

$$k = \frac{2 \times 1.745 \times 10^{-5} \times 1550.42}{0.002 \times 4.5\,(1550.42^2 - 85.622^2)} = 4.7848 \times 10^{-11}\ m^2$$

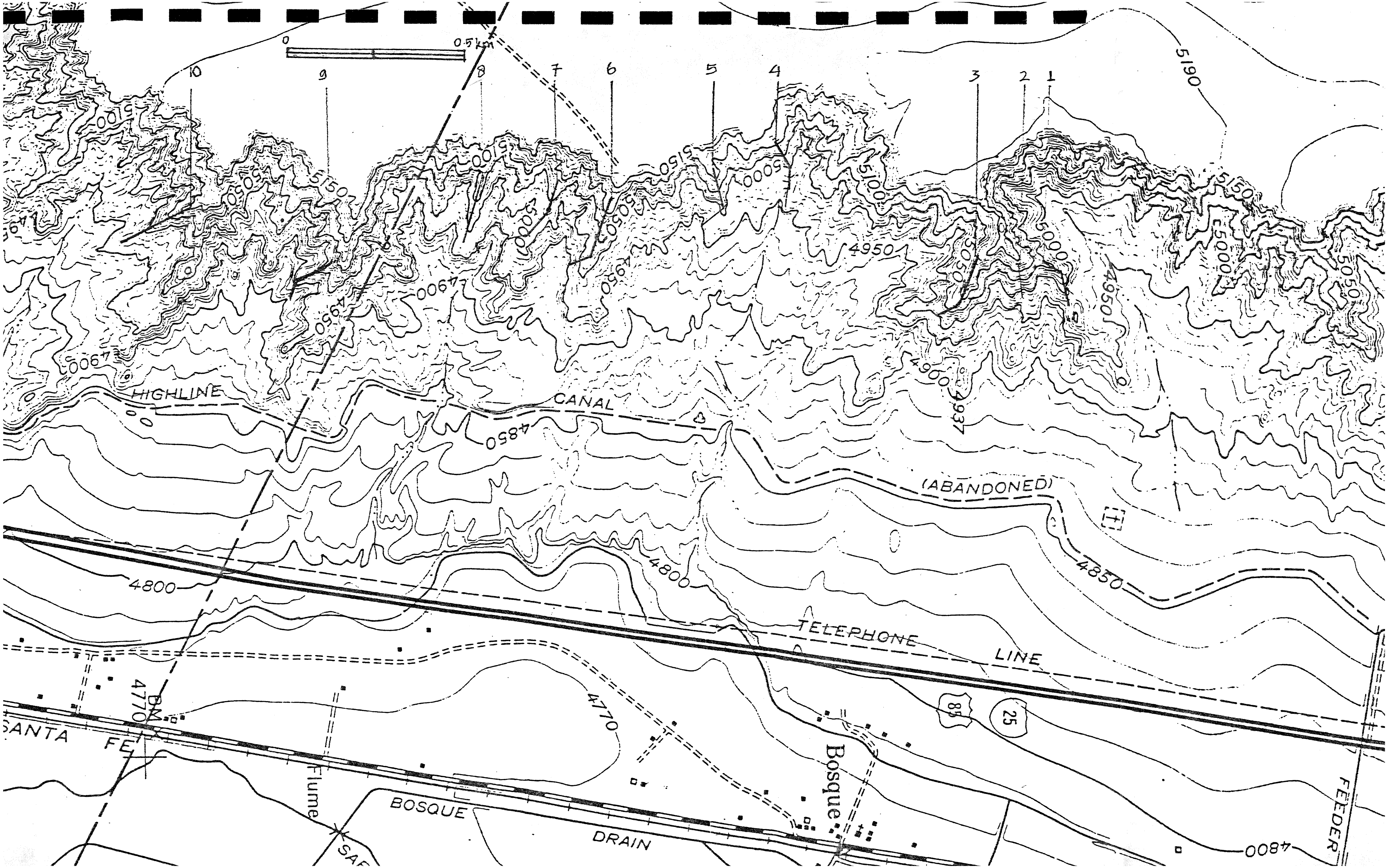
0
0.5 km
10
9
8
7
6
5
4
3
2
1
5190
5100
5150
5050
5000
4950
4900
HIGHLINE
CANAL
4850
4937
(ABANDONED)
4800
TELEPHONE
LINE
85
25
4770
BM
SANTA
FE
Flume
BOSQUE
DRAIN
Bosque
FEEDER